FINAL REPORT ON

DEVELOPMENT OF A 425-FOOT DIAMETER

PASSIVE COMMUNICATIONS SATELLITE

WITH SELF-ERECTING PROPERTIES

Contract No. NAS5-3943

Prepared by

G. T. Schjeldahl Company
Northfield, Minnesota

for

Goddard Space Flight Center
Greenbelt, Maryland

GPO PRICE $

CSFTI PRICE(S) $

Hard copy (HC) 3.00

Microfiche (MF) .65

ff 653 July 65

FINAL REPORT ON

DEVELOPMENT OF A 425-FOOT DIAMETER

PASSIVE COMMUNICATIONS SATELLITE

WITH SELF-ERECTING PROPERTIES

Contract No. NAS5-3943

Prepared by

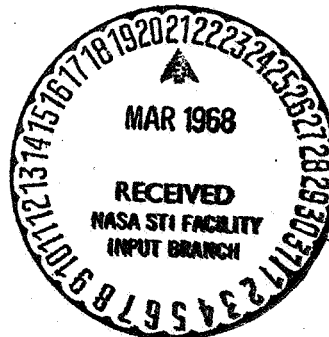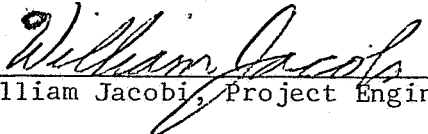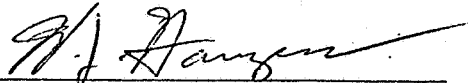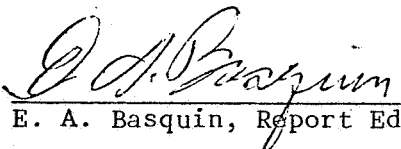G. T. Schjeldahl Company
Northfield, Minnesota

for

Goddard Space Flight Center
Greenbelt, Maryland

Prepared by:

William Jacobi, Project Engineer

Approved by:

W. J. Hangen, Program Manager

E. A. Basquin, Report Editor

ABSTRACT

This report describes the work done to develop a material with an improved ratio of radar cross-section to unit weight over ECHO II material. The material was primarily intended to be used in a passive communication satellite of reduced cost and increased reliability.

An open leno weave of fiberglass coated with copper was developed which would make a 425-foot diameter sphere weigh 2600 pounds. Preliminary tests show it to be radio reflective through 4 GHz.

Small model cylinders and flat plates of this material erected without inflation aids, but small model spheres did not erect fully. A design for an erection aid showed promise, but could not be fully tested within the scope of the contract. Additional work on these concepts is recommended to fully establish the parameters of the material.

TABLE OF CONTENTS

TABLE OF CONTENTS (Conc.)

LIST OF ILLUSTRATIONS

LIST OF ILLUSTRATIONS (Cont.)

LIST OF ILLUSTRATIONS (Conc).

LIST OF TABLES

1.0 INTRODUCTION

This report describes the effort of the G. T. Schjeldahl Company, begun in June 1964, to develop a self-erecting, radar-reflective material, usable in a large, but lightweight passive communications satellite. This effort was performed under contract No. NAS5-3943 to NASA Goddard under the technical direction of W. C. Nyberg.

The successes of Echo I and Echo II have shown that passive communications satellites are feasible. Echo I, 100 feet in diameter made of 0.5-mil metalized Mylar*, weighed 140 pounds. Echo II was fabricated from a three-ply laminate of 0.00018-inch aluminum on either side of 0.00035-inch Mylar, which was to be strain-rigidized in orbit. It was 135 feet in diameter and weighed 540 pounds. A number of limitations are encountered with devices such as these. The radar cross-section of these satellites is relatively small. The total cost of a passive communications network would be high because of the large ground stations required. Using larger satellites would decrease ground station costs, but the weight of larger Echo II satellites is prohibitive, and the distorting force of solar radiation on a large opaque satellite is high. Furthermore, previously orbited satellites required a complex inflation system which introduces some system unreliability.

Materials development for improved satellites was thus felt necessary. Goals established for materials performance were that the material had to be (1) extremely lightweight, significantly reducing the weight per unit RF cross-section area of Echo materials; (2) approximately 90 per cent transparent to solar radiation to minimize drag and solar pressure effects; (3) rigid enough to withstand buckling forces from solar pressure with a safety factor of 5.0 since it was desired that the surface contour remain accurate; (4) the reflectivity in the 8-9 GHz range was to be 95-98 per cent that of a similar solid surface; and (5) capable of erecting without inflation aids or mechanical devices.

Therefore in summary, the objective of this program was to develop a material which would increase the RF cross-section of a passive communications satellite without a substantial increase in weight or the area acted upon by solar pressure. Other secondary objectives were to reduce the complexity of manufacture, to simplify requirements of the canister, and to eliminate the need for an inflation system. It was hoped that these objectives would increase the reliability of a passive communications satellite network and reduce the total systems cost.

---

*Registered du Pont Trademark

2.0 SUMMARY

The first step taken towards the development of this material was that of selecting an open mesh material that could be coated with a metal for radar reflectivity. The open fabric or scrim material was essentially transparent to solar radiation and after metal deposition on its surface would be radio-frequency reflective. Prior to this contract, Schjeldahl had shown that a lightweight fabric woven from fiberglass yarn exhibited a remarkable memory; it could be folded into a tight package and upon release would spring out to the original shape. The fiberglass fabric had a relatively high modulus of elasticity and an excellent strength-to-weight ratio. Based upon this and the availability of fiberglass materials in general, this program scope was limited to fiberglass as a base material.

Preliminary work indicated that a major intrinsic property required for the self-erecting phenomenon was a high flexural rigidity. Work was done to enhance this inherent property of the fiberglass.

Originally, charring the size on the fiberglass fabric seemed the best solution to increasing the rigidity; however, further work showed that the proper application of sizing and/or binding materials could create the same effect.

Figure 1 is a representation of the composite developed under this contract. It shows the basic fiberglass matrix thoroughly saturated with a sizing material which has then been coated with GT 201* resin. The binder is then coated with copper by electroless deposition.

During this program a number of fabric weights and styles were investigated, and a leno-pattern weave was found most suitable for the mesh. Weight was a problem since commercial weavers do not normally prepare material as light as required. The final weight of the material developed in this contract would theoretically provide a 2600-pound, 425-foot diameter sphere. A 425-foot sphere fabricated from Echo II-type material would weigh approximately 5700 pounds. One type of fiberglass fabric yielded a material that theoretically could provide an 1180-lb, 425-ft-diameter sphere. However, the material was so light that it did not have sufficient strength to be manufactured into shapes. Further discussions with the weavers revealed that this fabric was considered too light to be woven successfully on a production basis on existing machinery. Because the extremely lightweight fabric desired could not be obtained, much of the work during this program was performed on a material heavier than the initial goals set forth. However, this heavier fabric demonstrated the features of the erectable materials concept.

In developing material, and measuring its properties, it was necessary to design equipment for making self-erecting material on a pilot-plant scale. This equipment, built and used to plate and coat fiberglass mesh materials

---

*Proprietary GTS Co. adhesive

which exhibit self-erecting properties, was used a number of times to prepare materials that were fabricated into objects for evaluation.

Preliminary tests show that material prepared as described in this report is radio frequency reflective through 4 GHz. Due to the limitations of Schjeldahl facilities, this testing was not carried any further.

Calculations in the last section of this report indicate that the material appears to be rigid enough to withstand the solar pressure in space.

Tests established the ability of this material to erect without inflation aids or mechanical devices. Small cylinders and flat plates erected very well; however, small spheres did not erect completely unless some erection aids were employed. A design is presented in this report that aids the erection of a sphere. Though showing promise in this laboratory, this design did not perform as well as expected in the deployment tests at Goddard Space Flight Center. It is felt at this time that the period of free fall of the spheres was not sufficient for a more complete erection.
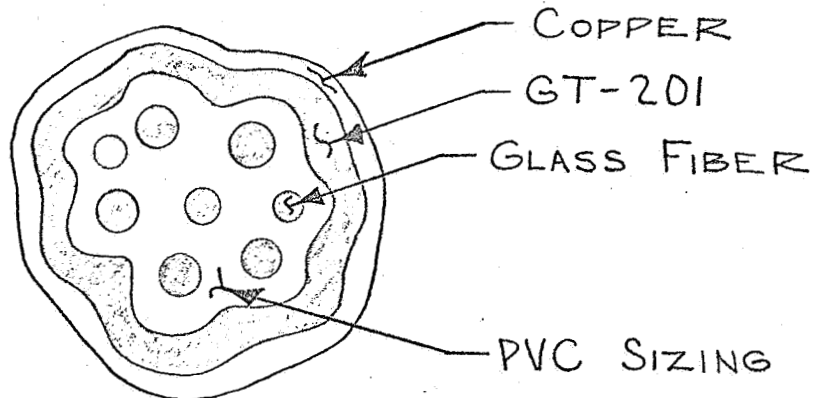
Figure 1   Cross-Section of
           Self-Erecting Material

3.0 CONCLUSIONS

1. The material developed under this program is self-erecting, lightweight, RF reflective, has a small effective surface area (essentially transparent solar radiation) and has a relatively high rigidity.

2. The vacuum deployment tests at Goddard Space Flight Center, wherein the small spheres did not completely assume a spherical shape, indicate that space erectables are limited at this present level of development.

3. A modulus of elasticity higher than that of fiberglass is apparently required for the base material to achieve the ultimate in erection properties.

4. The material at its present state of development is potentially useful for a number of applications including space antenna surfaces wherein its lightweight, reflective properties can be used with a minimum of auxiliary erection aids.

5. Continuous roll-to-roll electroless plating of fabric has been demonstrated by the pilot plant equipment built under this contract. The large number of pilot runs indicates that the conductive copper coating can be applied to a suitably sized and bound glass fabric with acceptable quality. The objective was to produce fabric with a resistance of 2 ohms per square, which is equivalent to the resistance of metalized Mylar used in the Echo I satellite. The present pilot plant can handle a 48-inch-wide web, prepare its surface, and plate or deposit a copper coating on it. The speed of the equipment, however, leaves much to be desired, since it is capable of running only one foot per minute during the plating operation. This web speed is limited by the plating bath residence time.

6. At the present state-of-the-art, the material received from commercial weavers is considered acceptable. The material received from the weaver early in the program had many defects, such as improper thread spacing, drop picks and general unraveling of the fabric itself. Most of these defects were undoubtedly due to the lightness of the fabric and the small quantity ordered. The latest material received was prepared by a new process that applies sizing on the loom itself. This material has very little thread wandering and excellent uniformity of weave pattern. It appears that material to produce self-erecting material weighing 0.25 to 0.33 of an ounce per square yard is improbable, as present weaver capability is limited to production of heavier fabric. The latest styles received have been much heavier, in the range of 0.6 to 0.7 of an ounce per square yard.

7. The sizing investigations revealed many likely candidates for fortifying the flexural rigidity of glass fabric; however, the bulk of these were water sensitive and hence unacceptable for use in the electroless copper baths. It had been hoped that the process could be simplified by plating the size directly. These sizing agents, even though water sensitive, could be used to prepare self-erecting material using vapor-deposited aluminum as a conductive coating. The most acceptable size investigated was a commercially available PVC. This size is platable if properly cured, and significantly enhances the rigidity of the self-erecting material.

4

8.   A GT 201 has been found to be the most acceptable coating, as it not only adequately binds the fiber bundles together at the intersections, but also presents a suitable plating surface. GT 201 is water insoluble and is "space-proven". Another significant advantage of this thermosetting polyester coating is that it makes the fiberglass fabric heat-formable to a predetermined shape.

9.   Electroless copper deposition seems to be completely acceptable and has performed adequately in the equipment described above. After thorough investigation of the products available as protective coatings for a copper surface, none were found that protect it under high humidity and high temperature conditions. It is recommended that future use of copper be limited to areas of low humidity and that it be protected in atmospheres of low humidity prior to use.

10.   A standard bitape butt seal seems to be completely acceptable for use on this material. A bitape seam is space environment proven, having been used on a large number of similar space objects.

11.   It is apparent that the theoretical development of forces on thin wall structures is scanty, and further work should be done to clarify them.

4.0 RECOMMENDATIONS

1. There should be a rigorous theoretical analysis of the structural stresses that will normally be encountered by this material in large space structures.

2. A study of the dynamics of deployment should be made, as the possible areas of failure during deployment are largely undefined.

3. A thorough examination of the experimental techniques presently available will have to be made so that material of this nature can be suitably evaluated for its intended use. These should include:

- Using a concentrated load on a thin-walled spherical shell to simulate solar pressure.

- A pressurization test wherein a bladder inside of a sphere of self-erecting material will be inflated to failure of the self-erecting material.

- A large number of cylinder tests to thoroughly examine the buckling modes involved in collapse.

- A study into the extended life characteristics when stressed over long periods in a space environment.

4. Radio frequency reflectivity of materials of this nature, and the effect of discontinuities in the conductive coating must be studied.

5. A study should be made to determine the relationship of surface imperfections to a failure of shapes deployed in space.

5.0 MATERIAL DEVELOPMENT

5.1 FABRIC BASE

Early in the contract it was proposed to process the yarn before it had been woven. It was proposed that virgin yarn of the proper weight be bought from a spinner, and then subsequently coated, heat treated, coated, heat treated again, and then plated to a specific conductivity value. Later in this contract it was shown that it is much more suitable to pursue the concept of plating and binding a fabric on a roll-to-roll basis.

5.1.1 Fiberglass Fabric

Most of the self erecting material development uses a fiberglass fabric for its base. The composition of the glass is as follows:

Silicon dioxide	50 to 56 %
Calcium oxide	16 to 25 %
Aluminum oxide	12 to 16 %
Boron oxide	8 to 13 %
Sodium & potassium oxide	1 to 4 %
Magnesium oxide	0 to 6 %

The properties of the fiberglass are:

Specific gravity of the fibers	2.55
Tensile modulus of elasticity and tension	10.5×10^6 psi
Elongation	3 to 4 %

The yarn has been woven. It is described with a series of numbers and letters, with the following example being the most usual type used on this contract. ECD 450 1/1 is defined as follows: The first letter defines the glass composition, namely E glass; the second indicates the type of fiber, namely C for continuous filament; the third letter defines the average filament diameter from which the yarn was made. D indicates a filament diameter of 0.00021 inches. The 450 is the yield in hundreds of yards per pound of the basic strand; 204 D-size filaments were wound together to produce the 450 yarn. (900 yarn has 102 filaments per strand). In the next set of numbers, the fraction, the first is the number of single strands twisted, and the second the number of these strands plied together. The total number of strands is the product of these two numbers. The yarns are then woven into fabric

Figure 2 shows this type of pattern and how each transverse fiber is held in place by twisting the machine direction yarns. The fiberglass used almost exclusively throughout this contract was a 10 by 20 leno-weave fabric, the 10 indicating the number of yarns in the machine direction and the 20 indicating the number of yarns in the machine direction. The machine direction yarns are twisted together in the weaving process so that the final fabric appears to have only 10 fibers in the machine direction.

7
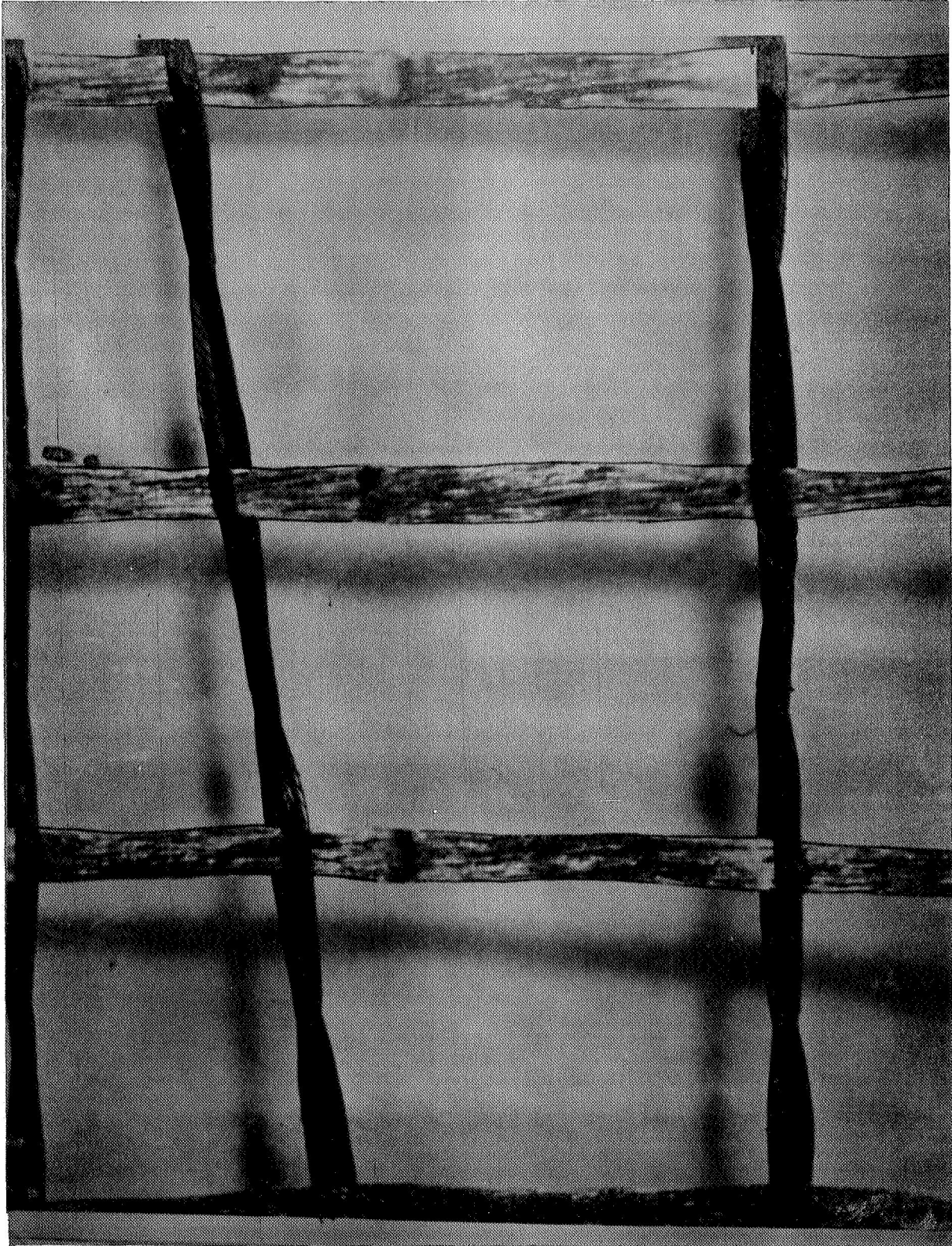
Self-Erecting Material (X250) Showing Leno Pattern Weave

Figure 2

As the fabric is woven it is sized with a lubricant normally consisting of a starch. Early in the program this sizing was burned off in a high temperature oven at 600 degrees F for 30 to 60 minutes. However, it was found that although this treatment increased the rigidity of the fabric, the most efficient means of realizing high rigidity was through sizing and adequate binding of the fabric itself, since heat treating materially weakened the fabric.

Most of the fabric used on this contract was prepared by Hess-Goldsmith Company, New York City, and their style numbers will be used to identify the fabric received. Table 1 lists the different types of fabrics that were processed into deliverable items.

Fiberglass material processed early in 1966 was very light, 0.6 of a milligram per square centimeter. This extremely lightweight fabric is almost beyond the limits of existing weaving equipment. When this material was received it was by-and-large acceptable; however, there were many weaving imperfections. The flaws consisted of the following:

1. Lack of transverse threads indicating that the pick was broken.

2. Nonorthogonal alignment of the fiber bundles.

3. Uneven spacing of the machine fibers.

4. A tendency to wander on the roll.

5. A lack of proper tensioning throughout the roll, making it very difficult to process.

Because the weaver was apparently unable to prepare acceptable lightweight fabric, a concession was made for the sake of development and a more readily obtainable fabric weight was used during the remainder of 1966. This fabric weighed approximately 1.8 milligrams per square centimeter and had much fewer flaws. Late in August of 1966 an order was placed with Hess-Goldsmith for two different types of fabrics, made from ECD 450 yarn and ECB 450 yarn. The ECB type yarn is made up of thinner filaments. Beta yarn has twice as many filaments as D yarn with equivalent weight. It was hoped that the two types of material could be processed identically, and some information could be gained regarding the advisability of using B yarn in the future. However, due to production problems the weaver could not deliver the B yarn fabric in time for inclusion in the program, and this comparison could not be made. This last material received in December, the ECD 450 fabric, was sized on the weaving machine. Also received in this order was a sample of fabric where the material was unbalanced to the extent where the transverse fibers were much larger than the machine direction threads. This fabric was processed during the months of December and January and some of the models were made from it. The model tested at Goddard prepared from this fabric performed better than a model prepared out of balanced material.

The fabric weight appears to be a very definite design limitation as present commercial weaving practices severely limit the minimum

TABLE 1

COMPILATION OF SEVERAL GLASS FABRIC STYLES

Vendor Style No.	Mesh Configuration Threads/Inch		Properties
	Machine	Transverse	Wt. mg/cm^2
Hess-Goldsmith I8601	10	10	1.77
J.P. Stevens 1659/45	10	10	5.65
J.P.Stevens 1620/45-857W	20	20	5.78
Hess-Goldsmith No. 191	10	10	5.3
J.P. Stevens 166/48	5	5	2.08
Hess-Goldsmith I8539	10	10	.67
Hess-Goldsmith I8683-150	10	10	4.22
Hess-Goldsmith I8683-450	10	10	2.17

weight of self-erecting material that can be produced. The minimum
weight of fabric where the thread spacing is 10 by 10 per inch appears
to be near 0.5 oz/sq yd. This results in a 425-ft-diameter sphere weight
of close to 2,000 lbs. This weight is higher than the initial design
goal of the contract and new weaving techniques will have to be used to
produce lighter fabric.

If less fibers per inch are required, as a lower frequency
is used for reflective work, the weight of the fabric could be reduced and
a much lighter fabric developed and produced by the weavers. However,
the requirement for large sample sizes might preclude any efficient devel-
opment work along these lines. The weavers are interested only in large
quantities of fiberglass fabric purchases. The few hundred yards that have
been used in this development work are very small when compared to the
millions of yards that are normally produced. There are many other types
of fiberglass yarns available, however, commercial acceptance has not been
high on these and, therefore, they are not available in the form of fabric.
Owens Corning produces a type S glass which has a much higher modulus, almost
1-1/2 times greater than E glass. However, this production has gone solely
into the manufacture of roving-type yarns and very little has been woven.

5.1.2 Dacron-Glass Combination Fabric

A sample of fiberglass Dacron combination yarn was secured
from Owens Corning. This combination, GDD 941 (1/2) 4.4S, is a 40-denier
Dacron yarn twined with an ECD 900 1/0 glass yarn. To evaluate this yarn
it was necessary to prepare a fabric so that a comparison to the present
glass fabric could be made. A hand loom, shown in figure 3, was used to
make a simple, plain weave fabric from the fiberglass-Dacron yarn and the
ECD 900 1/2 1.0Z yarn. After these fabrics were loomed and suitably sized
their tensile strengths and flexural rigidity were measured.

Data presented in tables 2 and 3 compare the fabrics made of
fiberglass yarn and of the combination yarn. The weight increase with a
polyvinyl alcohol size was not as high as intended. However, this work
will serve as a guideline in comparing the two materials.

Comparing the sized fabrics, the average tensile strength of
the combination yarn was 66 per cent of that of a fiberglass fabric. The
rigidity of the combination fabric was only 52 per cent of that of the
fiberglass fabric. Because of the low rigidity and poor tensile strength
this material was not investigated further.

5.1.3 Future Concepts

It is felt at this point that the use of the thread-laying
facilities at Schjeldahl for producing fabric should be investigated. It
has become increasingly apparent that commercial weavers have neither the
inclination nor the ability to weave material that is suitable for use in
large space structures. Using the thread layer, it would be possible to
program the proper thread spacing and custom-make a fabric on a continuous
basis. This undoubtedly is more acceptable than relying on commercially
available fabrics. Figure 4 is a drawing of the present equipment; with very
little development work it could be modified to make acceptable material for
this contract.

Figure 3   Hand Loom

TABLE 2

Rigidity of Hand-Woven Samples

Material Description	Rigidity (mg-cm)			
	10°	20°	41.5^o	Average
Glass	354.0	309.2	336.1	333.1
Glass - A29	460.3	414.3	460.26	444.9
Glass PVOH	401.8	426.8	399.1	409.2
Glass A29, PVOH	462.9	493.9	429.7	462.2
Dacron/glass	180.4	176.7	145.0	167.3
Dacron/glass A29	298.4	276.8	258.8	278.0
Dacron/glass PVOH	175.2	226.7	197.3	199.8
Dacron/glass A29, PVOH	199.0	203.2	236.9	213.0

TABLE 3

Tensile Strength of Hand-Woven Samples

Material	Starch	A29	PVOH	Tensile	Elongation
Glass	X			11.5	4.1
Glass	X	X		15.9	4.1
Glass	X		X	15.2	4.7
Glass	X	X	X	16.6	4.3
Dacron/glass	X			7.9	4.3
Dacron/glass	X	X		11.0	5.8
Dacron/glass	X		X	8.8	5.0
Dacron/glass	X	X	X	11.4	4.83

CREEL FOR MACHINE DIRECTION THREAD ARRAY

GATE DRIVE

CONTROLS

DATA READER

TO TACHOMETERS AND OTHER FEEDBACK XDUCERS

VARIBLE GUIDE GATE FOR M.D. THREADS

REVOLVING DRUM WITH THREAD SPOOLS FOR TRANSVERSE DIRECTION ARRAY
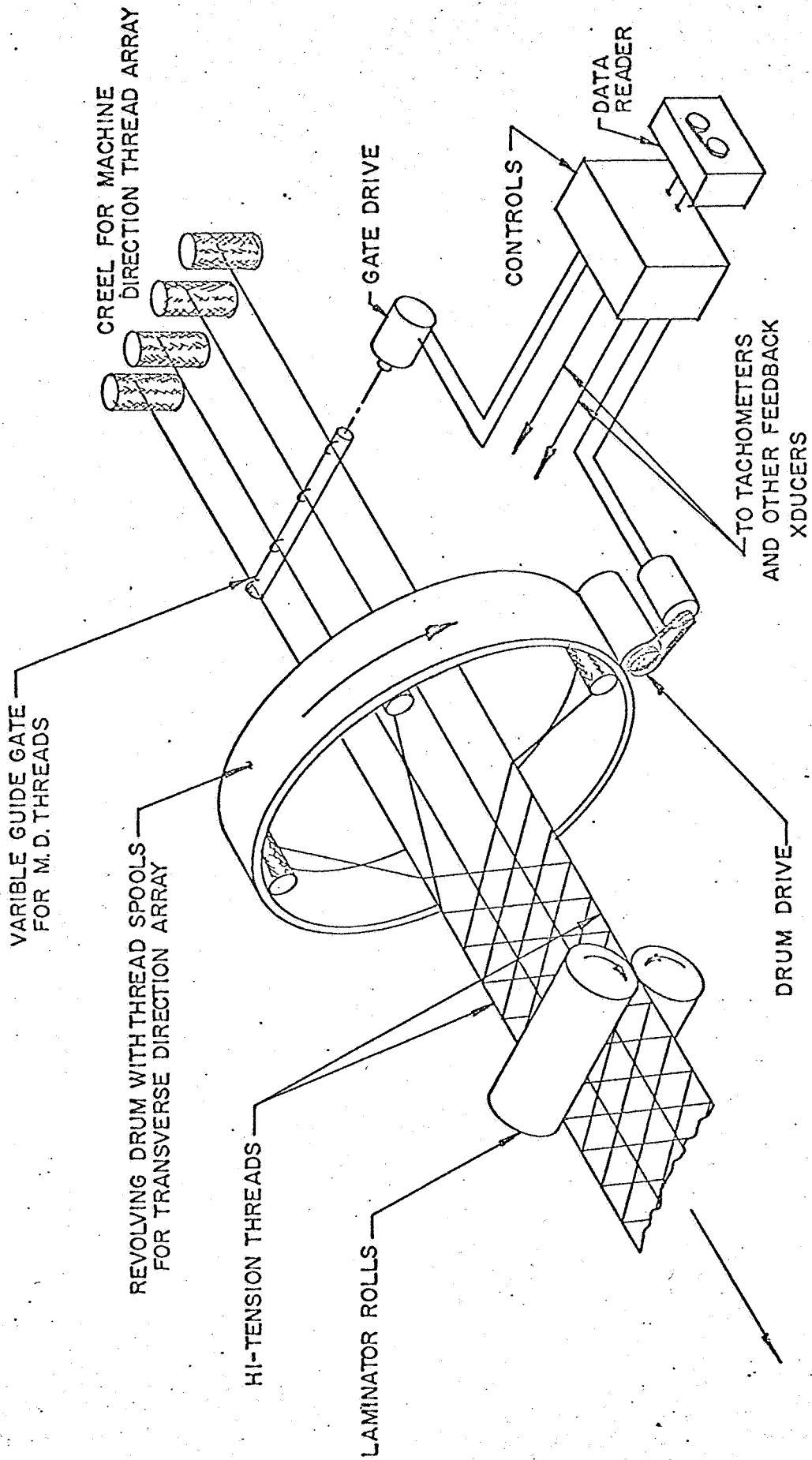
HI-TENSION THREADS

LAMINATOR ROLLS

DRUM DRIVE

Figure 4: CONCEPTUAL LAYOUT FOR FLYING THREAD LOOM AND AUTOMATIC CONTROLS

14

5.2 SIZING

The effect of sizing agents was investigated during this program. Processing steps to the fabric prior to plating consist of pretreating, or sizing, including heat cleaning and application of sizing to the fabric. This step encapsulates the filaments in the fiberglass yarn increasing the fabric's rigidity. The binder step cements the yarn bundles at the intersections and provides a smooth platable surface. The binder step many times performs both functions, sizing and binding. The elimination of the binding step was investigated, however, the majority of the sizes did not have adequate resistance to the plating solutions.

5.2.1 Heat Treating

The original concept of self-erecting material pointed towards the use of hot air charring to enhance self-erecting properties. Therefore, an experiment was designed to determine the proper heat treating conditions. Twelve-inch square pieces of glass fabric were fixed to aluminum sheets and placed in a forced air oven at several temperatures for various time intervals. Temperature was varied from 200 to 600 F and exposure times from 5 to 60 minutes, as shown in Table 4. From these data a topographical chart, figure 5, was made showing the rigidity as a function of time and temperature. This chart shows that the highest rigidity is in the region bounded by dotted lines. Because of the size of the optimum area it was felt that close control of this process would be unnecessary. As will be pointed out in subsequent sections, this work, although helpful in pinpointing the optimum heat treatment conditions, has been superseded through the use of sizing agents.

5.2.2 Sizing Materials

In order to develop a material with high rigidity, it was felt that the proper sizing agent could make the fabric stiffer. Ten sizes were studied as listed in Table 5. In most cases two concentrations of the size solutions were used. The base glass fabric used for this study was Hess Goldsmith Style I8601.

Table 6 shows the flexural rigidity and tensile strength of the laboratory samples. These samples were prepared by placing a 13- by 14-inch sample of glass fabric into a cardboard frame and applying a solution of the sizing agent. The sizing agents increased the rigidity of the fabric somewhat; the most effective being animal glue, polyvinyl alcohol, GT-201, and Silane A 1100. The highest tensile strength was noted in the Silane A1100 and GT-201 sized samples. The gain in weight was nearly the same regardless of type of size used; a 5 per cent solution increased the weight approximately 3 per cent and a 10 per cent solution, 6 per cent.

The effect of GT 201 on the fabric rigidity is shown in figure 6. The highest rigidity is observed with a 20 per cent weight addition. There is a decrease in flexural rigidity as the ratio of GT-201 to fiberglass increases. The results show that a 20 per cent increase is desired, varying with the style material used. The weight addition of GT-201 in the production runs was approximately 20 per cent.

TABLE 4

Determination of Optimum Heat Treating Conditions for Highest Rigidity

Material	Temperature of Oven (°F)	Time (Minutes)	Weight (mg/cm^2)	Rigidity mg cm
Hess Goldsmith				
I8539	200	5	.69	9.9
"	200	30	.69	20.1
"	200	60	.69	11.5
"	300	30	.69	13.5
"	300	5	.70	18.1
"	300	20	.69	17.0
"	400	10	.69	29.8
"	400	45	.69	91.5
"	400	60	.68	72.8
"	500	10	.67	11.4
"	500	15	.68	107.2
"	500	60	.67	152.2
"	600	5	.67	67.7
"	600	10	.67	35.4
"	600	30	.67	24.9
"	450	30	.66	115.9
"	450	60	.69	104.8
"	500	30	.67	119.1
"	500	45	.68	123.0
"	500	60	.67	115.8
"	550	15	.67	96.7
"	550	45	.66	53.0
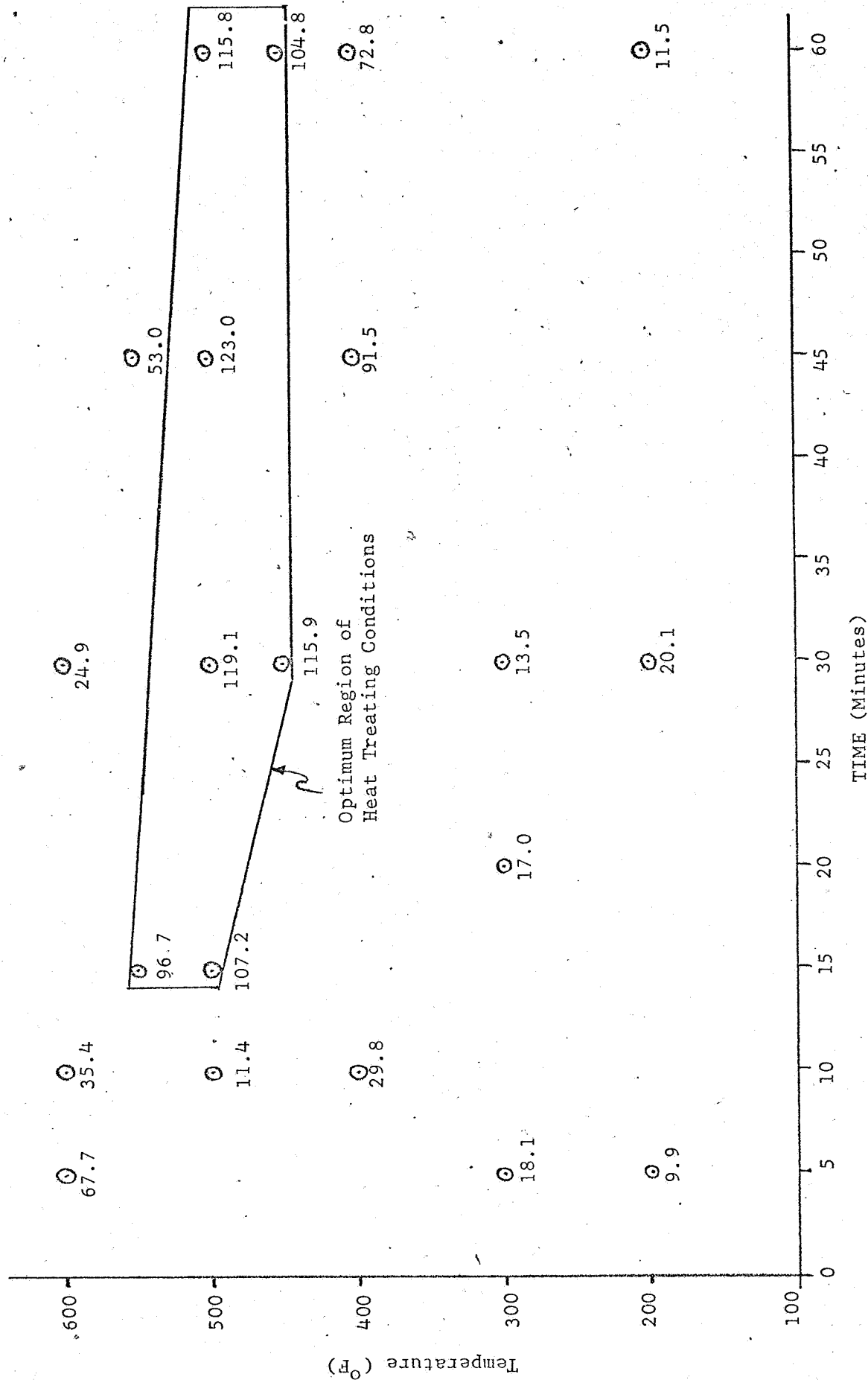
Figure 5 Rigidity as a Function of Time and Temperature
(Figures indicate sample rigidity in mg-cm)

17

TABLE 5

Materials Used in Sizing Study

	Trade Name	Description	Supplier
1.	TS100	Polyvinyl acetate copolymer emulsion	Rhom & Haas
2.	HA16	Acrylic copolymer emulsion	"
3.	ASE60	Carboxylic terminated acrylic polymer	"
4.	Silane A1100	γ-Glycidoxypropyltrimethoxysilane	Union Carbide
5.	Selectus	Edible gelatin	Swift and Co.
6.		Starch	Corn Products
7.		Dextrin	Corn Products
8.	Hercules	Animal glue	Swift and Co.
9.	GT-201	Proprietary thermosetting resin	G.T.S. Co.
10.	52-40	Polyvinyl alcohol	E.I. du Pont

TABLE 6

Flexural Rigidity and Tensile Strength of Laboratory Samples

Lab. No.	Size	Weight (mg/cm^2)	Rigidity (mg-cm)	Tensile Strength (lb/in)
I8601		1.82	135.5	
301-14-1	Glue	1.93	1169.3	27.8
301-14-2	Glue	1.83	848.2	24.3
14-3	Gelatin	1.89	818.7	19.8
14-4	Gelatin	1.84	939.9	26.6
15-1	TS100	1.91	734.4	28.8
15-2	TS100	1.83	476.3	19.5
15-3	PVOH	1.90	1121.3	28.8
15-4	PVOH	1.84	999.2	26.3
15-5	HA16	1.87	515.9	18.7
15-6	HA16	1.77	419.	18.6
15-7	Dextrin	1.89	965.2	26.8
15.8	Dextrin	1.86	706.3	22.1
16-1	GT-201	2.24	1109.1	38.8
16-2	Starch	1.88	894.2	27.5
16-3	Starch	1.78	773.4	24.3
16-4	ASE60	1.84	710.3	24.0
16-5	ASE60	1.78	699.37	22.9
16-6	GT-201	2.33	1137.6	34.6
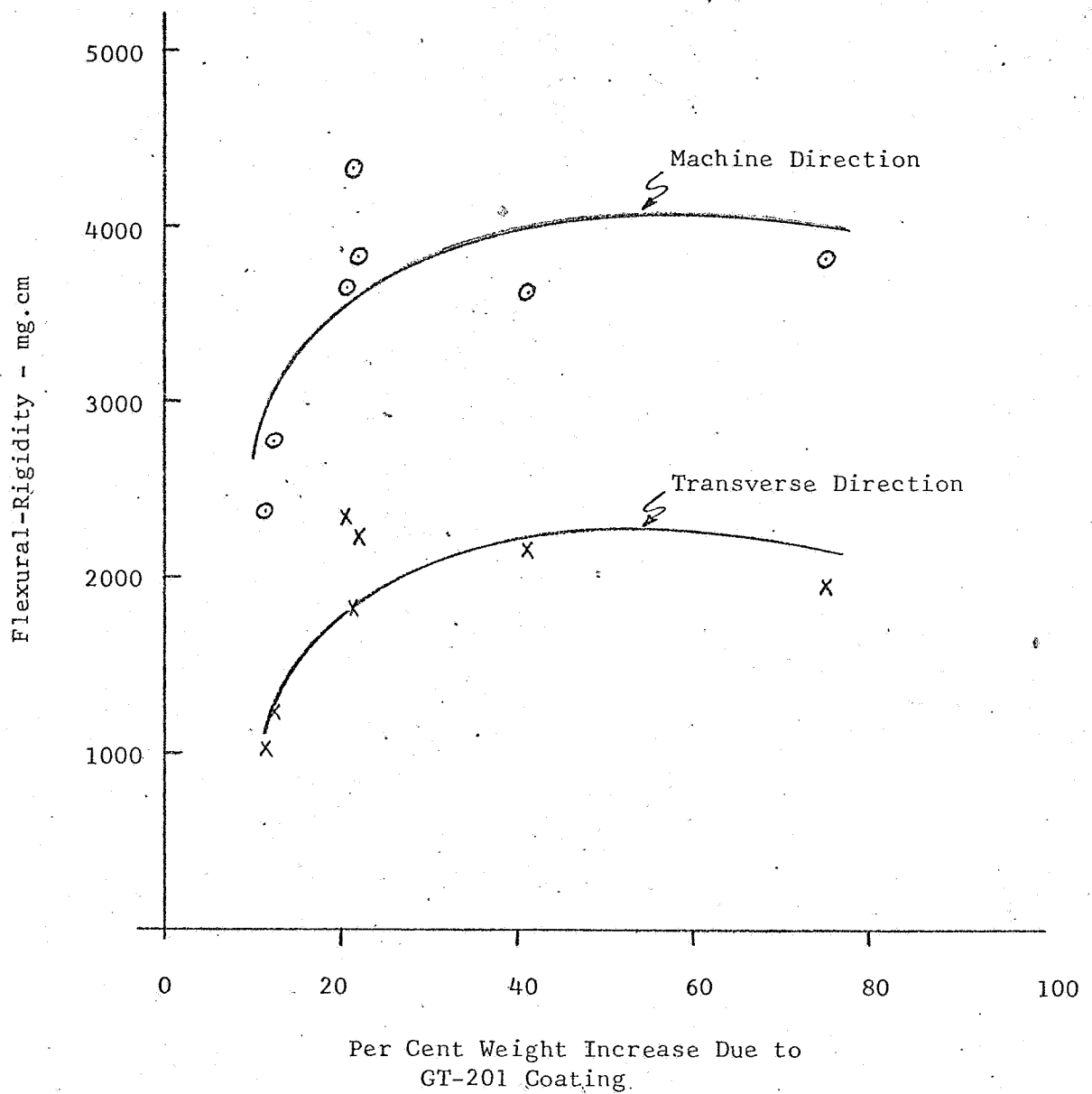
Figure 6   Effect of GT-201 Coating Increase on
Flexural Rigidity

5.2.3 Weaver-Applied Sizing

Samples of Hess Goldsmith style No. 451 were received during June of 1966. Style 451 has a 36 by 18 one pick leno weave, with machine direction threads B150 1/0 and transverse threads B150 1/2. The design weight is 2.98 ounces per square yard. Hess Goldsmith's laboratory pre- pared three different samples with three types of sizing applied to the fabric. Listed below are the numbers for these sizes and a description of them.

> 451-A - a polyvinyl chloride size
> 451-B - a neoprene size
> 451-C - an acrylic size

Table 7 shows the tensile strength and elongation for each of these materials in the machine direction. As can be seen from these data, the type of sizing has no marked effect on these properties. To determine the suitability of any of these sizes the unsized fabric had to be received and evaluated. The rigidity of these samples and their weight are shown in table 8. An average weight increase of the three sizes was 8 per cent. The rigidity as measured, indicated that Hess Goldsmith style 451-A is the most rigid.

To determine the susceptibility of these coatings to water soak- ing, a test was devised as follows. Samples were soaked approximately 20 minutes in water and the rigidity and tensile machine direction were measured wet. Table 9 shows the rigidity of number 451-A, number 451-B, and number 451-C in an as-received condition, after a 20-minute soak, and after drying. Style 451-A was effected least with a 60.7 per cent decrease in rigidity. After druing, the rigidity of all three increased to a level higher than the initial rigidity. This is probably caused by more complete wetting of the fiberglass during the soaking as the resins became softened by the water.

Another property that was considered important in the evaluation of water sensitivity was the tensile strength of a sample cut on a 45-degree angle.

Measurement in this direction should give the water resistance of the sizing agent more accurately, as the strength of the yarn intersections is being tested. The results are listed below. Style No. 451-A and No. 451-C increased in strength after a 20-minute soak while the tensile strength of 451-B decreased after the soak.

Tensile Strength of Samples Cut 45 Degrees to Machine Direction

(Figures are Pounds per Inch of Width)

	451-A	451-B	451-C
As received	38	29	24
After 20-minute soak	49	20	34

TABLE 7

Tensile Strength and Elongation of Hess, Goldsmith Styles 451-A,-B,-C

(1 inch wide samples)

	451-A		451-B		451-C	
	Tensile Strenth (lb)	Elongation (%)	Tensile Strength (lb)	Elongation (%)	Tensile Strength (lb)	Elongation (%)
Sample 1	120.0	9.0	109.0	7.0	108.0	8.0
Sample 2	122.0	9.0	114.0	7.5	95.0	8.0
Sample 3	120.0	8.0	109.0	9.0	111.0	8.0
Sample 4	120.0	8.0	115.0	8.0	105.0	8.5
Sample 5	125.0	8.0	110.0	8.5	98.0	8.5
Average	121.4	8.4	111.4	8.0	103.4	8.4

TABLE 8

Rigidity of Style 451 Fabric

(1 inch wide samples)

	451-A Rigidity (mg-cm)	451-B Rigidity (mg-cm)	451-C Rigidity (mg-cm)	451 No Size Rigidity (mg-cm)
$10°$	6,708.2	1,649.6	2,902.5	112
$20°$	5,183.6	1,745.6	2,677.7	179
$41.5°$	1,776.0	1,557.1	2,401.2	123
Average	4,555.9	1,650.8	2,660.5	138
Weight mg/cm^2	10.9	11.2	10.5	10.1

TABLE 9

Water Sensitivity of Size as Supplied by Hess, Goldsmith

Figures in Table are Rigidities (mg-cm)

	451-A	451-B	451-C
As Received			
10°	6,570	2,450	2,630
20°	6,350	1,930	2,310
41.5°	5,400	1,670	2,210
Average	6,107	2,017	2,383
Soaked in Water 20 Minutes			
10°	2,460	202	750
20°	2,480	156	540
41.5°	2,260	177	540
Average	2,400	178	610
Dried			
10°	10,500	5,230	4,080
20°	8,900	4,000	2,780
41.5°	6,300	3,920	2,380
Average	8,567	4,383	3,080

As a result of this experiment it appeared that the polyvinyl chloride sized fabric could survive the effects of water during copper deposition. Platability of this size was subsequently successfully demonstrated.

5.3 PLATING

The material used in a passive communications system should have good radar reflective properties; experience has shown that a resistance of 2 ohms/square is necessary. Much effort was expended to develop a method of making self-erecting material conductive. The method that was established was a proprietary electroless plating process manufactured by Enthone. An electroless plating bath will deposit a metal (in this case copper) on a catalyzed surface. The process is autocatalytic, so metal deposition continues. Figure 7 plots time versus thickness of the metal coating. The supplier of this process states that approximately 0.001-mil is deposted per minute, but calculations show that the average rate was 0.0008 mil/min in laboratory runs. A residence time of 10 minutes in the plating baths should result in a deposit of 0.008 to 0.01 mils of copper, with resistance of 2 $\Omega/\square$.

The rate in the laboratory was established by plating 6-inch square samples of I8539 fabric coated with GT-201. After treatment with the sensitizer and activator, the samples were held in the plating baths for various lengths of time, then dried and weighed. The plated samples were then placed in an ammonium persulfate bath to remove the copper deposited, after which they were again then weighed to determine the copper removed. Table 10 shows the results of these experiments.

TABLE 10

Results of Plated Samples

Residence Time in Plating Bath	Amount of Copper mg	Rate of Deposition mg/min
2	1.09	.55
5	1.90	.38
7	4.88	.7
10	12.23	1.22
12	12.65	1.05
Average		0.78

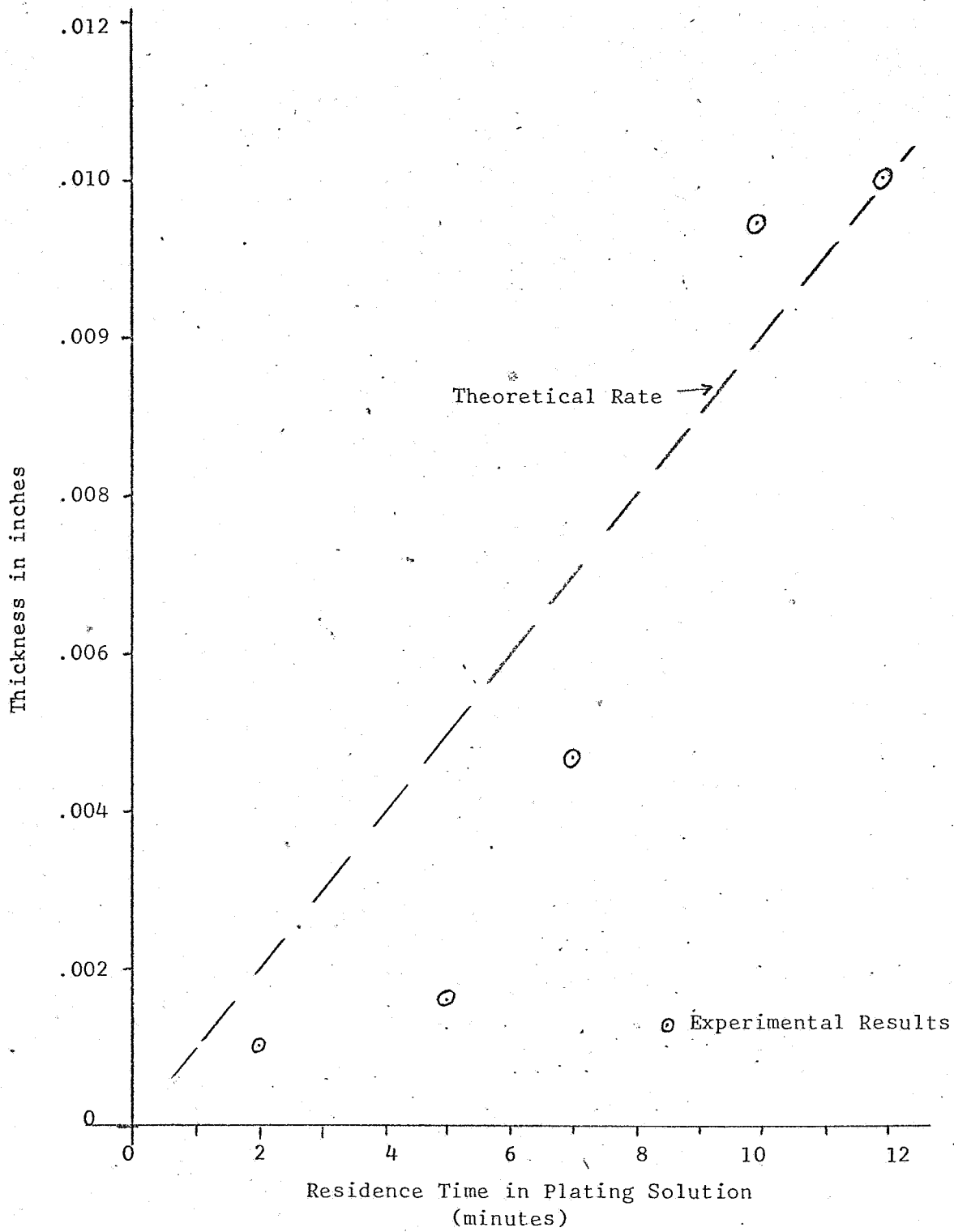The above rate calculations do not consider the increase in diameter.

Figure 7 Residence Time VS Copper Thickness

5.3.1 Batch Plating

The use of the batch system was used early in this contract to prepare material. Large flat pans were used to immerse the fabric in the sensitizer, activator, and plating solutions. Spray nozzles were used for water rinse after immersion in each solution. The procedure involved a one-minute sensitizer treatment, one-minute activator treatment, and an eight minute copper plating treatment. Plating was difficult because of the number of hand processes involved, because the panels being plated, 4 by 15 feet, were awkward to handle, and inability to maintain recommended operating temperatures caused poor plate quality.

The binder was applied in a semi-batch operation. Large flat panels were placed on a fixture and hand-sprayed with the General Electric SS4090 silicone resin. The coating weight and uniformity varied over the panel and in weight from panel to panel. However, this material was to be used in the measuring of RF reflectivity and the inconsistencies in silicone coating were deemed unimportant. Material processed in this manner was unacceptable for making spherical segment as it had a great number of flaws. The material had been affected by the plating solution due to improper rinsing.

5.3.2 Single-Tank Continuous Plating System

The difficulties encountered in the bath plating of fiberglass fabric prompted the investigation of a continuous process. The equipment designed for this use is pictured in figure 8. It consisted of one process tank, one rinse tank, and one rewind roll. The residence time in each solution depended on the amount of material submerged in the processing tank. A number of pilot runs were made using a four-inch-wide web of material. It was found that using a single processing tank for the three steps was impossible because the rollers became contaminated by the solution in the previous step. After much development work with this machine, it was decided to use a series of tanks for adequate plating. It was also found that paint holders handled the web best. The nap on the paint rollers grabbed the open fabric very effectively and distributed the stress on the material as it was being transported from one tank to the next. It was also found that a more suitable plating mixture for this operation was a 2:5:9 bath that consisted of two parts Cu 400-A, five parts Cu 400-B, and nine parts deionized water. It was found that control and the plating quality of a bath of this makeup was far superior to the baths used earlier, made up of one part of Cu 400-A, one part Cu 400-B, and one part deionized water. On the limited runs on this machine it was believed that no web handling rollers would be required at the bottom of any of the tanks. However, this proved to be erroneous after the continuous plating machine was constructed and a large-scale run was attempted.

5.3.3 Multiple Tank Plating System

The plating machine ultimately developed, shown in figure 9, consists of two sections as shown in figure 10. The specification for running this machine is appended.

27

Figure 8   Single Tank Plating Equipment
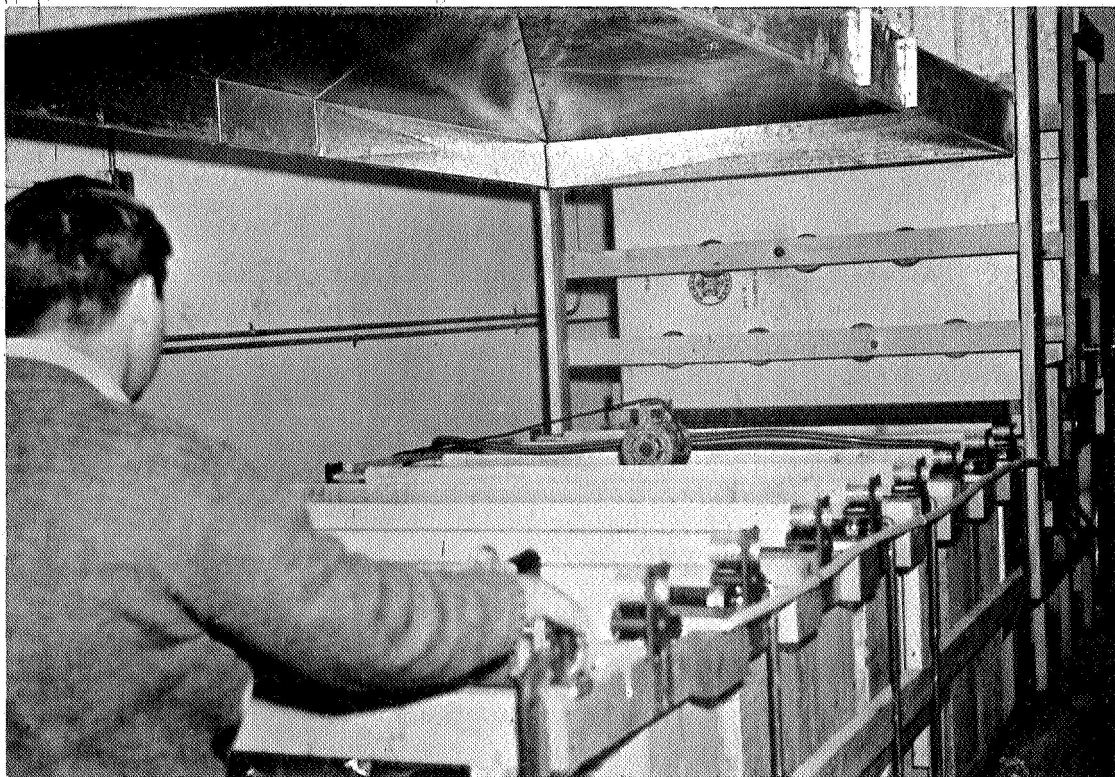
Figure 9   Continuous Plating Equipment (from unwind end)

TANKS — 1 & 3 — WOOD 12 x 18 x 54
2, 4, 5 & 8 — SHEET METAL 12 x 18 x 54
6 & 7 — WOOD 12 x 30 x 54
9 — SHEET METAL 12 x 12 x 54
10 — SHEET METAL 6 x 2 x 54

DRYING CHAMBERS — SHEET METAL 12 x 72 x 54

RUBBER ROLL

2ND UNWIND

UNWIND

D_2

D_1

TANK 9 - NOT USED

SECTION B

SECTION A

REWIND

DRY

RETREATMENT AND BINDING

DRY

WASH

PLATE

PLATE

WASH

WASH

ACTIVATOR

WASH

SENSITIZER

UNWIND
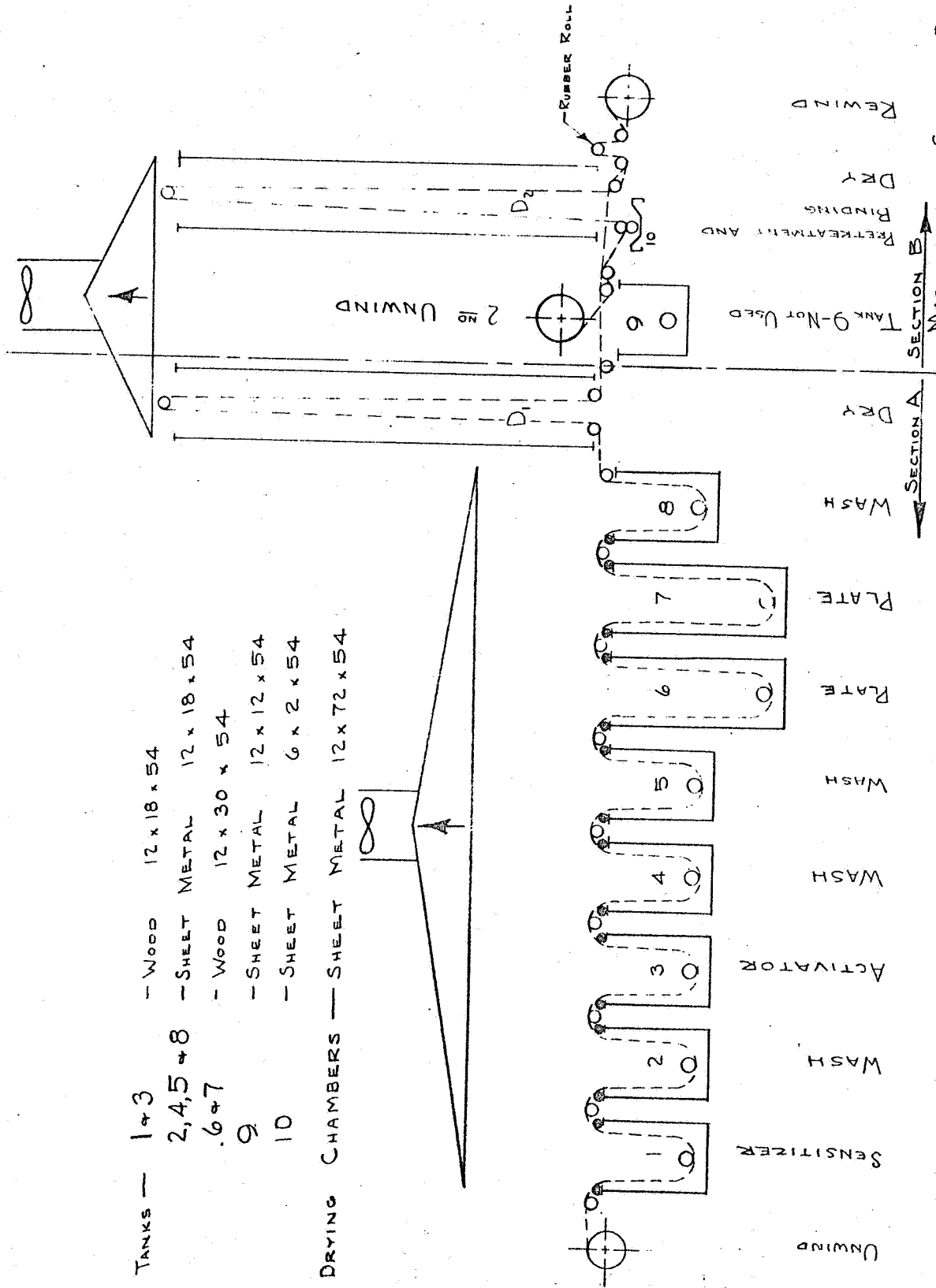
MACHINE FOR COPPER PLATING
SELF ERECTING MATERIAL
24456-12   2-2-67

Figure 10

29

Section A is used for electroless copper plating. It consists of eight tanks and a drying tower. The tanks are filled with the solutions indicated on figure 10. All tanks have air agitation except 5 and 8. The material is processed through all of the tanks as indicated and then through drying tower No. 1. It is then run directly to the rewind station and re- wound. All of the top rolls up to tank 8 are driven. The rolls in the bottom of the tanks (1-5 and 8) are 3-inch-diameter PVC, are not driven, and turn in PVC brackets suspended from the top of each tank. The rollers in tanks 6 and 7 are 1-1/4-inch diameter pllyethylene, mounted on brackets from the top of the tanks. In drying tower No. 1 room temperature air dries the web after plating. The material is not silicone-rubber-coated but stored in a plastic bag with a desiccant.

The equipment has the following operating features:

1. Web width: 48 inches maximum
2. Web speed: 1.0 ft/min. (6 in/min optional)
3. Amount of material required to thread machine: 55 ft
4. Residence times:
      Sensitizer solution   1.7 min
      Activator solution   1.7 min
      Plating solution   10 min
      Drying tower   10 min
5. Process control temperatures:
      Sensitizer and activator   18 to 22 C
      Plating   20 to 22 C
      Rinse tanks   40 to 50 C
      Drying towers   No. 1 -   18 to 22 C
                         No. 2   60 to 70 C
6. Operating facilities requirements:
      Air pressure   70 psi
      Water   deionized
      Gas   for water heater
      Electrical   110 V. 60 Hz
      Exhaust fans   explosion proof

Normal operating speed is 1.0 ft/min although a number of runs were made at 6 in/min. The slower speed allows the use of only half the normal amount of chemicals and is more economical for shorter runs.

Section B of the machine is used for applying the pretreatment and/or binder to the material. The second unwind is used along with the coating tank (10) and drying tower 2. The machine is webbed as shown in figure 10. Tank 9 is not used in any of the operations. The transfer coat- ing rolls and the rubber roll are driven, all others are free turning alumi- num rollers. Drying tower 2 uses banks of infrared lamps for dying and curing the coatings. A temperature of 60 to 70 C is maintained.

5.3.4 Aluminum Plating

Vacuum-deposited aluminum was investigated as means of pro- viding conductance, but was not pursued beyond the preparation of two

4- by 6-foot panels for evaluation by GSFC. The equipment is limited to coating 5- by 11-foot pieces, and there is a tendency to shadow at fiber bundle intersections. These two limitations precluded any further development work.

6.0 PRODUCTION RUNS

Each material produced during the program was consecutively numbered.
The processing of this material involves five operations: fabric procure-
ment, pretreatment, binding, metal deposition, and sheath coating. The
process steps are defined below.

1. Fabric Procurement – This is simply an identification of the
base fabric, e.g. Hess, Goldsmith I8601

2. Pretreatment – Any process that a fabric is subjected to,
such as heat treating or sizing is des-
cribed in this subheading.

3. Binder – This process is analogous to the sizing
process described above; however, for our
purposes it is advantageous to split it off
as separate item. This will allow us to
consider materials whose primary purpose is
to tie or bind the threads together to in-
crease the integrity of the fabric.

4. Metal Deposition – This describes the process that is used to
deposit a metallic coating on the self-
erecting material.

5. Sheath Coating – This process step protects the metal
deposit and, as it is the final coating on
the material, it becomes a major factor in
the ultimate surface properties.

The process steps number was added with a dash to the run number to
indicate the number of processes applied to the base fabric. Thus, 134-4
would indicate fabric No. 134 processed through metal deposition.

This numbering system was first used for the material processed in
August. Arbitrarily, the first run was numbered 129. Sample data sheets
appear in the Appendix.

6.1 NOTES ON PRODUCTION RUNS

The properties of the various runs are summarized in table 11. Ad-
ditional data appear below.

Run No. 129

This material used as its base Hess Goldsmith style 8539 and it is the
first material processed on our pilot plant equipment on a continuous roll-
to-roll plating basis. The material had many shortcomings in that the re-
sistance varied from 2 ohms per square to essentially infinite. A large

portion of this material was unacceptable for further fabrication that had been intended. A number of 4- by 6-foot panels were fabricated and also two 30-inch-diameter spheres.

Run No. 130

This material also had Hess Goldsmith I8539 material as its base. The operation of the continuous plating machine was fairly acceptable during this run and material was produced with an average resistance of 1 ohm per square. This material was later fabricated into two large spherical segments.

Run No. 131

This material used Hess Goldsmith style 8601 which is a heavier fabric than 8539. The plating again proved satisfactory and the average resistance was 0.7 ohms per square.

Run No. 132

This run was the first to substitute a water solution of Silane A1100 for heat treating. The rigidity of this material was very high. A number of samples were made from it, and it was also used in basic development work in the search for a protective coating for the self-erecting material.

Run No. 133

This run used the same base fabric as run 132 only it was heat treated for 30 minutes at 550 F. As can be seen from the summary sheet, most of the properties were decreased in comparison to run 132 and run 134. This material was also used in the fabrication of a number of panels and was used in the study of increased resistance after exposure to adverse conditions.

Run No. 134

This material, the same base as No. 132 and No. 133, was neither sized nor heat treated. The significant thing about it was that is showed that a GT-201 coating could produce a satisfactory material without pretreatment.

Run No. 135

This material used as a base J.P. Stevens fabric 1655 which has approximately the same weight as Hess Goldsmith I8601, but has five threads per inch in each direction instead of the normal ten. This material was not plated but merely coated with GT-201. The rigidity in the machine direction was extremely high, almost seven times more than had ever been experienced before. This material was used to construct a number of spheres to evaluate the self-erecting properties, and showed that asymmetric material has improved self-erecting properties.

Run No. 136

This material represented the first of a series of runs that were made on two new fabrics felt to offer improved self-erection. This unbalanced fabric had transverse direction fibers much heavier than machine direction fibers. Fabric description was Hess, Goldsmith I8683-150. The fabric weight is approximately twice that of Hess, Goldsmith I8601 and it was used in the sphere tested during the third test at Goddard.

Run No. 137

This material was balanced and had a PVC size applied by the weaver on the loom. It had much better physical properties than any of the similarly prepared fabrics in the past. This material was also used in the Goddard dynamic test chamber.

Run No. 138

When this material was ordered it was felt that a GT-201 coating would be superfluous as the size applied by the weaver was to be water insoluble. The results of attempts to plate this material without previous coating with GT-201 is shown in this run. As can be seen, the rigidity in all directions is not equal to that of run No. 137. After further checking, the weaver revealed that the PVC size coating was not properly cured on the loom, and therefore could not be plated before a GT-201 coating was applied.

Run No. 139

This particular run was to be used in the fabrication of a spherical segment similar to those that had been built in January of 1965. Table 12 compares rolls 1 and 2 to show the reproducibility of the production runs. As can be seen the rigidity in the transverse direction is almost identical but the machine direction is approximately 33 per cent difference. This appears to be the limit of reproducibility.

Run No. 140

This production run is similar to production run No. 130 except that it was not heat treated nor protected by silicone rubber sheath layer. Comparison of the radio frequency reflective data of end caps of this material and material shipped in January 1966 should reveal the effect of a silicone sheath coating.

Run No. 141

This material was run to make up enough material so that the end caps could be completed and shipped before the due date.

Run No. 142

This was a duplication of run No. 136. It has more rigidity in the machine and 45 degree angle directions, probably due to a heavier coating of GT-201.

Run No. 143

   This was a duplication of run No. 141 and had approximately equal
properties to this material. This run was also used to fabricate an end cap
section which was shipped to NASA Goddard.

Run No. 144

   This was a duplication of run No. 142 and shows the reliability of the
production facilities. This material was used in a number of tests which
are described elsewhere in this report.

TABLE 11

Material Inventory Summary Sheet

Run No.	Date	Fabric Description	Finished Weight mg/cm²	Resistance Ω/□	Rigidity mg/cm			Tensile Strength lb/in			Bend Radius Tensile Strength lb/in			Processing Steps
129	12/4/65	H.G.I-8539	1.0	2-∞	MD 178.2	TD 23.4	45° 59.2	MD 13.7	TD --	45° 0.3	MD 4.2	TD --	45° 0.7	Heat-treated, GT-201, Electroless copp silicone coated
130	2/4/66	H.G.I-8539	1.3	1.0	MD 172.0	TD 30.0	45° 22.0	MD 10.9	TD 2.5	45° 0.5	MD 2.9	TD 1.5	45° 1.0	Heat-treated, GT-201, Electroless copp silicone coated
131	5/13/66	H.G.I-8601	2.78	0.7	MD 859	TD --	45° --	MD 27.6	TD 19.8	45° 0.68	MD --	TD --	45° --	Heat-treated, GT-201 Electroless copp silicone coated
132	8/30/66	H.G.I-8601	2.1	3.7	MD 916.38	TD 592.20	45° 175.18	MD 26.6	TD 25.8	45° 0.95	MD --	TD --	45°P --	Silane A-1100 GT-201 Electroless copp

Material Inventory Summary Sheet (cont.)

Run No.	Date	Fabric Description	Finished Weight mg/cm²	Resistance Ω/□	Rigidity mg-cm	Tensile Strength lb/in	Bend Radius Tensile Strength lb/in	Processing Steps
133	8/30/66	H.G.I-8601	2.25	2.2	MD 646.9 TD 450.4 45° 152.3	MD 23.5 TD 16.8 45° 0.65		Heat-treated, GT-201, Electroless copper
134	8/30/66	H.G.I-8601	2.11	0.63	MD 848.0 TD 595.6 45° 229.0	MD 28.9 TD 25.4 45° 1.2		GT-201 Electroless copper
135	10/20/66	1655	2.39	--	MD 6,145.5 TD 798.8 45° 933.5	MD 26.8 TD 6.4 45° 1.1		GT-201
136	12/15/66	H.G.8683-150	4.56	0.14	MD 779.5 TD 5,586.0 45° 678.8	MD 26.6 TD 105.2 45° 3.7		GT-201 Electroless copper
137	12/15/66	H.G.8683-450	2.29	1.6	MD 946.8 TD 628.9 45° 350.6	MD 26.6 TD 40.8 45° 1.9		GT-201 Electroless copper

Material Inventory Summary Sheet (cont.)

Run No.	Date	Fabric Description	Finished Weight mg/cm²	Resistance Ω/□	Rigidity mg-cm	Tensile Strength lb/in	Bend Radius Tensile Strength lb/in	Processing Steps
138	12/15/66	H.G 8683-450	2.15	--	MD 593.2 TD 249.8 45° 190.7	MD 32.4 TD 32.8 45° 0.6	MD -- TD -- 45° --	Electroless copp
139 Roll I	1/9/67	H.G. 8683-450	2.36	5	MD 967.9 TD 601.5 45° 351.4	MD 23.1 TD 31.3 45° 3.5	MD 6.7 TD 9.1 45° 5.1	GT-201 Electroless copp
139 Roll II	1/9/67	H.G. 8683-450	2.36	8.3	MD 1,208.3 TD 604.2 45° 392.7	MD 28.4 TD 38.2 45° 5.5	MD 6.9 TD 12.2 45° 5.4	GT-201 Electroless copp
140	1/18/67	H.G. 8539	1.02	1.2	MD 255.1 TD 146.9 45° 52.5	MD 13.6 TD 5.9 45° 0.9	MD 1.4 TD 0.8 45° 1.0	GT-201 Electroless copp

38

Material Inventory Summary Sheet (conc.)

Run No.	Date	Fabric Description	Finished Weight mg/cm²	Resistance Ω/□	Rigidity mg-cm	Tensile Strength lb/in	Bend Radius Tensile Strength lb/in	Processing Steps
141	1/18/67	H.G. 8683-450	2.51	.4	MD 1,017.1 TD 667.2 45° 413.0	MD 25.4 TD 39.1 45° 5.4	MD 7.6 TD 9.4 45° 10.2	GT-201 Electroless copper
142	1/18/67	H.G. 8683-150	4.91	2.1	MD 1,275.0 TD 5,603.0 45° 1,293.2	MD 27.0 TD 124.8 45° 8.5	MD 4.5 TD 26.5 45° 9.6	GT-201 Electroless copper
143	1/13/67	H.G. 8683-450	2.58	4	MD 1,146.1 TD 715.1 45° 455.5	MD 24.5 TD 38.0 45° 4.7	MD 6.1 TD 10.3 45° 6.6	GT-201 Electroless copper
144	1/19/67	H.G. 8683-150	4.48	4	MD 948.4 TD 4,838.7 45° 1,136.3	MD 25.1 TD 119.6 45 4.7	MD 4.8 TD 13.0 45° 9.1	GT-201 Electroless copper

7.0 MATERIAL TESTING

A copy of G. T. Schjeldahl Company Specification Q 132 is appended to show the testing techniques used in this contract. All of the tests described except the "folded rigidity" were conducted on the materials produced. The results appear elsewhere in the report. This section describes the testing involved.

7.1 TENSILE TEST

The tensile strength is tested in an Instron testing machine by loading a 1-inch-wide sample in tension. The load is applied at a constant jaw separation rate of 2 inches/minute. The transverse and machine direction samples were cut so that the yarn bundles ran the entire sample length. As the fabric has 10 threads per inch the samples were cut 10 threads wide. The samples cut at 45 degrees to thread direction were also 1-inch wide. Five samples were tested in each direction, and the average ultimate tensile strength computed.

7.2 BEND RADIUS TEST

The Instron testing machine was also used for this test with the fixture shown in Section 7.1 in Q 132. The sample was forcibly bent over a 0.008 radius and then loaded to failure at the crease.

7.3 RIGIDITY TEST

The fixture shown in figure 11 was used to measure the flexural rigidity of the material. This method is defined in ASTM D1388, and is an extension of the heavy elastic theory described by Bickley[1]. The material is positioned on the fixture as a cantilever, and its length is extended until the tip is deflected to touch a fixed angle of 41.5 degrees. At this deflection the length of overhang is twice the bending length. The bending length is then used to calculate the rigidity using the equation

$$G = Wc^3$$

where

G = flexural rigidity (mg-cm)
W = weight/unit area (mg/cm^2)
c = bending length (cm)

This property is very important in the calculation of buckling of thin shells.

---

1. Bickley, W. G. The Heavy Elastica , Phil. Mag. Vol. 17, No. 113, March 1934.
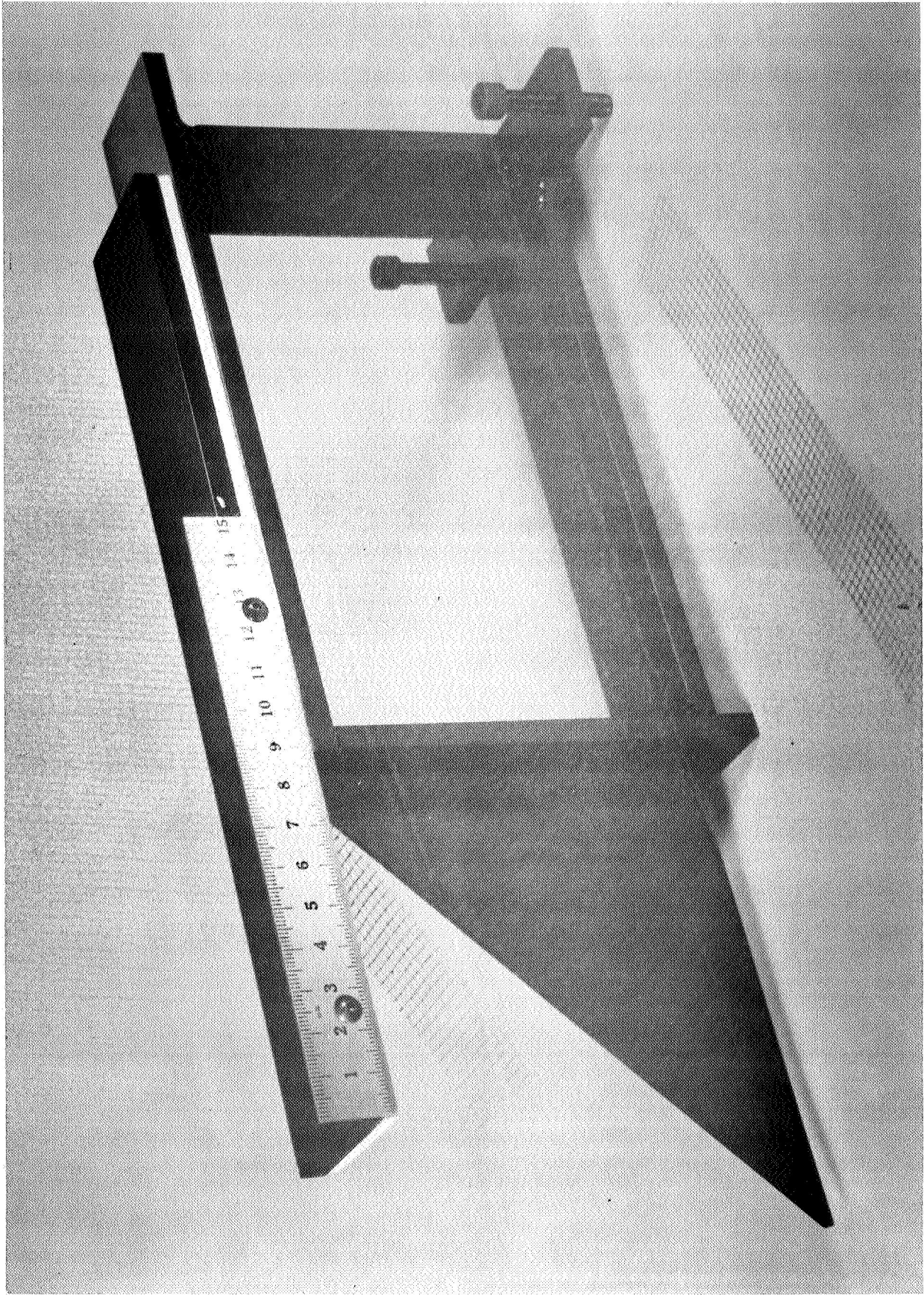
Figure 11   Fixture for Measuring Flexural Rigidity

7.4 FLEXING ENDURANCE

As this material will be used in large space structures that will be folded and packed in a canister, it is necessary to determine the fold resistance of the material. Fold resistance has no discrete units and there are several methods of evaluating it.

One of these is the bend radius tensile strength presently used to evaluate this material. This test determines the strength of a material as it is folded on 1/128-inch radius bend. This is described in more detail in G. T. Schjeldahl Company Q 132.

Another is the folded rigidity test (Sec. 9 of Q 132) which attempts to measure the stiffness remaining after the material has been creased 180 degrees while under a static load.

During this contract two tests concerned with cyclic flexing were used. Both techniques involve flexing a sample 180 degrees around a known radius bend, and then folding it back on itself around a similar radius bend. These tests flex a loaded sample cyclically until failure occurs. The number of cycles-to-failure is recorded as a property of the material.

7.4.1 NASA Flex Tester

NASA designed and supplied a testing machine which, besides flexing the sample, has provision for measuring resistivity. The results of this testing are shown in Table 12.

Figure 12A shows this machine and figure 12B shows an enlarged view of the fiber bundles after failure. Figure 13 shows the mechanism used to rotate the fixture.

Table 12 presents the increase in resistance as a function of flex cycles. Three points are selected to show this, 0 cycles, 100 cycles, and 800 cycles.

TABLE 12
Resistance $\Omega/\square$

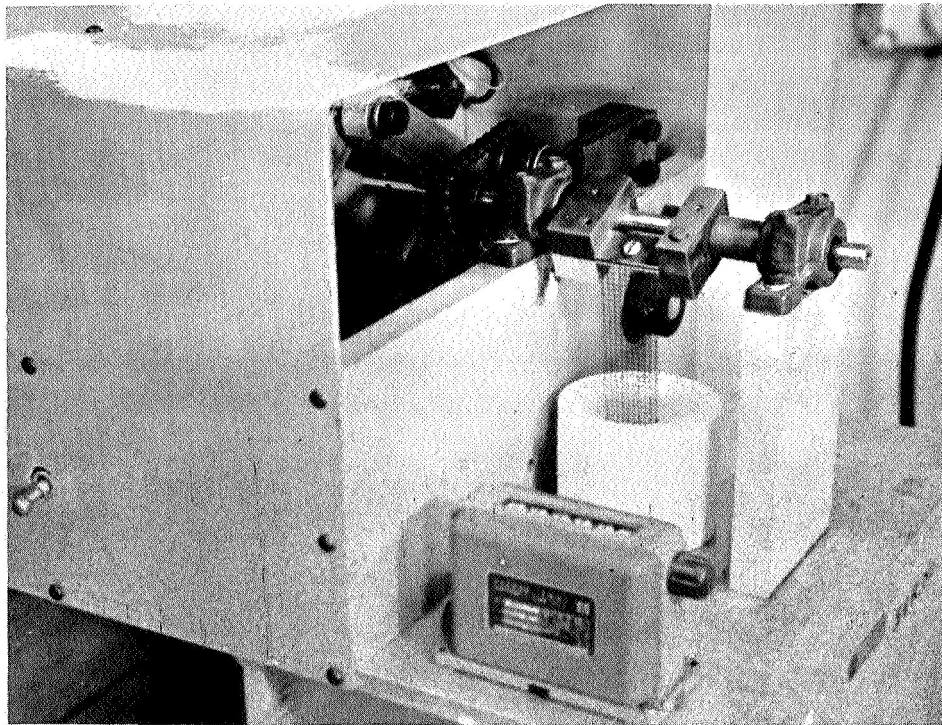|		0 Cycles	100	800
134.4	MD	5	12	175
	TD	5	135	240
133-4	MD	5	140	∞
	TD	5	25	115
132-4	MD	5	180	880
	TD	∞	--	--
131	MD	1	1.75	35
	TD	1.25	1.75	55

42

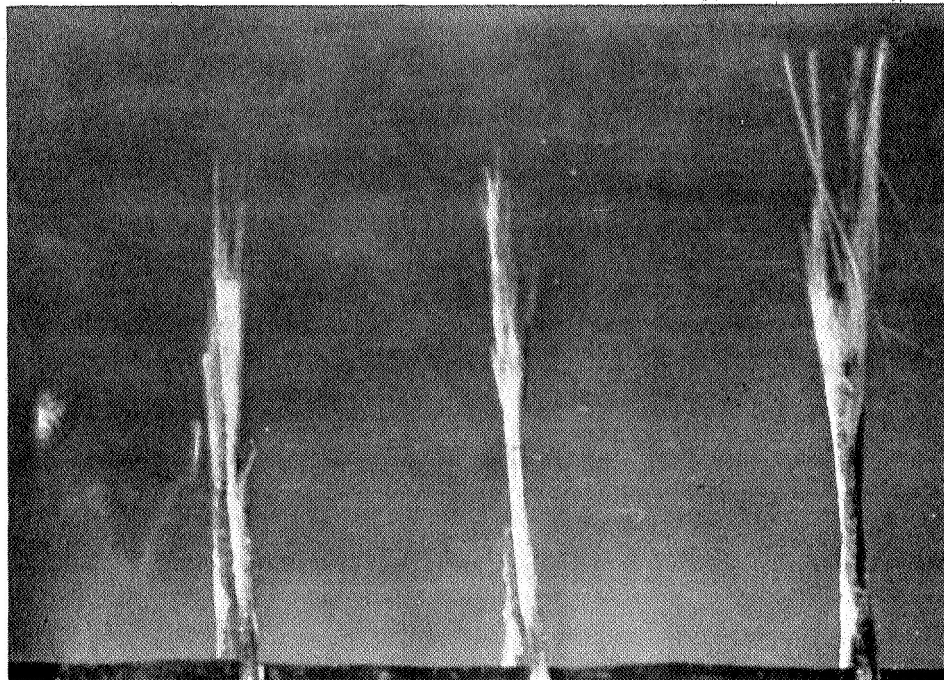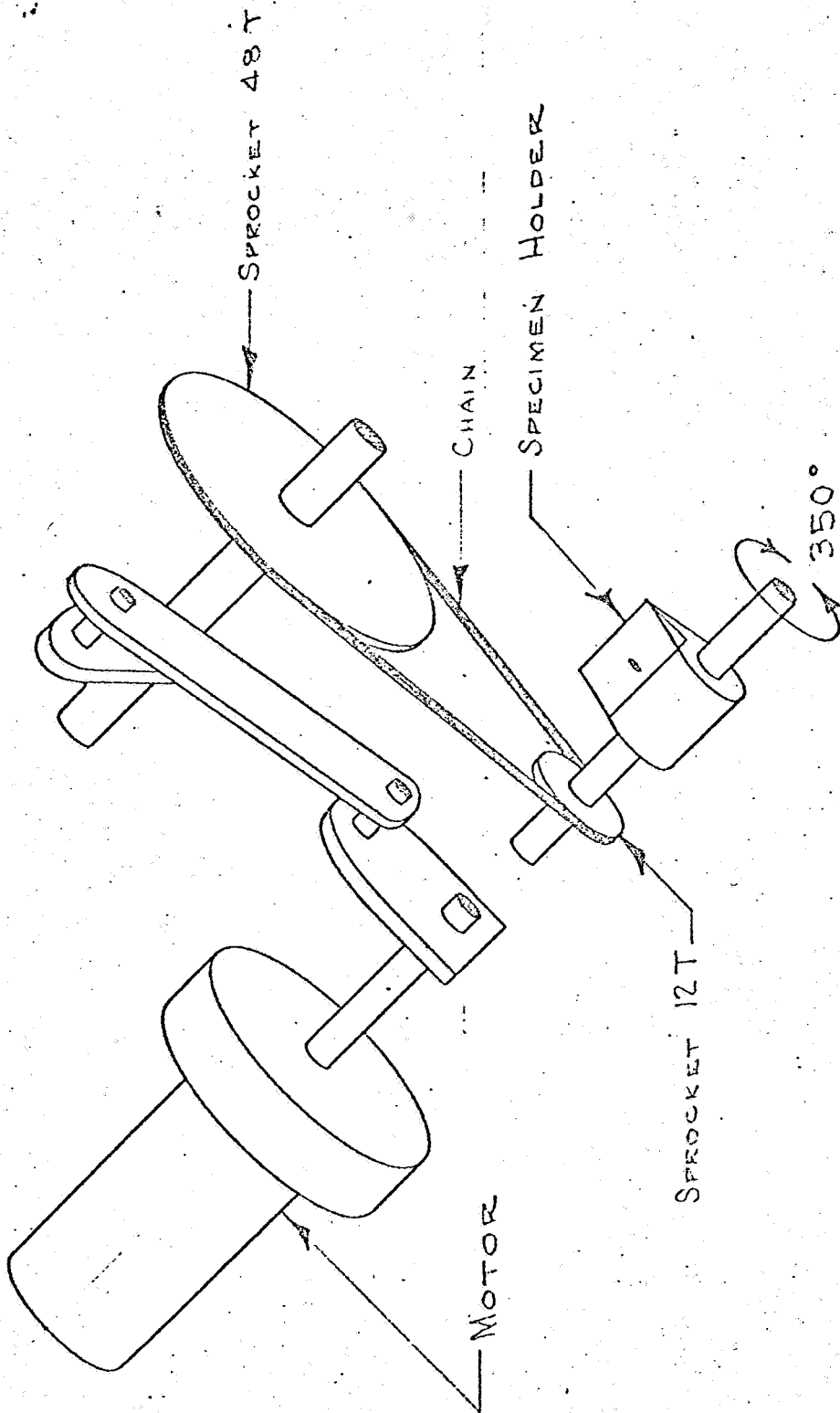Figure 12A   NASA Cyclic Flexing Test Equipment

Figure 12B   Self-Erecting Material at Failure Point
(X 150)

MESH - FLEX TESTER,
MODIFICATION   6-29-66
24456-13

Figure 13

44

7.4.2 Schopper Tester

The Schopper fold tester, as described in ASTM method D 643-63T, folds a material sample over a mandrel under tension. It was felt that this method would reveal flex resistance more suitably and quickly than equipment supplied by NASA. Samples of runs 132, 133, and 134 were tested in both the machine and transverse direction. (Measuring the flexing resistance of samples cut at a 45 degree angle was attempted, but no data are reported as the samples were too weak to test.) Ten samples of each type were tested initially, but because of the large variation, more were tested. Ultimately as many as 57 samples were tested. Table 13 lists the average flex life with the variance. Figure 14 presents histograms relating population of events at specific failure points.

A computer program, using Student's "T" distribution to check for significant differences, was used to compare the means. Using a 90 per cent confidence level, the following conclusions were drawn.

1. 132-4 MD less than 133-4 MD
2. 133-4 MD less than 134-4 MD
3. 132-4 MD less than 134-4 MD
4. 132-4 TD greater than 133-4 TD
5. 133-4 less than 134-4 TD
6. 132-4 TD greater than 134-4 TD

TABLE 13

Number of Folds to Failure on Schopper Test

Sample	Direction	Lot Size	Mean	Standard Dev.
132-4	MD	52	5.85	2.90
	TD	51	15.90	14.43
133-4	MD	55	8.36	4.32
	TD	42	5.19	5.25
134-4	MD	55	16.24	7.87
	TD	56	11.16	10.75
All	MD	162	10.23	6.85
All	TD	149	11.10	11.78

Following the above comparisons, the means of the samples in both directions were related. The following conclusions were made.

7. 132-4 less than 134-4
8. 132-4 greater than 133-4
9. 133-4 less than 134-4

Pairing number 1 was run again, this time using a 99 per cent confidence level. The conclusion did not change.
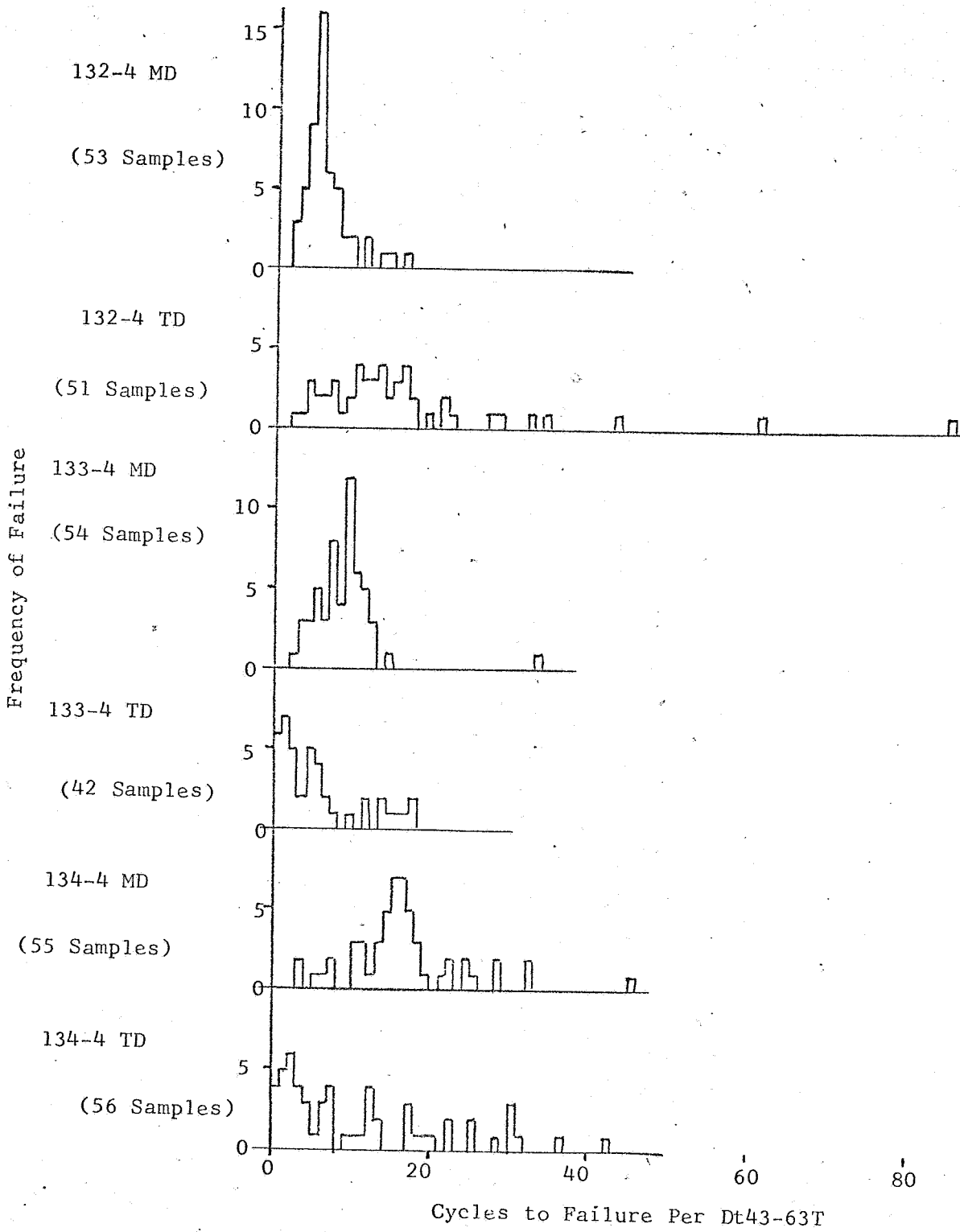
Figure 14   Histograms of Schopper Test Results

10. 132-4 MD less than 133-4 MD

When all the machine direction samples were compared to all the transverse direction samples, at a 90 per cent confidence level the conclusion was as follows.

11. Machine direction equal to transverse direction.

7.5 RESISTANCE CHANGE WHILE SAMPLE IS STRESSED TO FAILURE

To determine the continuity of self-erecting material during elongation to failure, it was necessary to monitor resistance of a sample continuously while under tension. A recording ohmmeter was not available for this purpose, so a Brown recorder was used to measure the voltage drop across the sample while it was in the jaws of an Instron testing machine. The current flowing through the sample was held constant by a 95,000 ohm resistor connected in series with the mesh sample so the potential would be proportional to the resistance. The sample of self-erecting material was placed in insulated jaws of an Instron testing machine and then connected as part of a circuit. Resistance was plotted as a function of time. The stress on the sample was monitored on the Instron in respect to time. Because there is a constant jaw separation rate, time is proportional to strain (or elongation). Combining these two charts produces a relationship between resistance and strain as shown in figure 15. It was originally intended to plot resistance as a function of stress; however, the material reaches its ultimate strength long before there is any change in resistance. The resistance began to increase rapidly at 100 to 150 per cent elongation, which is far beyond the material's ultimate elongation of 3 to 5 per cent, because only one or two threads are broken at the yield point, and the electrical continuity is maintained by unbroken cross threads.

Testing of this nature was discontinued as it appeared to have very little significance for evaluating self-erecting material.

7.6 EFFECT OF TEMPERATURE EXTREMES ON THE TENSILE STRENGTH AND RIGIDITY

During the development stage, the tests performed on these materials were limited to ambient temperatures. As the materials reached a plateau in their development, it became important to trace the effect of temperature.

7.6.1 Rigidity

To test the flexural rigidity at temperatures other than ambient, the technique was changed from that described in section 7.3. A fixed cantilever method was used for these tests because of inability to use the equipment pictured in figure 11. Samples were placed in a controlled temperature chamber in a fixture as shown in figure 16. A one-inch-wide sample was placed on blocks B and C and then A was placed on top of B and the samples.
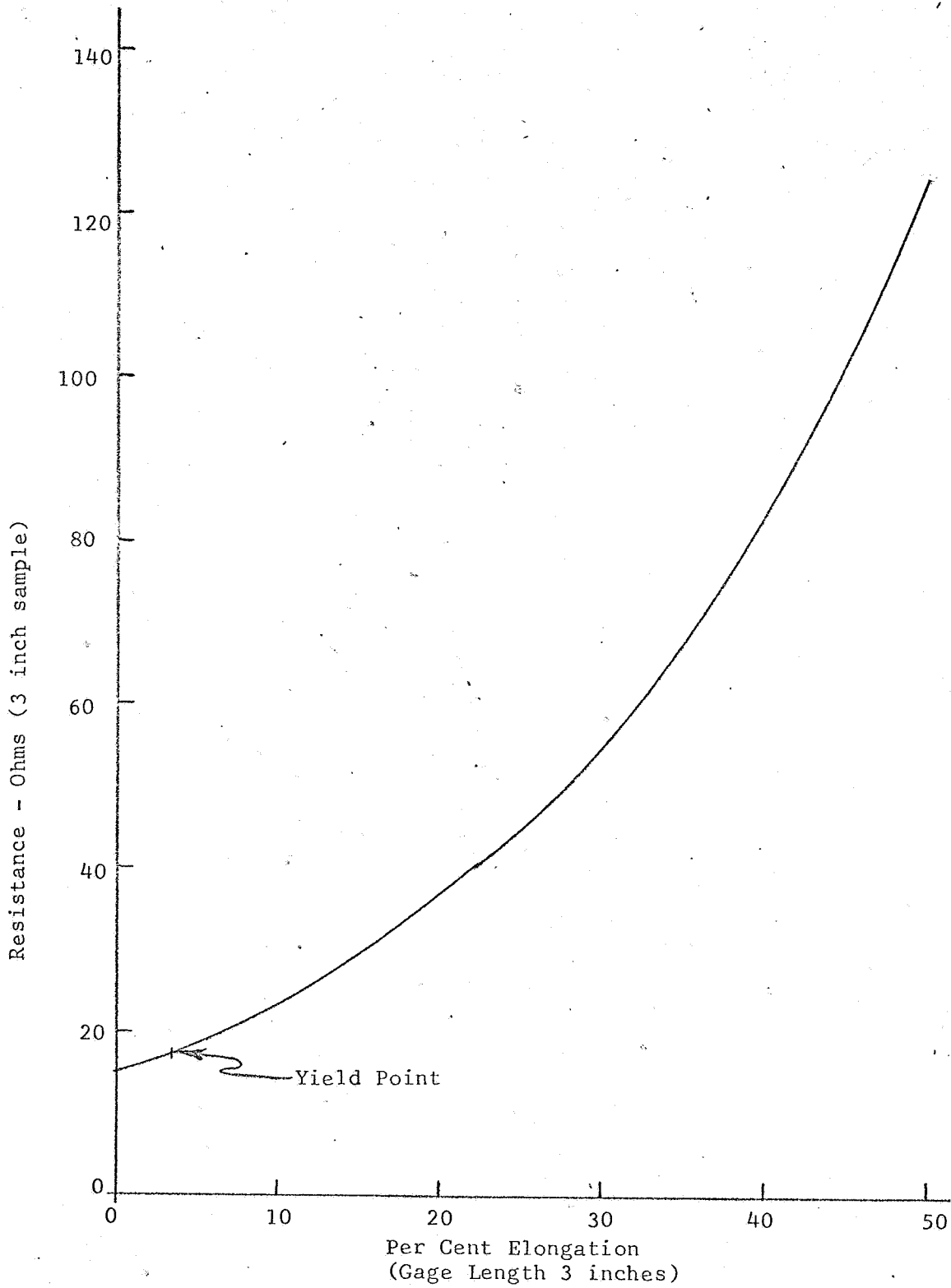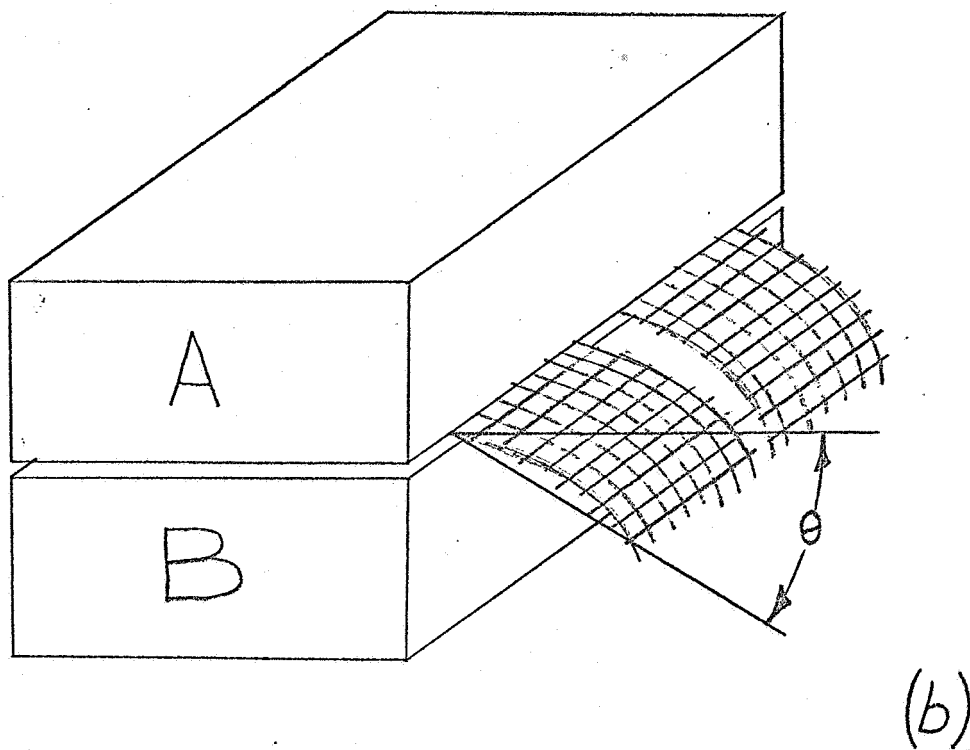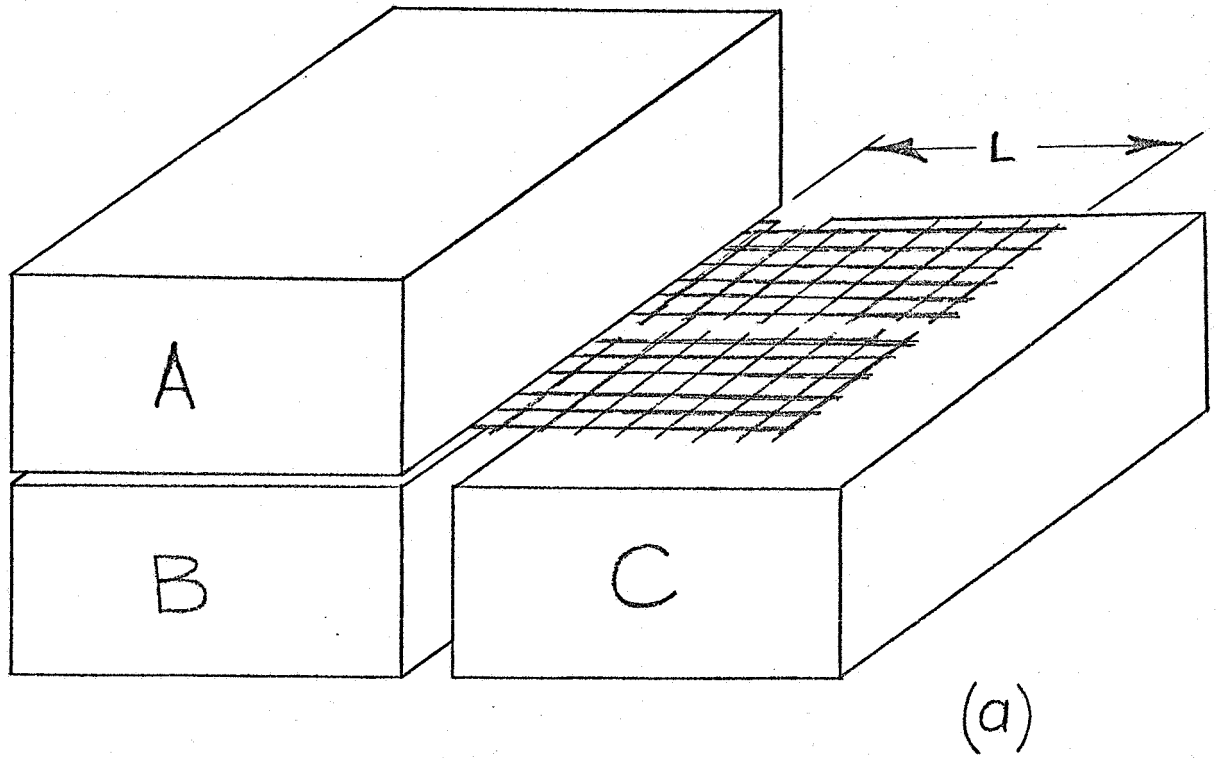
Figure 15 Effect on Resistance due to Elongation

48

Figure 16   Procedure Used to Determine
              Flexural Rigidity at Non-
              ambient Temperatures

After a conditioning period block C was removed allowing the sample to deflect under its own weight. The samples were positioned so that ℓ was known. The angle of deflection, θ, is then measured. From figure 17, which shows the relationship of ℓ to c as a function of θ, the bending length can be calculated, using the formula

$$G = Wc^3,$$

where G and W have the same meanings as in 7.3.

The results of this testing are shown in figure 18. As can be seen the rigidity is not affected by either temperature condition.

7.6.2 Tensile Strength at -70 and 212 F

Three materials were taken as representative of the developments during this contract. These were No. 140, 143, and 144. Table 14 lists the tensile strength at -70 and 212 F

TABLE 14

Tensile Strength at -70 and 212 F
(lbs/in)

		-70 F	212 F
140	MD	8.4	7.0
	TD	2.0	1.5
143	MD	10.5	14.0
	TD	17.0	29.0
144	MD	23.0	19.5
	TD*	86.0	69.5

143 and 144 material was exposed to vacuum for 48 hours. Table 15 shows that the tensile strength is little affected by vacuum conditions.

---

* 144 TD slipped in the jaws and the values shown here are low.

The relationship between the deflection angle θ and the ratio of c/ℓ for a cantilever, where c is the bending length and ℓ is the length of overhang.

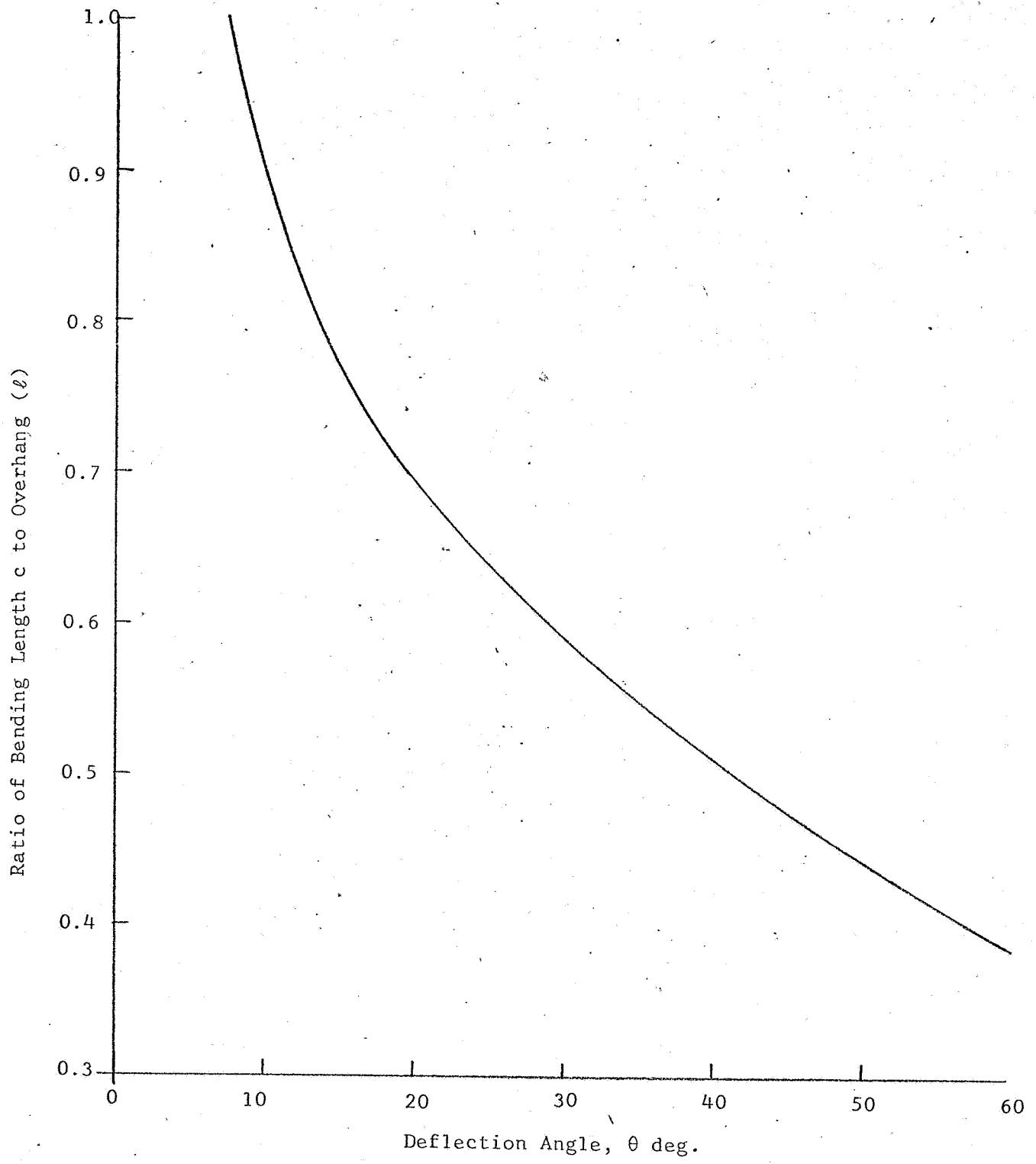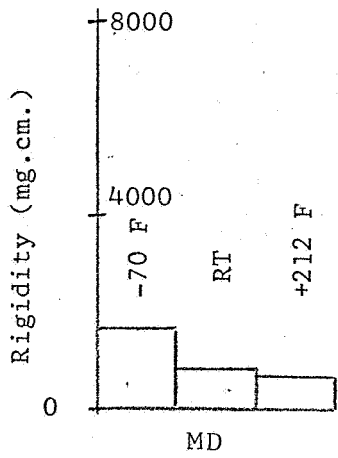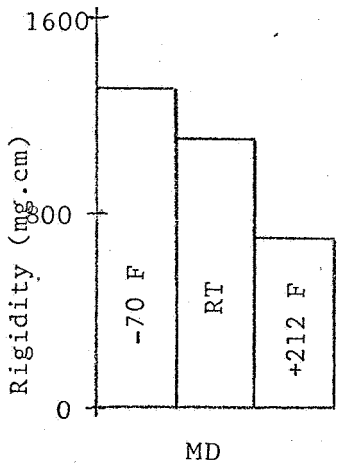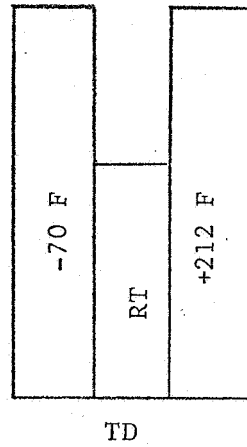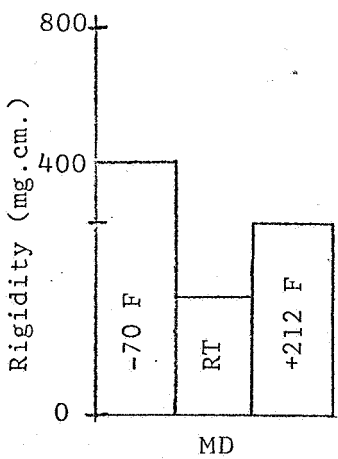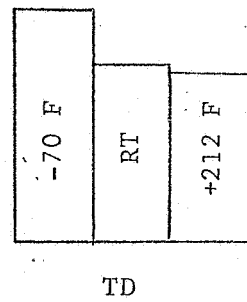Figure 17 Ratio of Deflection Angle to c/ℓ
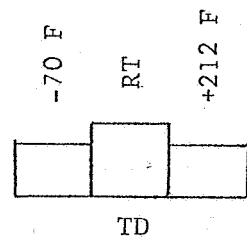
Figure 18   Effect of -70 F and +212 F
on Rigidity

TABLE 15

Tensile Strength in Vacuum

(lbs/in)

		-70 F	212 F
143	MD	25.5	25
	TD	45.5	28
144	MD	24.0	23
	TD*	98.5	72

7.7 REFLECTIVITY

A sample of self-erecting material was evaluated for radio frequency reflectance with a coaxial transmission line device for measuring the reflection coefficient. This equipment is located in the St. Olaf College physics laboratory.

It was found that this particular apparatus requires an electrical contact to the mesh. Because of this, no reflectivity measurements could be made on mesh-coated silicone rubber. The equipment was also limited by its lack of output above 2 GHz. Figure 19 shows this curve. As can be seen, the RF reflectivity is 90-96 per cent of the standard copper sheet.

7.8 EXPOSURE TO ULTRAVIOLET RADIATION

This material is to be used in an environment where it will be exposed to large amounts of ultraviolet radiation; therefore, it is important that the effect of uv radiation be measured. A number of tests were run to determine the changes in tensile strength, weight per unit area, rigidity, and conductance after exposure to uv radiation.

The uv radiation source was a General Electric UA-2 lamp; Figure 20 shows its radiation curve. The tests were conducted in a vacuum chamber where a pressure of 10^{-5} torr is maintained. A quartz plate window has nearly 100 per cent transmission in the ultraviolet portion of the spectrum. Samples are approximately 14 inches from the source which is outside the vacuum chamber. Control samples were also placed in the vacuum chamber but shielded from the ultraviolet radiation. The temperature of the samples in the vacuum chamber was maintained at approximately 70 F.

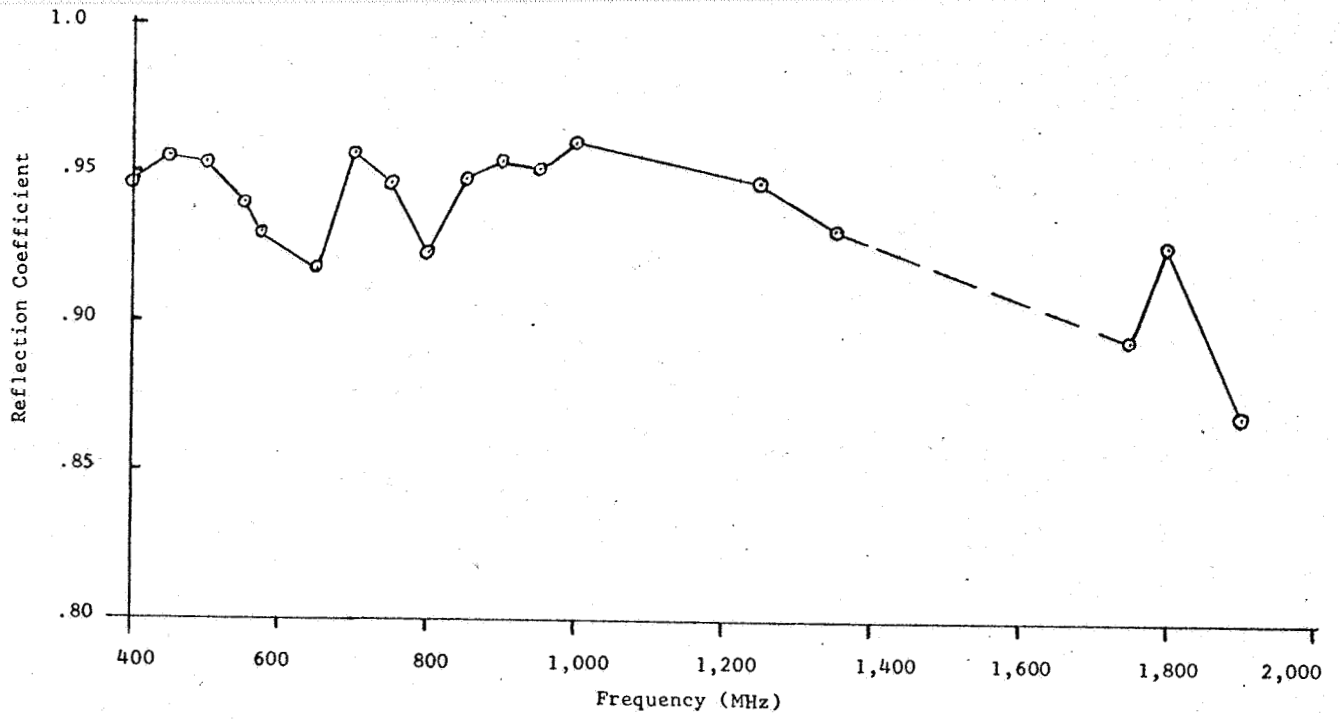*144 TD slipped in the jaws and the values shown here are low.

Figure 19   Reflection Coefficient versus Frequency
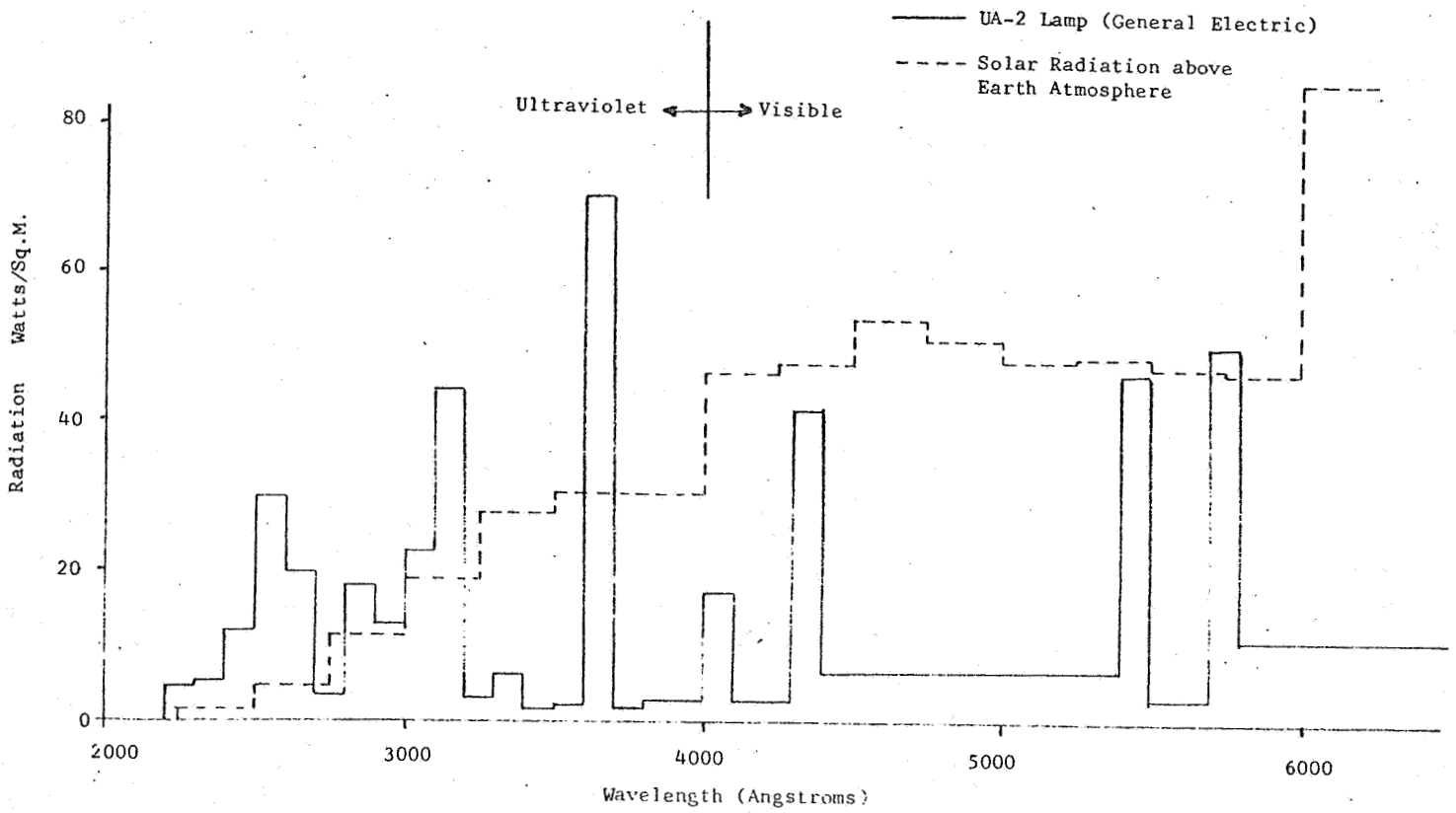For Sample No. 216-85-1

Figure 20   Radiant Energy vs Wavelength

Because of the limited space in the vacuum chamber, only 10 samples could be exposed to ultraviolet radiation at any given time. The samples were placed in the vacuum chamber at different times to provide data on degradation due to radiation exposure for three intervals, namely: ten days, thirty-five days, and forty-five days. The samples shielded from the UV source were measured and thus the effects of vacuum was determined.

Figure 21 shows the increase in resistance of radiated and shielded samples over 45 days. It shows that the resistance of samples exposed to radiation increased much more quickly than that of the shielded samples. After 45 days the increase was the same for both.

As can be seen in figure 22, there were no significant changes in tensile strength, bend radius tensile strength, or rigidity.

The weight loss of the samples was about 0.5 per cent.

7.9 BLOCKING

To determine the effects of vacuum bagging and the possibility of blocking by this material during storage, a one-inch wide strip, 12 inches long of 131 material and 143 material were accordion folded and placed under a static load of 14 psi in a vacuum. The samples were loaded in this way for 48 hours. The samples were to be pulled in tension to determine the amount of blocking between adjacent layers of material. Upon taking them out of the vacuum chamber and releasing the load, both materials sprung completely out as there was no blocking between adjacent surfaces. The materials chosen for this test were No. 131, which had been coated with General Electric SS4090 silicone rubber, and No. 143, which had no protective coating applied to it. It was concluded that neither of these materials had any tendency to block under the conditions described.

7.10 PERPENDICULAR TRIPLE FOLD

Test samples 4- by 12-inches were folded into a perpendicular triple fold, then placed in the Instron jaws and pulled at the rate of 20 in/min causing material to unfold while passing over itself. The samples were then inspected to determine thread breakage. Two different materials were tested under the same conditions in the machine and transverse directions. Results are shown in Table 16.

RIGIDITY

45 Days
35 Days
10 Days
Initial

No Ultraviolet

45 Days
35 Days
10 Days
Initial

Ultraviolet

Rigidity (mg-cm)
800
400

TENSILE

45 Days
35 Days
10 Days
Initial

No Ultraviolet

45 Days
35 Days
10 Days
Initial

Ultraviolet

Strength (lbs)
20
10
0

TENSILE

45 Days
35 Days
Initial

No Ultraviolet

RADIUS

BEND

45 Days
35 Days
Initial

Ultraviolet

Strength (lbs)
10
0
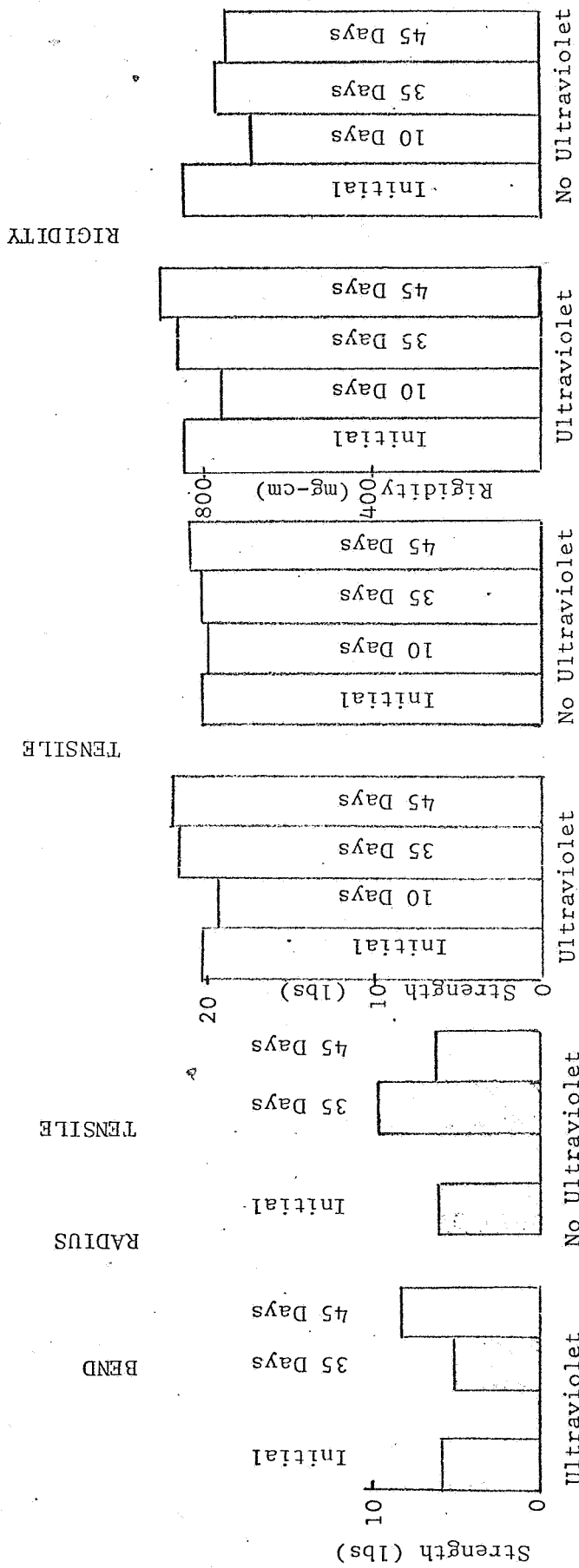
Figure 22   Effect of UV Radiation and Vacuum on
Self-Erecting Material Properties

No Ultraviolet

Ultraviolet
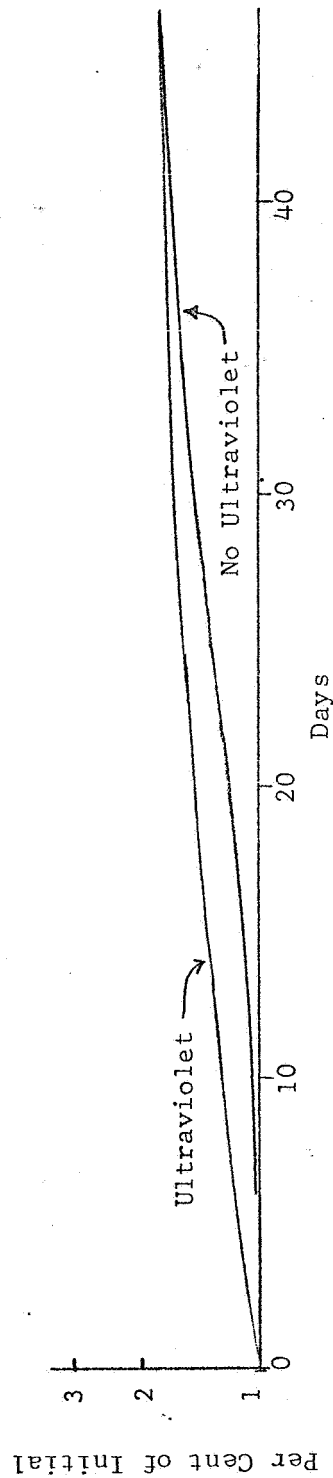
Days
10   20   30   40   0

Per Cent of Initial
3
2
1

Figure 21   Effect of UV Radiation on
Conductivity

TABLE 16

Thread Breakage After Folding

143-4	MD	Sample 1	2 threads broke
		Sample 2	no threads broke
	TD	Sample 1	no threads broke
		Sample 2	1 thread broke
105-113-1	MD	Sample 1	7 threads broke
		Sample 2	15 threads broke
	TD	Sample 1	6 threads broke
		Sample 2	8 threads broke

Unlike inflating balloons, spheres made of self-erecting material extend in the pole to pole dimension first; then expansion occurs at the equator. Because of this erection mechanism, the triple fold test is not applicable.

7.11 CORROSION

A number of protective coatings were evaluated. Figure 23B shows one of four test chambers built to evaluate various protective coatings and the effect of various atmospheres on self-erecting material. The following coatings were evaluated:

Enthone	Entek 45
	Entek 56 (coating time 45 seconds)
	Entek 56 (coating time 60 seconds)
Iridite	7P
Kenvert	18
Kenvert	31
Kenvert	32
Silicone	SS-4090 (General Electric)
	Silane A 1100 (Union Carbide)

Enthone Entek 45, Iridite 7P, Kenvert 18, and Kenvert 31 were used only for initial test samples, as all removed most of the copper sheath resulting in a substantial increase in resistance. Iridite 7P, Kenvert 18, and Kenvert 31 are conversion coatings which form a protective oxide layer.

No. 132 material was used as the control. All samples were twelve inches long; electrical connections were made by potting the ends in conductive epoxy.

Initial results showed an accelerated test procedure would be advisable. Figure 23A shows the modifications made to one of the chambers. Through the use of a temperature controller the chamber was maintained at 100 F ± 1 F.
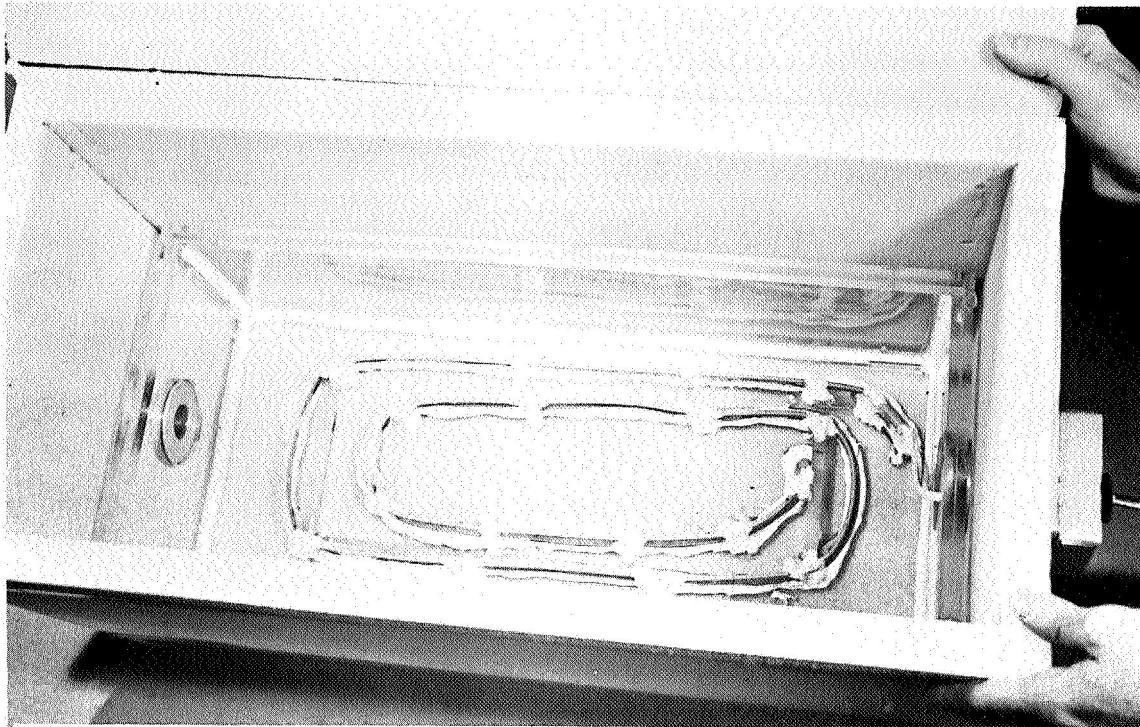
57

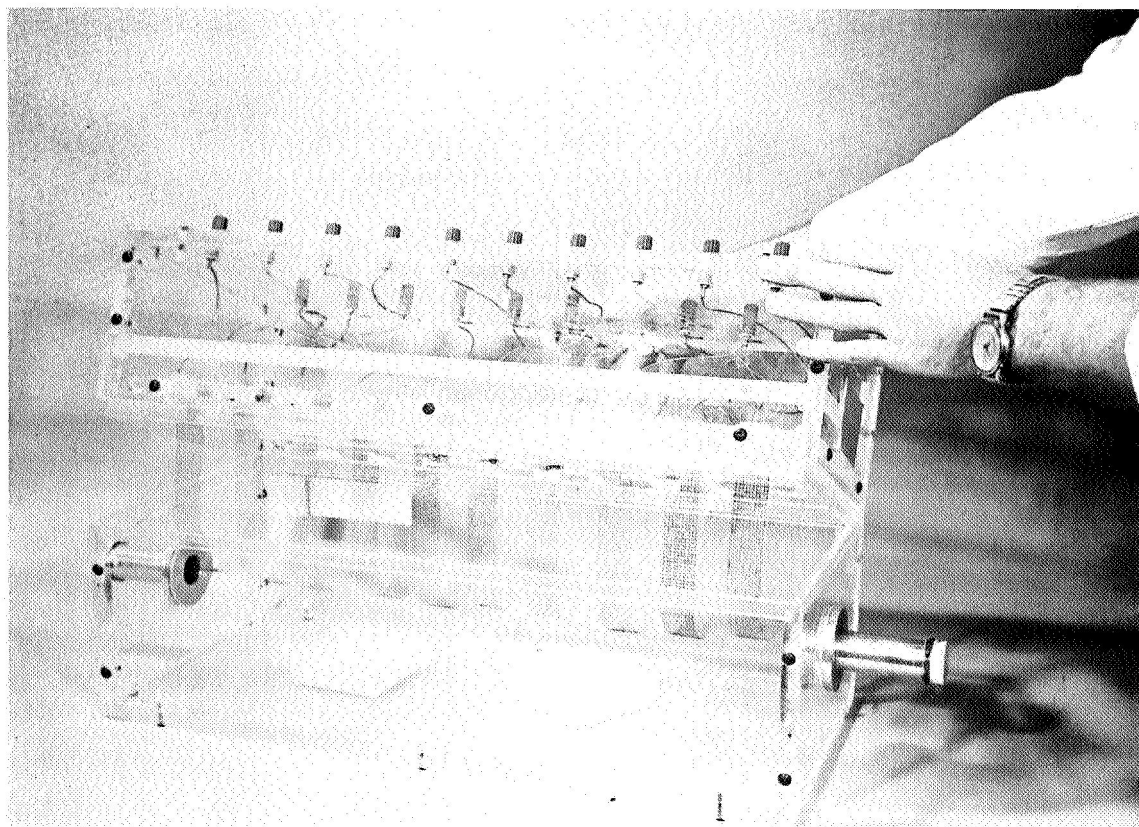Figure 23B   Interior of 100 F Controlled Atmosphere Chamber

Figure 23A   Controlled Atmosphere Chamber

Figure 24A shows the effect of various atmospheres on unprotected No. 132 control material exposed for 30 days. The samples tested at zero relative humidity and room temperature remained unchanged for the test period while the resistance of samples exposed to 100 per cent oxygen dropped after being placed in the chamber, and remained virtually unchanged for the remainder of the test because oxygen-saturated copper is more conductive than copper exposed to air only.

Figure 24B compares No. 132 material exposed to 100 per cent relative humidity at room temperature and at 100 F. These samples were unprotected.

Figure 25A compares the various protective coatings on 132 material. These samples were subjected to 100 per cent relative humidity at 100 F to accelerate corrosion. These initial tests showed that either silicone rubber (SS-4090) or E-56(60) offered the best protection.

Additional samples were made to evaluate the E-56(60) protective coatings more completely. The larger number of samples showed resistance increased slowly for the first ten hours but increased at the same rate as the control after that. (See figure 25B).

Figure 26A compares all material tested. These samples were unprotected and exposed to 100 per cent relative humidity at room temperature.

Figure 26B shows the resistance of each material as a function of time. It is interesting to note that the samples (134 material) which had an initial resistance over 100 ohms increased at a faster rate and showed a higher per cent of increase than the samples having an initial resistance below 100 ohms.

Figure 27A compares the resistance of two samples exposed to room conditions for 100 days. Both samples were identical except for the conductive epoxy used to pot the ends. Final resistance after 100 days was 15.2 ohms for each sample. While the copper sheath did discolor, very little change took place in the resistance.

Figure 27B compares a set of samples exposed to 100 per cent relative humidity at 100 F. Some of the samples were coated with Union Carbide A-1100 Silane, a coating used to protect copper foil from oxidation; others were coated with SS-4090 silicone rubber. Both sets of samples showed an extremely rapid increase in resistance. It was at this time that a number of measurements were made to determine the effect of soaking the samples in various solvents. All samples in this set had a high resistance initially.

From the controlled atmosphere tests which have been completed, it appears that material stored at room condition is extremely stable. The only better method is to store the material at zero relative humidity. All protective coatings tested had some damaging effect on the initial resistance of the material.
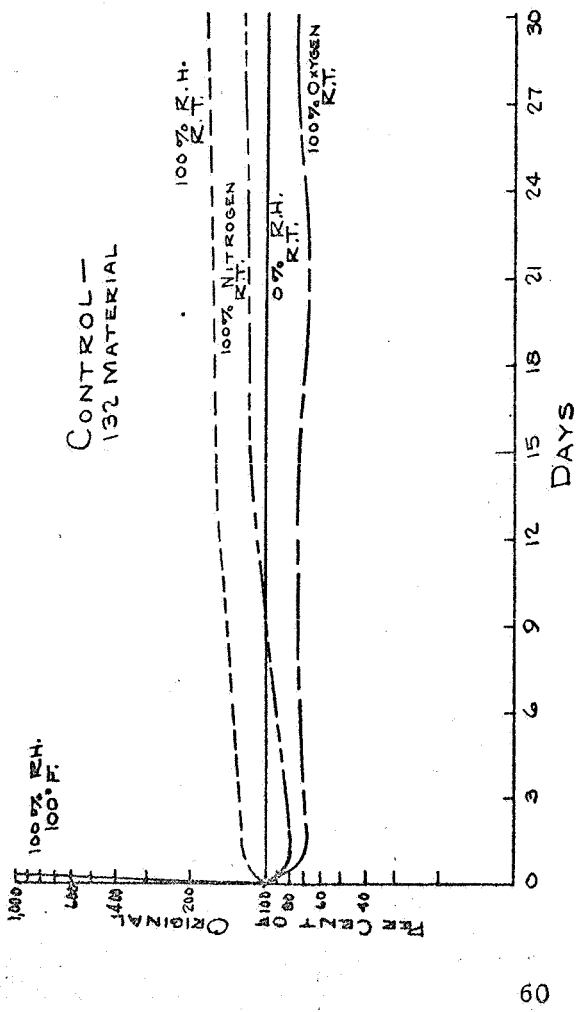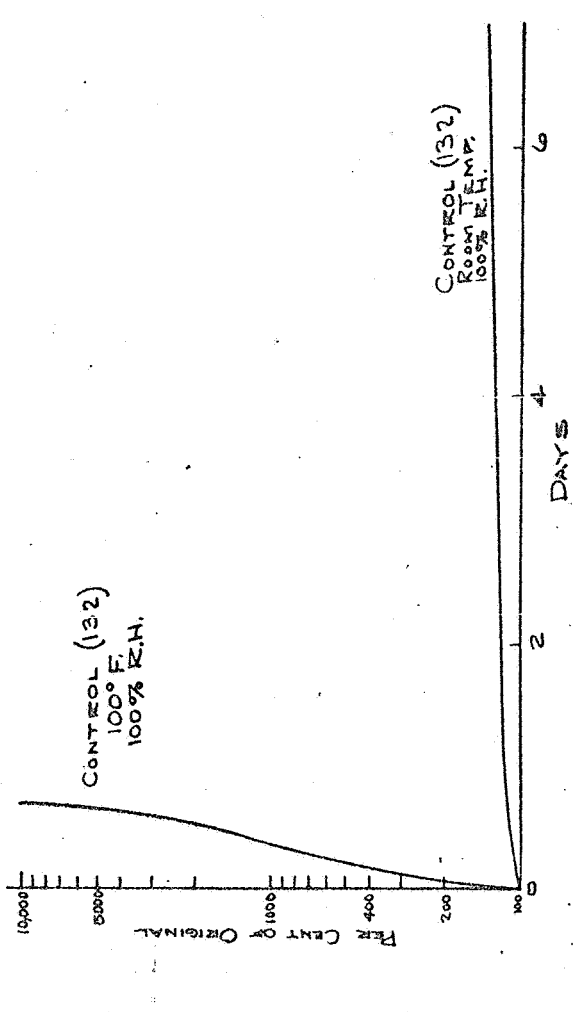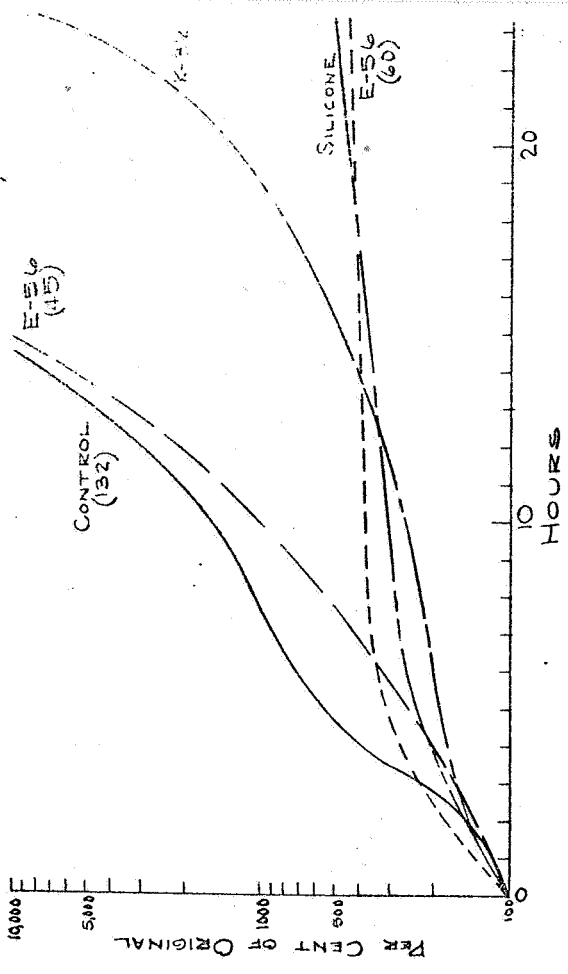
Fig. 25A

Figure 25B

Figure 24A

Figure 24B

Controlled Atmosphere
100° Fahrenheit
100% Relative Humidity

Control—
132 Material

Per Cent of Original

Hours

Days

ROOM CONDITIONS

105-135-1

105-135-1

105-135-2

RESISTANCE (OHMS)

100
80
60
40
20

0   25   50   75   10
         DAYS

Fig. 27B

100° F.
100% R.H.

CONTROL

SILICONE

A-1100
SILANE

PER CENT OF ORIGINAL

4,000

2,000

1,000
800
600
400
200

100

0   1   2   3   4
         HOURS
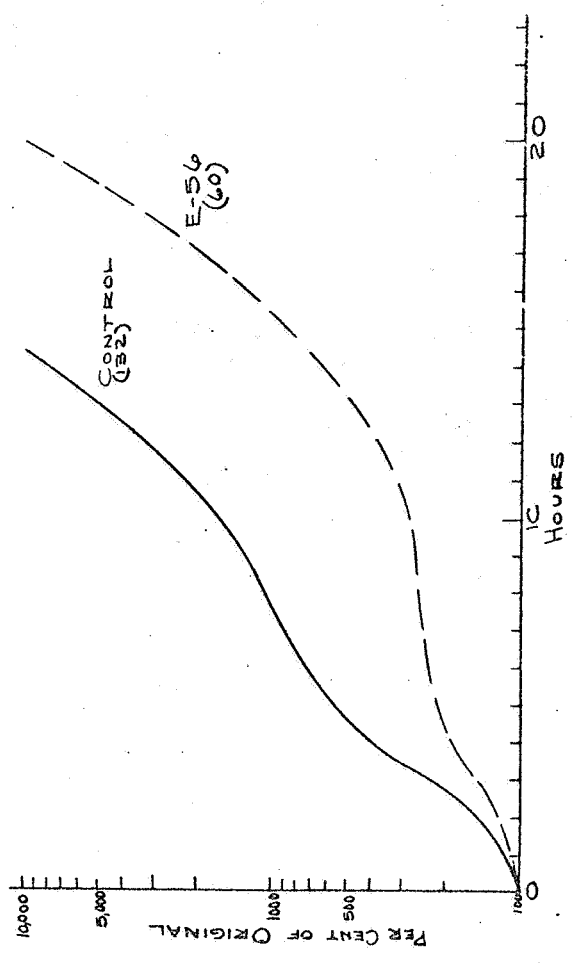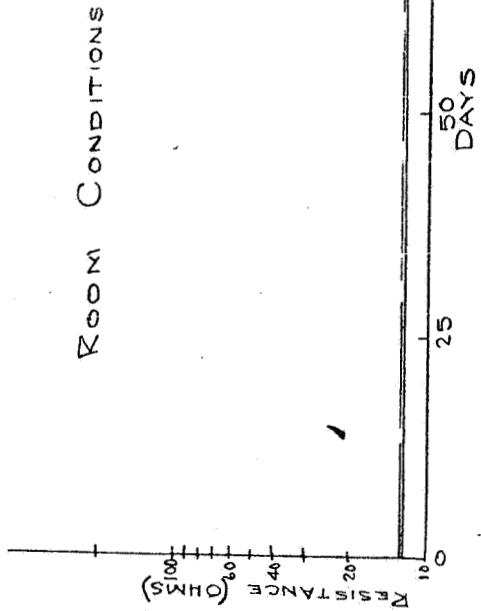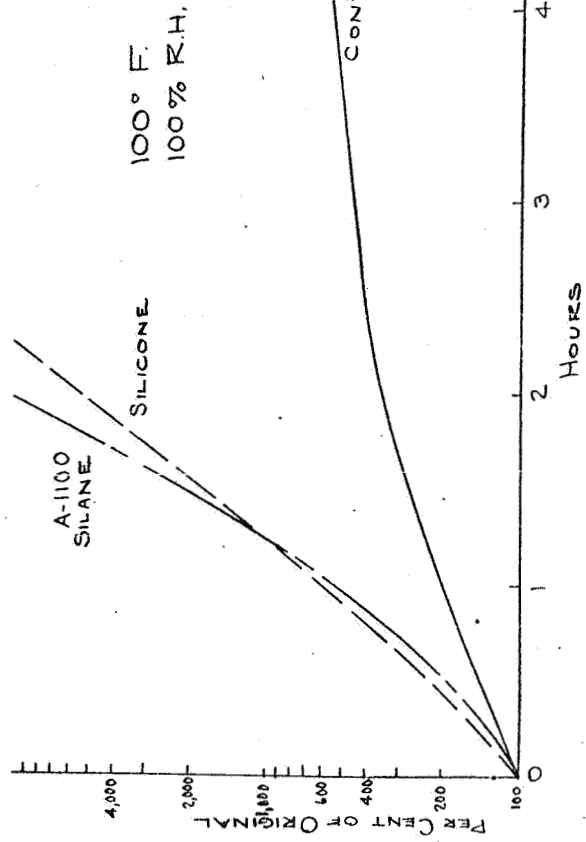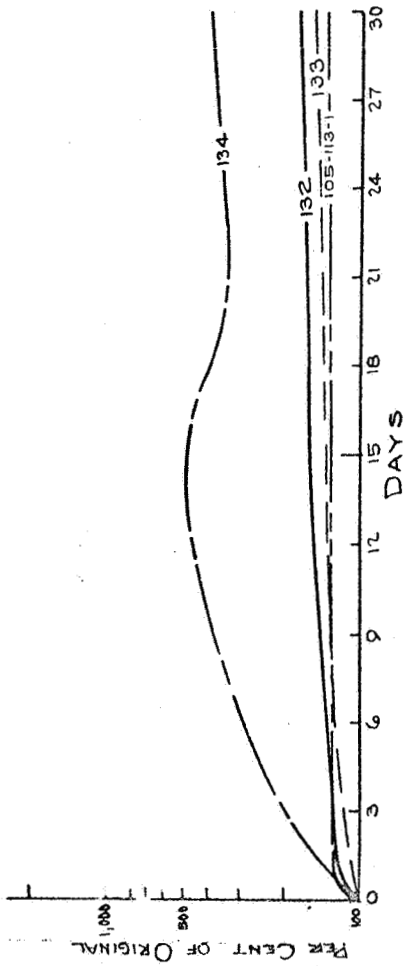
Figure 27A

CONTROLLED ATMOSPHERE
100% RELATIVE HUMIDITY
ROOM TEMPERATURE

134

132
133
105-113-1

PER CENT OF ORIGINAL

1,000

500

100

0   3   6   9   12   15   18   21   24   27   30
                    DAYS

Fig. 26A

134

133

132

105-113-1

RESISTANCE (OHMS)

1,000

500

100

50

10

0   3   6   9   12   15   18   21   24   27   30
                    DAYS

Figure 26 B

61

8.0 FABRICATION OF MODELS

8.1 SEAMS

8.1.1 Liquid Seams

The initial seaming technique bonded the material at the seams with a resin solution of GT-201. The solution was brushed onto the seam area totally encapsulating both pieces of fabric to form an overlapping seam. This seam was cured by forced hot air. This technique was found to be unsuitable for production procedures as it was difficult to keep the gores alined. This technique of bonding was abandoned at this poi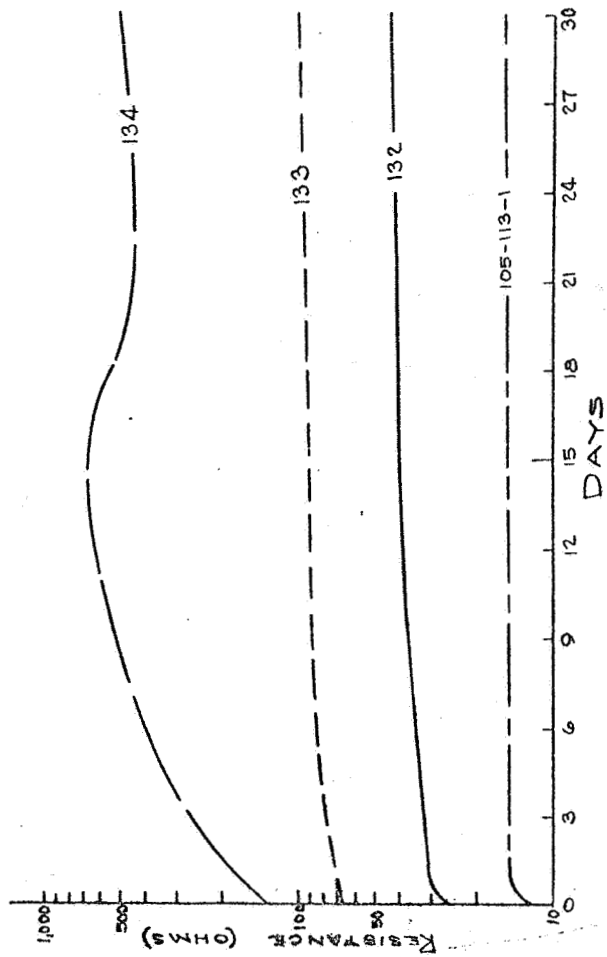nt although it was briefly used again later in the contract during the preparation of cylinders where flat end panels were cemented into place with a liquid silicone rubber solution. During the fabrication of these cylinders, this adhesive system was found unsuitable because of its extremely slow setting time. The use of a liquid or resin solution to prepare the seam was abandoned and all future fabrications used a bitape seam construction.

8.1.2 Bitape Seals

Using aluminum-coated material, several seam designs were evaluated. Aluminum-coated material was used because at the time copper-plated material was being coated with a silicone rubber sheath coating. The following designs were evaluated.

Design A	Standard overlapping bitape seal
Design B	A 3/8-inch overlap with 1/8-inch wide strip of 0.9-mil aluminum in a bitape seal
Design C	A 3/8-inch overlap with 1/8-inch wide strip of 1/2-ounce copper foil in the bitape seal
Design D	A 3/8-inch overlap with a bitape seal using a conductive tape

Table 17 shows the results of this work. Designs are compared to continuous material in respect to resistivity and tensile strength.

TABLE 17

Seal Evaluation

	Material Sample	Seal Configuration	Resistivity	Tensile Strength lb/in Width
1	105-119-1	continuous	16.7	40
2	105-119-1	A	75.0	18
3	105-119-1	B	38.3	13.6
4	105-119-1	C	71.7	15.0
5	105-113-1	A	--	0.8
6	105-119-1	D	48.2	10.0
7	105-119-2	continuous	4.7	32.0
8	105-119-2	D	18.3	16.8
9	105-119-2	A	8.0	18.8
10	105-119-2	B	8.3	12.7

Sample 5 is an overlap bitape seal. No resistivity measurement could be made on this because this particular sample had a sheath coating of RTV silicone rubber.

To determine the reproducibility of these seals five samples of designs A, B, and D were made. Design C was not run because of its similarity to B. Material used was run 131.

Table 18 lists these results. The figures given are for the resistance of a six-inch sample divided by the length of the sample. This type of resistivity measurement gives a fairly good representation of the effectiveness of a seaming technique.

TABLE 18

Seam Study of Sample No. 131

	Design A	Design B	Design D
	10.8	18.0	46.8
	8.8	16.0	30.0
	12.0	27.5	38.3
	13.3	21.7	32.5
	25.0	9.7	25.8
Average	13.98	18.58	34.68

The figures indicate that a simple overlapping seam provides the lowest resistance and therefore the best electrical contact.

Table 19 compares tensile strength of material 144 seamed by different methods. It shows that 30-gage tape does not seal through the openings in the mesh as effectively as the thinner tape.

TABLE 19

Comparison of Seam Types and Tape System

Material Bonded - 144-4 MD

	Tape Width	Overlap Joint	Butt Joint
15 Ga. Mylar by 1/4-mil GT-200	3/8	7.8 lb/in	8.1
30 Ga. Mylar by 1/4-mil GT-200	1/2	2.9	16.0

8.2 CYLINDERS

Initially it was desired to test the self-erecting material by deploying a simple right cylinder. The first models of this type were 7-1/2 inches in diameter and 12 inches high with flat ends in place. The ends were fastened to the edges of the cylinder with a solution of silicone rubber. Figure 28 shows how the cylinder erects under essentially 1-g. To evaluate this the cylinder was merely flattened perpendicular to its major axis. When released the cylinder popped up quickly and completely.

Following this a special deployment technique was devised to deploy the cylinders from a canister. The cylinder, supported by 3 strings, was packed in a canister consisting of two plates spaced so that the packing volume was 12- by 2- by 1/8-inches. These dimensions are based on a packing factor of 3.0. Motion pictures were taken at 80 frames per second during the cylinder deployment. Frames of these sequences have been selected and are grouped in figure 29. Figure 29a shows the packed canister prior to release, 29b at the point where the canister is falling away, 29c the cylinder well on its way to deployment, while 29d the ultimate shape of the cylinder.

A number of these tests were run on cylinders constructed of various weights of material. It was found that material from run No. 131 performed very well when the machine direction fibers were parallel to the ends of the cylinder. The rigidity in this direction has been measured at 850-900 milligram centimeters. Material from runs 130 and 129 was also deployed in this manner; however, it was found that material usually failed to erect so that the cross-section of the cylinder was circular. A schematic of the canister system is shown in figure 30.

The cylinder was then folded to a size approximately 2- by 2- by 3/4-inches and tossed into the air. Figure 31 shows the manner in which the cylinder deployed. The elapsed time during these pictures is approximately one-half of one second.

A number of techniques were used to pack the cylinder with flat ends, including packaging in the canister described above. The cylinder with flat ends was packed by rotating the ends in opposite directions and allowing the material to gather as the ends were brought together flat. Once the cylinder

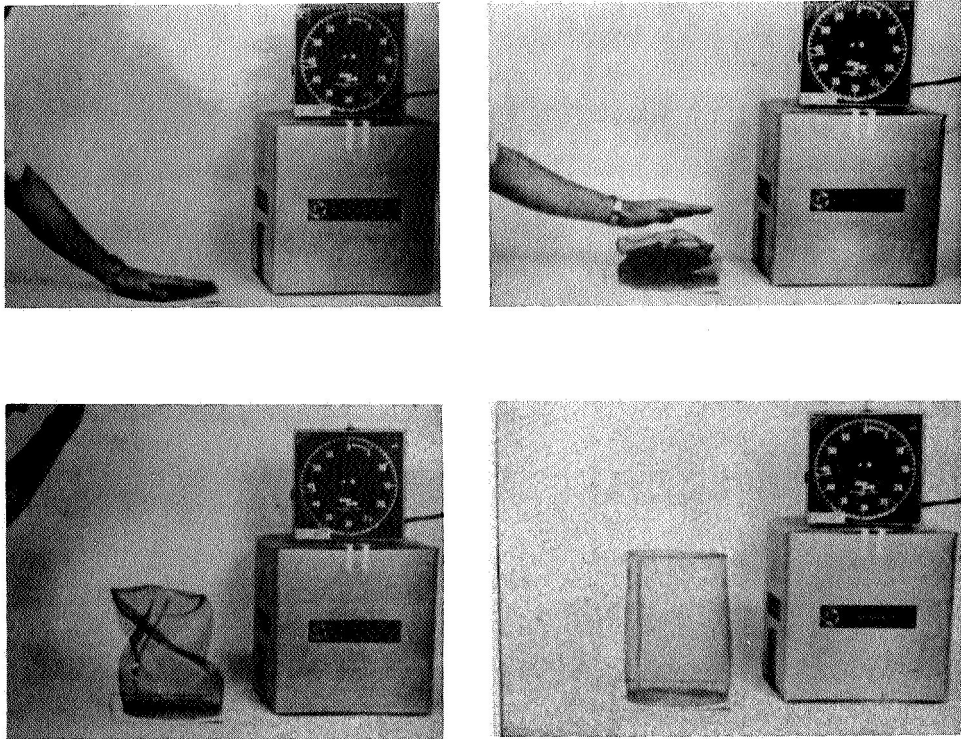Figure 28   Erection of Cylinder Under Its Own Weight
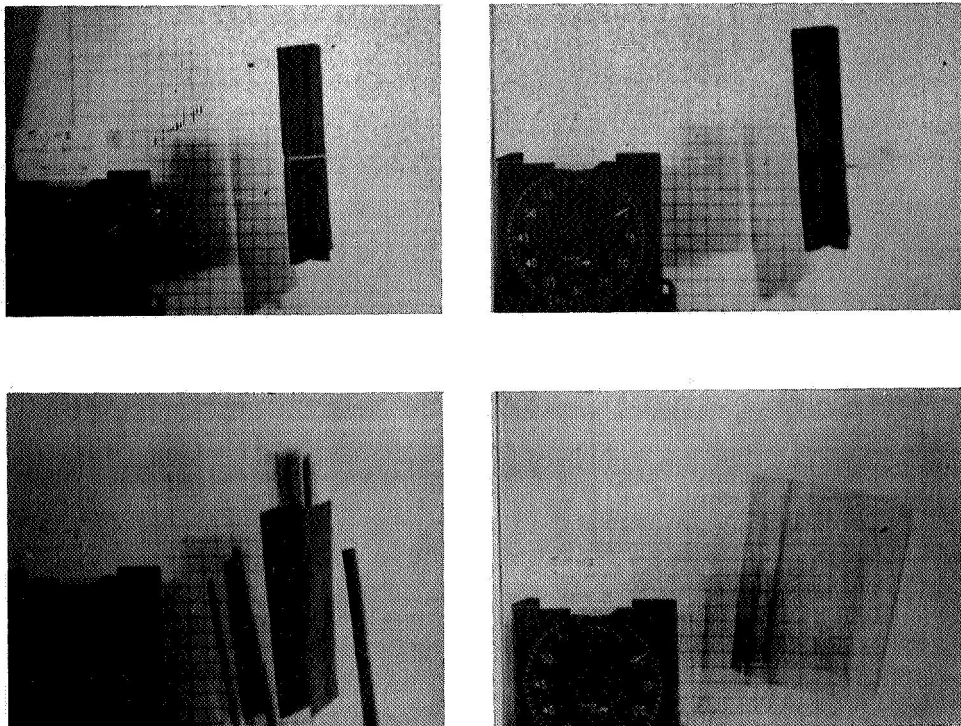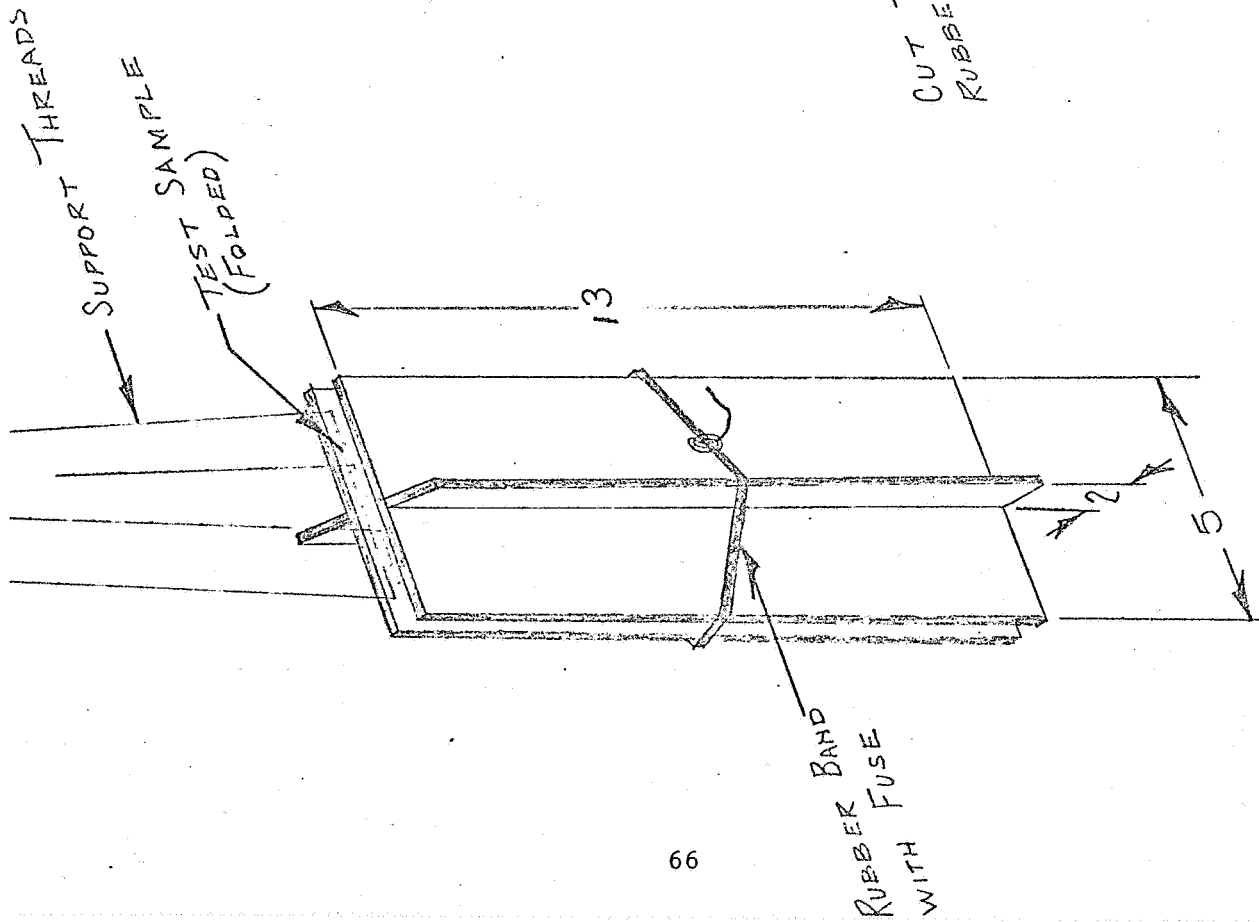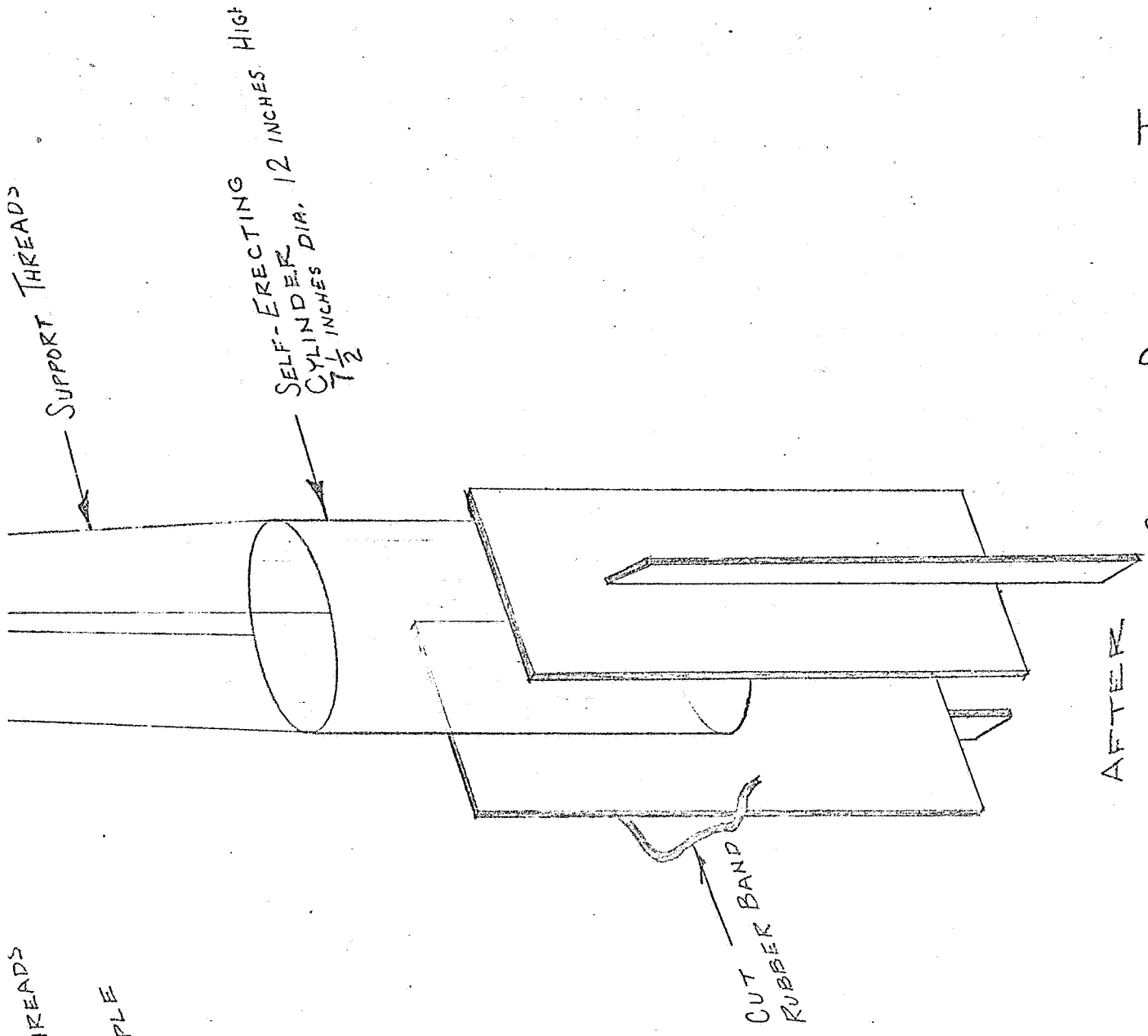

Figure 29   Erection of Supported Cylinder

CYLINDER DEPLOYMENT TEST
6-20-66

SUPPORT THREADS

SELF-ERECTING CYLINDER, 12 INCHES HIGH
CYLINDER DIA, $7\frac{1}{2}$ INCHES

CUT BAND
RUBBER BAND

AFTER

SUPPORT THREADS

TEST SAMPLE
(FOLDED)

13

12
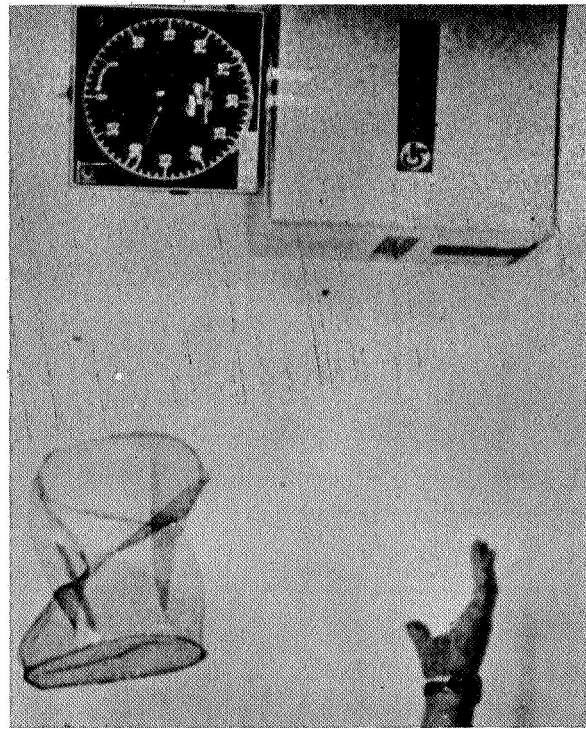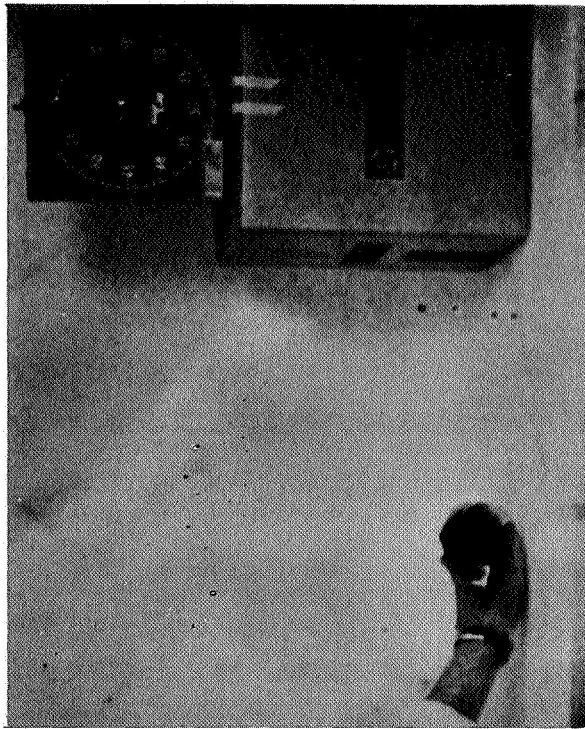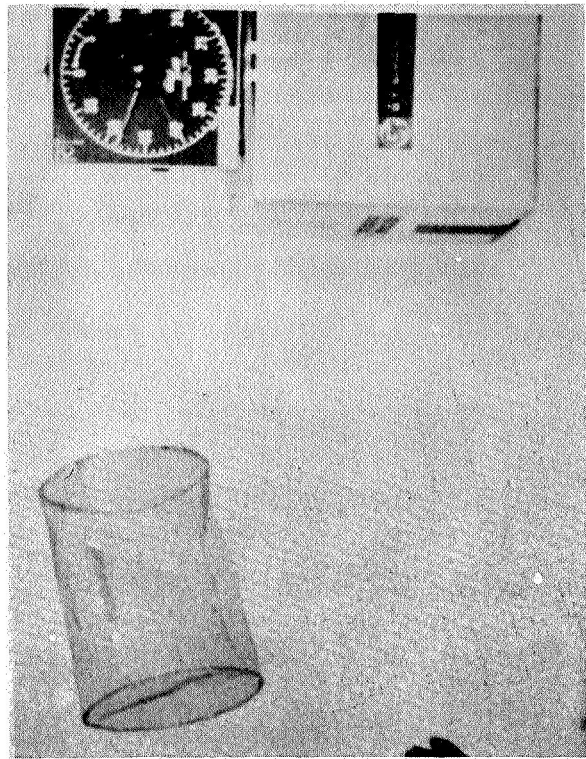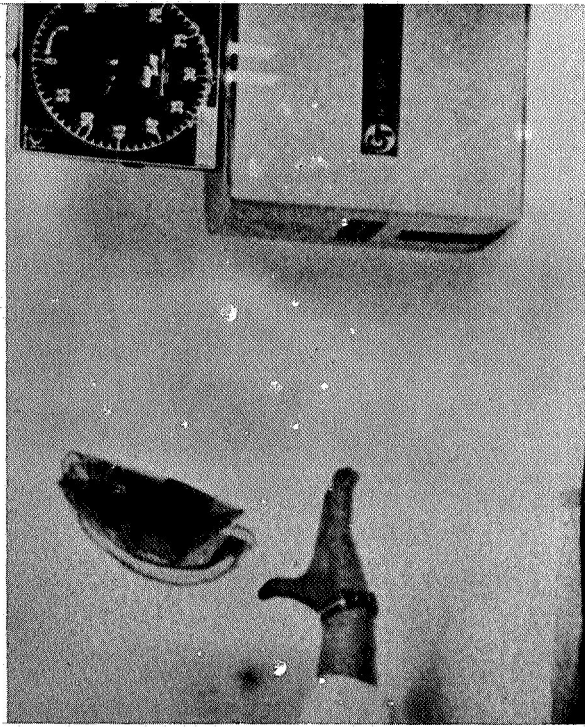
5

RUBBER BAND
WITH FUSE

BEFORE

Figure 30

66

Figure 31   Cylinder Erecting During Free Fall

has been collapsed parallel to the major axis, the resulting circular flat object is folded to the dimensions described above.

8.3 SPHERES

Because of the success of the erection of cylinders a number of models of a spherical configuration were made. The first models, 12-, 18-, and 30-inches in diameter, were of a gored type. Initially the spheres were to have an overlapping seam and a bitape construction. However, in attempting to package a 30-inch sphere prepared from 134 material, it is found that there was excessive breakage in areas next to the bitape seal. It was also noted that the material apparently did not have enough strength to support its own weight; in free fall, there was no indication that the material would erect itself. At this point material 135 was prepared. Material 135 has no conductive coating and has only 5 fiber bundles per inch in the machine and transverse directions. The rigidities of 132 and 135 are essentially equal in the transverse directions but material No. 135 is approximately 6 to 7 times more rigid in the machine direction. These two materials were fabricated into a number of spheres. In an attempt to determine the practical limit of size as a function of rigidity, three different size spheres were made; namely, 12-inch, 18-inch, and 30-inch diameter spheres. Figure 32 shows four of these spheres at rest on a table, the dark spheres being made of No. 132 material and the lighter of 135 material. The larger spheres shown are 18 inches in diameter while the smaller are 12 inches in diameter. As can be seen the larger sphere of 132 material does not have enough strength to stand spherically in the one-g environment, while the 18-inch sphere of 135 material stands very well under its own weight. The 30-inch sphere of 135 material buckles under its weight vertically to the same extent as the 18-inch sphere of 132 material.

8.3.1 Buckling

These model spheres were built to study folding techniques, and show that local buckling may be a problem. When a structural member is loaded in compression, the middle of the member deflects laterally in a direction normal to the plane of the member. If application of the load is continued the member collapses. This load at which the member fails depends upon the shape, dimensions, support conditions, and the physical properties of the material involved. In the case of a sphere, if the flexural rigidity is insufficient, failure may occur at stresses far below the elastic limit of the material. The pressure at which the spherical form becomes unstable or buckling occurs is called the critical or buckling pressure. The buckling may be overall buckling of the sphere or it may be localized in a small portion of the sphere.

Buckling had never been noticed before as the models did not have compound curvature. Self-erecting force apparently works very well over plane surfaces, or in objects such as cylinders, but buckling occurs in objects with compound curvatures such as spheres. This metastable position is disastrous since any object may have to pass through this buckled condition during its deployment.
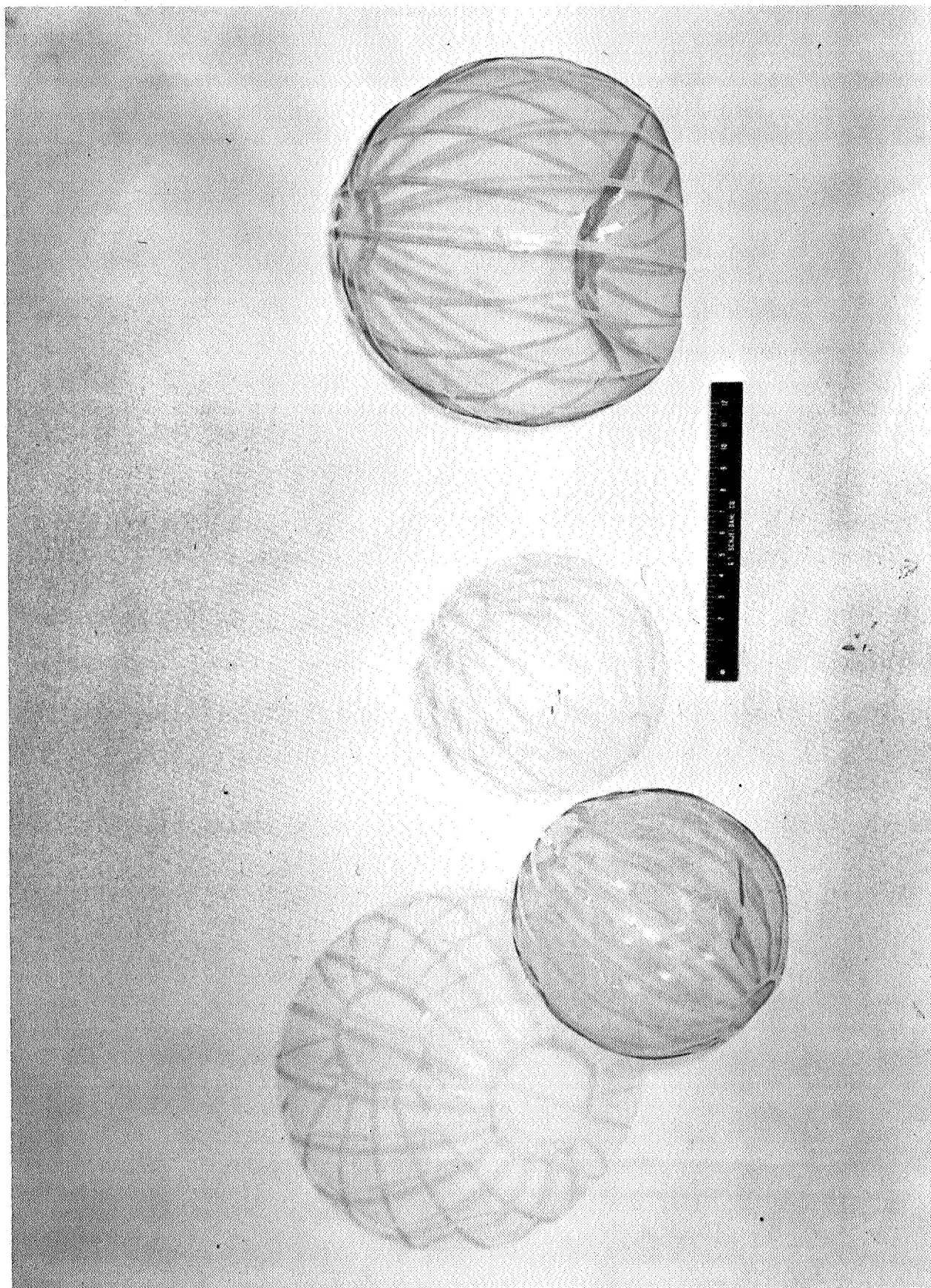
68

Figure 32   Gored Spheres Made of Self-Erecting Material

It has been found that a buckled area has fairly finite dimensions. The surface of a hemisphere can be depressed until a certain area has been buckled. Before this point is reached the material will spring back to its desired shape. Depression beyond this point or of a larger area causes buckling. It was concluded that the packaging configuration should keep the folded area smaller than the specific buckled area for a given material. Tests have shown that if the folding technique involves an area extending beyond a tape seam or exceeds 15 per cent of the total area of the sphere buckling will result.

A study was conducted in an effort to measure the effected area in a buckle after it had occurred. The shapes and sizes of various buckled areas in both spheres and hemispheres of various materials were tested and recorded. A probe of approximately 3/8-inch diameter was employed to permanently buckle the spheres. By probing the spheres from several positions, e.g., over a seal, across a gore, or over the polar cap, information could be developed regarding these buckled area. It was noted that one portion of the buckle paralleled or ended at the butt joint of a seal, usually involving a sharp crease in the tape material. It was noted that if the perimeter of the buckled area remained circular, the material would return to its spherical shape. In spheres of gore construction the area resisting permanent buckling best was the polar region, while the weakest area tended to be in the equatorial region. However, in spheres with gores cut at a 45-degree angle to the thread pattern, the gore area resisted buckling equally with the polar region.

Although the above testing is not exact, it does shed light on techniques and guidelines for proper folding of spheres.

8.3.2 Folding

Based on the study regarding size of buckled areas, a study into folding techniques of spherical objects was made. As it was desired that the folded areas be kept smaller than the minimum buckling areas, special techniques were employed. To minimize breakage of the fiber bundles it was found that the spheres must be carefully folded. Although the first fold can be maintained with a specific radius, when a secondary fold is made across the first, the radius of the first fold becomes zero. Because it is important that the radius of folding of self-erecting material never be less than 1/32-inch, it is very important that the primary folds be reinforced so that threads do not break during folding. It was also desired that the folding techniques would provide efficient use of the erection forces stored in the folding process.

The types of folding modes investigated in this study are pictured in figure 33. Type A uses the bitape seam as a hinge area and the center of the gore is folded lightly towards the inside of the sphere. This type worked out best and was also the most simple. Type B used the same principle only the self-erecting material was folded in the middle part of the gore in such a way that the midpoints of the gore were folded out from the center of the sphere. Type C was used with spheres with overlapping seams; no fold was made across the seal.

70

Type A

Type B
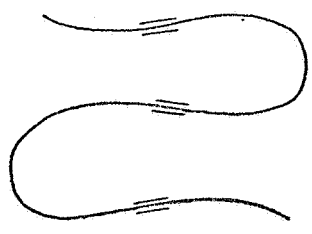
Type C

Figure 33   Types of Folding Techniques Used

8.3.3 Formed Spheres

A number of 12- and 16-1/2-inch diameter spheres were made by forming two hemispheres and then bitaping a seam around the equator. Such a sphere is shown in figure 34. Two techniques were used to prepare the hemispheres. One was the wet layup process which consisted of soaking sized glass fabric and softening the starch so that the fibers could be reoriented to form a hemisphere when pressed over a mold. A second technique used an oven to heat the material coated with GT-201, before pressing it on the hemispherical mold.

In packaging these spheres a tendency for buckling was observed. Further investigation of 135 material showed that the buckling mode was directional, forming preferentially in the machine direction. As the 135 material is extremely unbalanced with a ratio of rigidity between the machine and transverse direction of approximately 6 or 7 to one, this apparently reveals the nature of the buckle. The sphere made of 135 material was constructed with the hemispheres 90 degrees out of phase, so that half of the sphere was folded parallel to the machine direction and the other half of the sphere parallel to the transverse direction. It was found that the material folded parallel to the transverse threads always tended to erect itself. The other half of the sphere, where the folded areas were parallel to the most rigid dimension, would not fully erect. A cross-sectional view of a sphere that has been buckled perpendicular to the most rigid dimension shows that there is a smooth curve of the fibers in this buckled area. It is concluded that folding should be performed perpendicular to the most rigid dimension. This conclusion led to the request to the weaver that a portion of the fabric ordered be produced with asymmetrically with the transverse direction fibers much more rigid than the machine direction fibers.

The formed spheres had a distinctly larger critical buckling area than the sphere made of gores. However, it would be rather difficult to construct large spheres by forming.

8.3.4 Spheres of Biased Gores

It was found in static folding tests that there was decidedly more resistance to fiber breakage when material was folded at a 45-degree angle to the fiber bundles. This prompted the construction of a 12-inch diameter gored sphere made with material cut on a bias. This sphere was folded according to method A in figure 33; when deployed it erected to an object approximately 10 inches in diameter at the equator by 14 inches long from pole to pole.

8.3.5 Test Models

In preparing for the deployment test at Goddard Space Flight Center, 30-inch-diameter spheres were made from material produced in run No. 136 and run No. 137. No. 136 fabric had a high rigidity in the transverse direction and the gores were cut so that the transverse direction fibers were parallel to the equator of the sphere. The gores of these spheres were butt-sealed. The material from run No. 137 consisted of a balanced material cut at a 45-degree angle so that the gores could be folded without produced 180-degree folds in the fibers. These spheres were deployed under atmospheric conditions at the
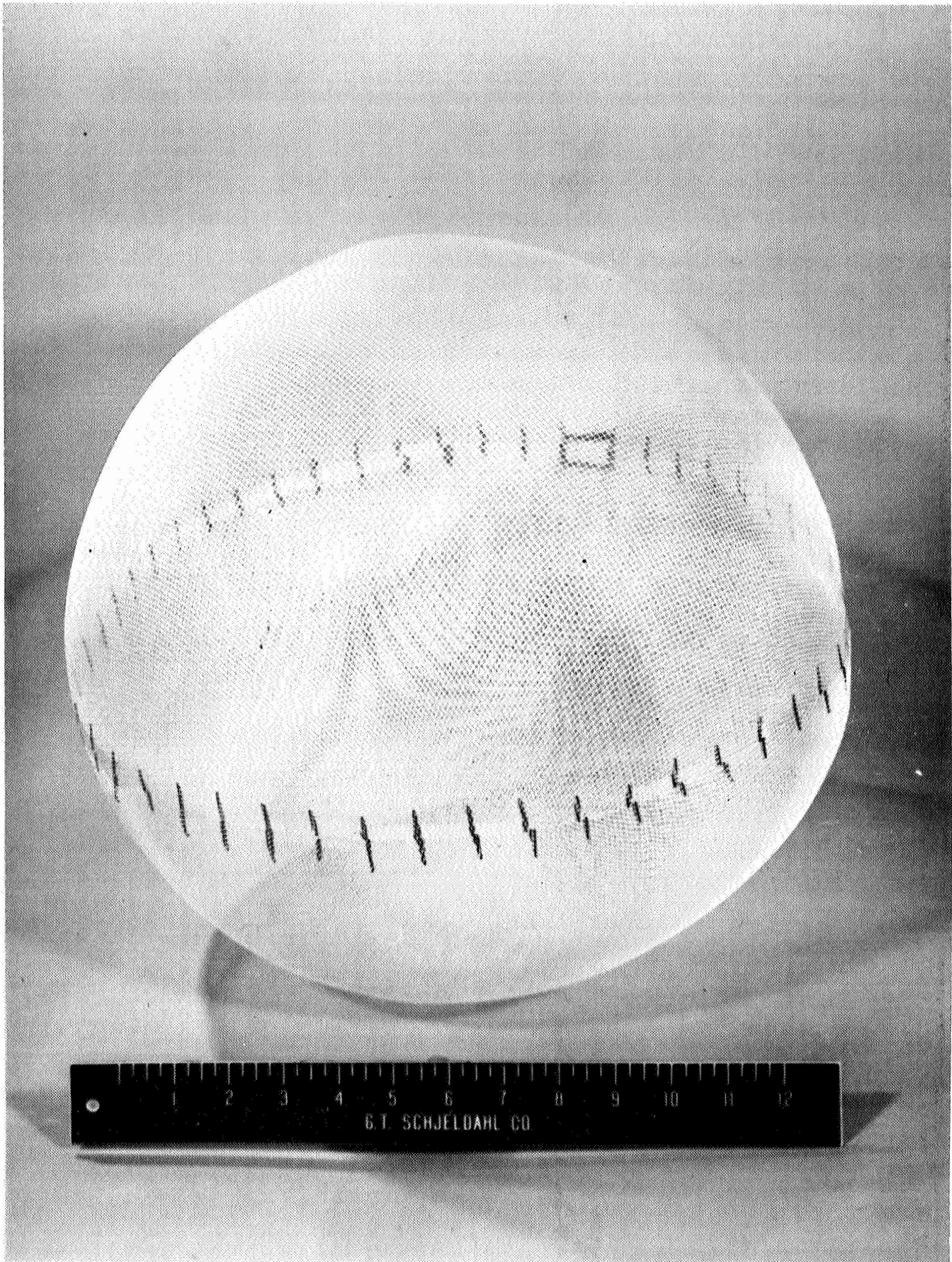
72

Figure 34   16 1/2-in. Dia. Sphere Made of 2 Formed Hemispheres

73

G. T. Schjeldahl Company; figure 35 shows a sequence of one of these deployments. As can be seen by the photographs the deployment was incomplete to the approximate dimensions of 15 inches diameter by 40 inches long. The sphere with the gores cut at a 45-degree angle was also tested under these conditions and did not deploy. These tests indicated that a more efficient means would have to be devised to realize and demonstrate the feasibility of erecting a 30-inch sphere.

It was found that a circumferential tuck in the spheres aided deployment. This tuck was made by folding one-half the sphere inside the other, and sewing the two halves together near the fold. When the sphere was then unfolded the sewed portion formed a circumferential flange. Figure 36 shows the details of this construction. A number of atmospheric deployment tests run at G. T. Schjeldahl showed the success of this. Using the spheres deployed in earlier tests, it was found that a sphere with a reinforced equator would deploy to 24 to 25 inches equatorial diameter and by approximately 32 inches polar diameter. It was felt that a sphere that had been folded only once would deploy itself completely.

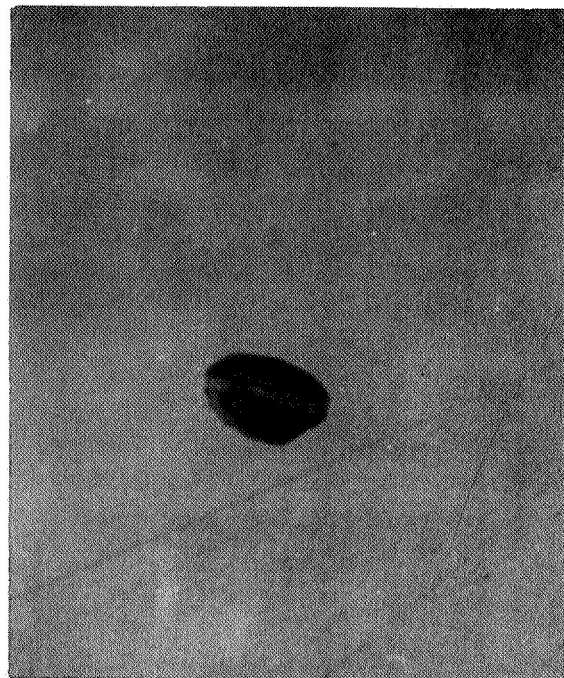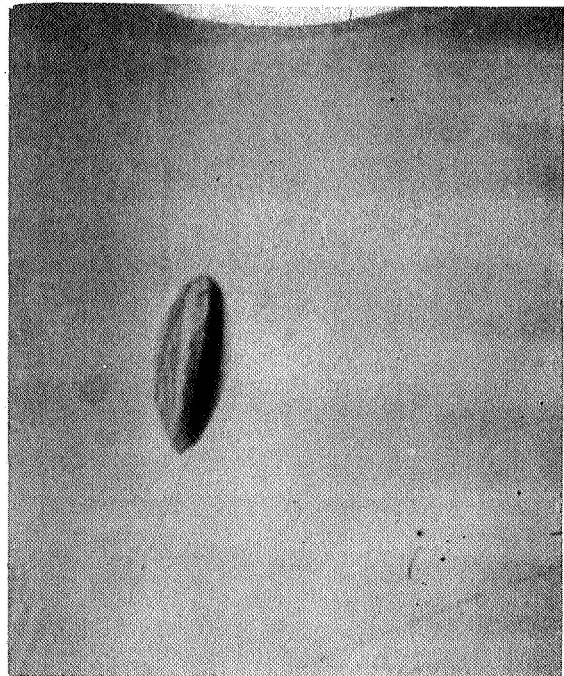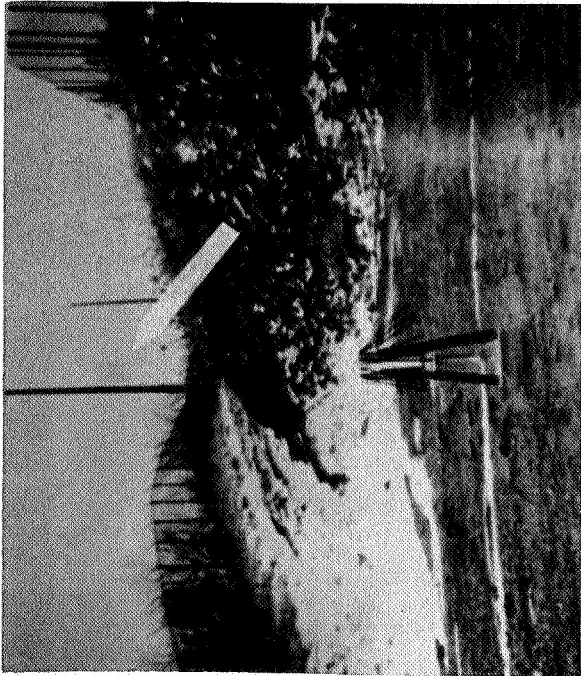Figure 35 30-in Dia. Sphere During Deployment in Atmosphere

FIN

SEWING

GORE

TYPE A

GT 300
BI-TAPE SEAL

SEWING

FIN

GORE

GT 300
BI-TAPE SEAL

TYPE B

SPHERE GORE

FIN AT EQUATOR

DETAIL A
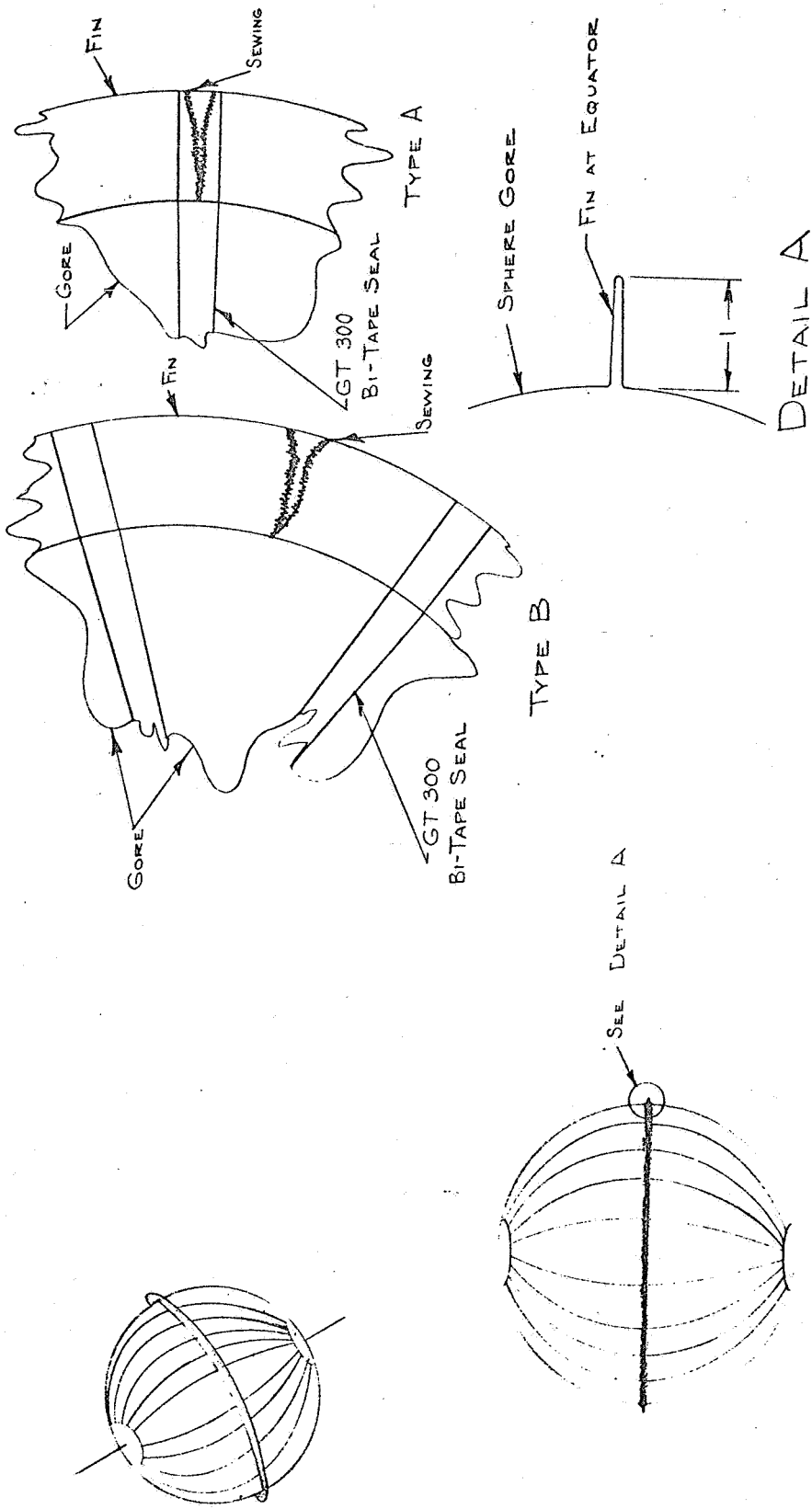
30-INCH SPHERE DESIGN
24456-11   12-22-66

SEE DETAIL A

Figure 36

76

70 mm Camera

70 mm Camera

16 mm Camera

Catapult

Figure 37   Dynamic Test Chamber at GSFC

9.0 DEPLOYMENT TESTS AT GSFC

Deployment tests at Goddard Space Flight Center in the dynamic test chamber were conducted to evaluate self-erecting properties in a vacuum under free fall conditions. The chamber had a number of monitoring devices; one 16-mm camera capable of taking 250 frames per second and two 70-mm cameras capable of taking 20 frames per second. The chamber was also equipped with a number of TV monitors, two of which were used. The placement of the cameras is shown in figure 37. The cameras were equipped with wide angle lens so that 80 to 90 per cent of each flight could be monitored by each camera. The deployment machine is described in the appendix.

At the beginning of the test it was decided that a program would be used to start the lights, camera, and fire the squib in the proper order. The timing sequence was as follows: First one bank of lights was turned on, after one second the second bank of lights was lit, after another second the cameras were started, and on the fourth second the squib on the deployment machine was fired. After four seconds the cameras were stopped, and after five seconds the lights were turned off. This procedure was followed in all of the tests run at Goddard.

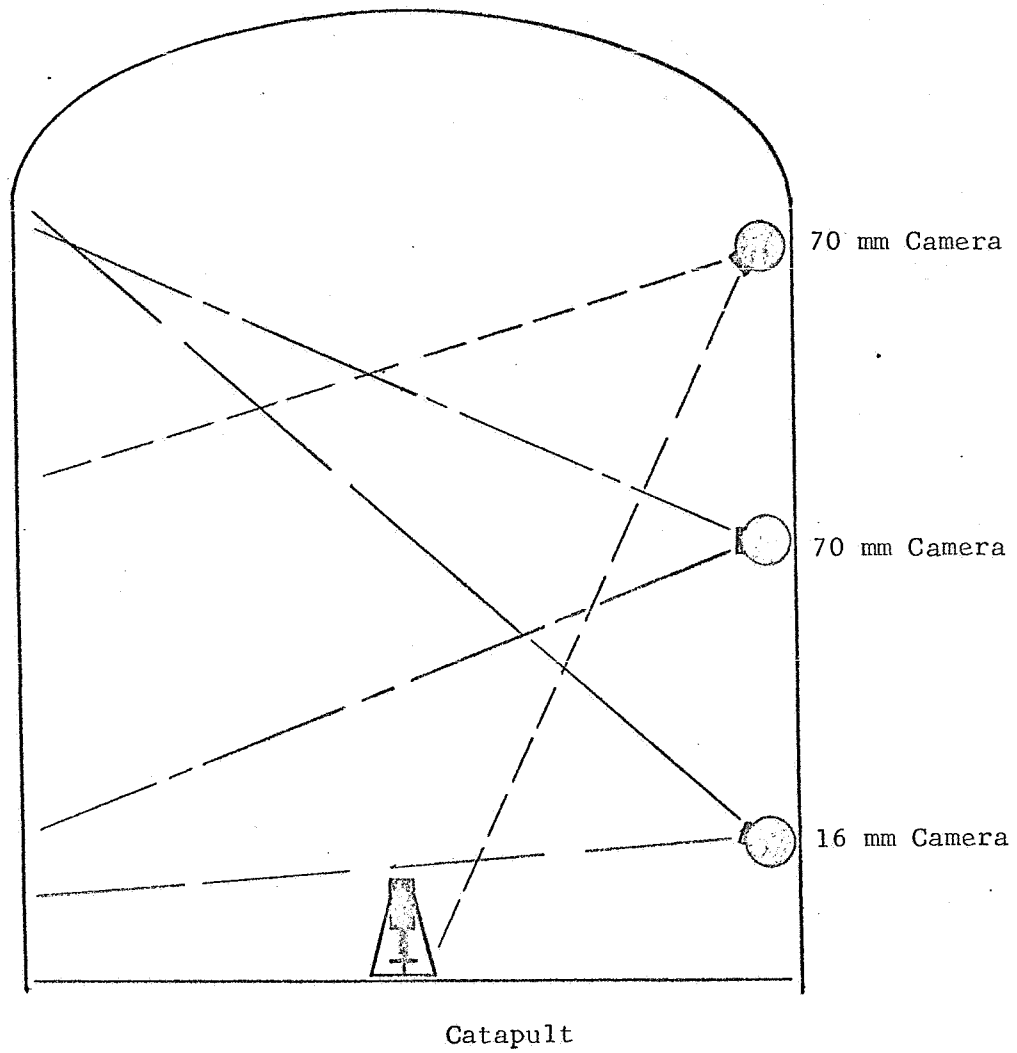The first test consisted of a sphere constructed of material No. 137. The gores of this sphere were cut at a 45-degree angle so as to minimize breakage during packaging in the canister. The sphere also had a tuck around the equator. The test proceeded as planned and the sphere deployed as a prolate spheroid approximately 12 inches in diameter with a pole-to-pole length of 40 inches. These measurements are based on the high speed motion picture film received from NASA. The test was run at a pressure of 0.9 of a millimeter of mercury. Upon release of the vacuum the sphere was examined and found to have no apparent defects from this test and a diameter of 20 inches and a length of 39 inches. This increase in deployed size was undoubtedly due to the air currents within the vacuum chamber and was at first considered to be the deployed size during the test.

Because of the final resting place of the sphere it was felt that the deployment machine was not perpendicular. Therefore, for the following tests the catapult was shimmed so that a more vertical flight would be observed.

The second test consisted of the deployment of two 18-inch diameter spheres from a canister of the size described in an earlier section. The pressure in the chamber at the time of deployment was 0.99 millimeters of mercury. The spheres were constructed of No. 137 material and had their gores cut at a 45-degree angle. One of the spheres was reinforced with six 20-mil piano wires. Figure 38 shows the two spheres in the free fall. Figure 38a is a still from the top camera sequnce, shortly after deployment. It shows that the reinforced sphere popped out of the canister and erected immediately. Figure 38b is a still picture during the descent of the spheres. Only the piano wire reinforced sphere erected.

The third test consisted of a sphere cut from 136 material with the gores cut with material more rigid in the transverse direction. The pressure at the
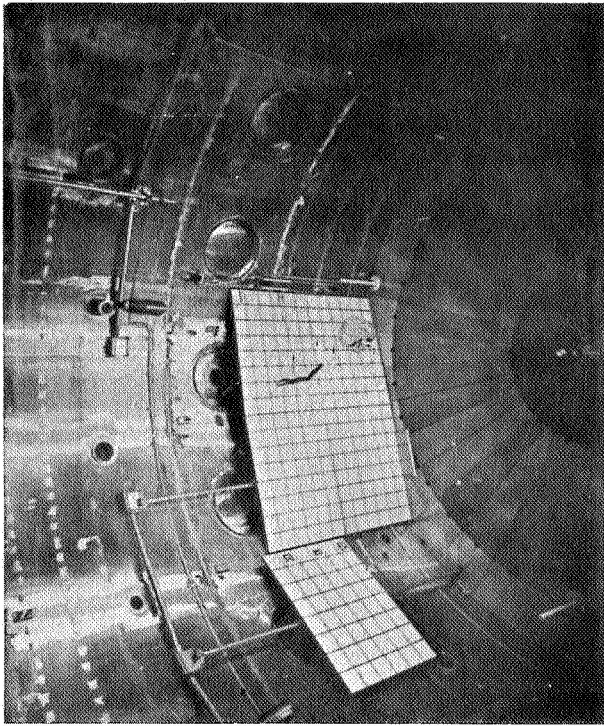
Fig. 38a

Fig. 38b

Two 18-in. Dia. Spheres during Deployment Tests at GSFC

Fig. 39a

Fig. 39b

30-in. Dia. Sphere During Deployment Tests at GSFC

79
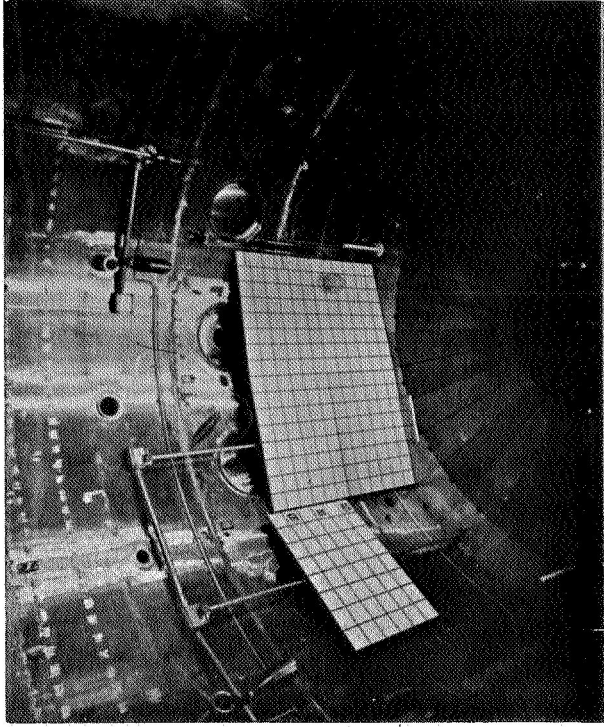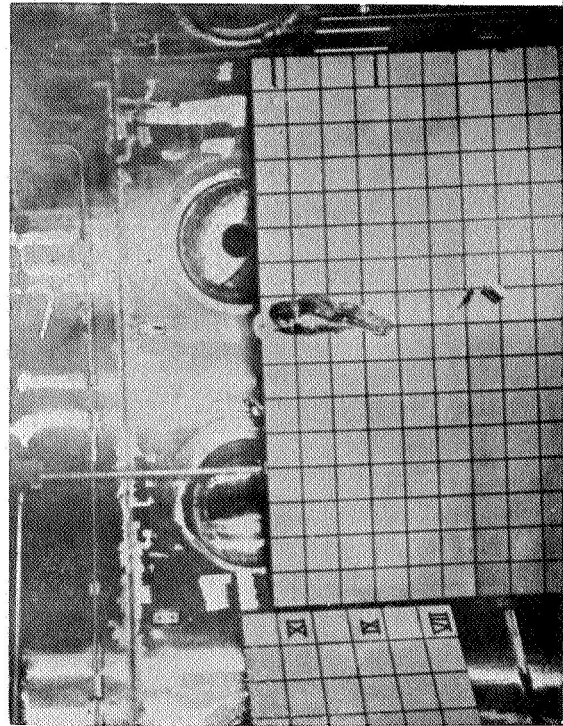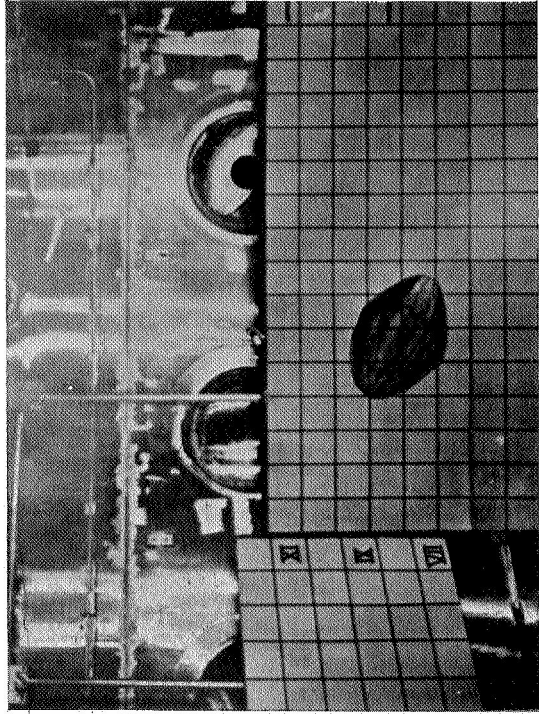
time of the test was 1.3×10^{-3} torr. Figure 39a shows this sphere just after release and after deployment, while 39b shows it on descent. At this point it was questioned if the time of free fall was long enough for the material to have erected. Motion picture records taken of these tests have shown that it was not.

The above tests were considered a success as there was no difficulty with the deployment machine nor any scheduling problems during the use of the dynamic test chamber.

APPENDIX I

STRUCTURAL ANALYSIS

This section includes four approaches to the structural analysis of large three-dimensional curvilinear objects under space conditions.

The first approach analyzes the problem from the standpoint of a cylinder. This approach provides a conservative solution because a sphere is a more rigid geometric shape than a cylinder.

The remaining three approaches consider a gored sphere. The second assumes no continuity along the seams and thus gives conservative results.

The third uses the theory of elasticity, assuming that there are no seams and that the object is made of continuous, homogenous, isotropic and elastic material. To allow for the inconsistency between assumed and actual material, a form factor, 1/30, has been introduced in the equations.

The fourth approach outlines the matrix method of analysis, a method especially suitable for mesh material. The material mesh size may be used as the mathematical mesh size for idealized structure. Furthermore, weave structure of the threads can easily and accurately be idealized for mathematical models. This method is also well suited for a high speed digital computer, and once programmed, an optimum analysis can be accomplished.

The results of analyses from these approaches are also included. It is evident that a sphere of 450 feet in diameter or even larger is structurally feasible with the materials developed under this contract.

All of these approaches assume that the material is absorbing all of the light striking its surface. This introduces an additional safety factor of approximately 3.0 as $\alpha = 0.3$.

1.0 A CYLINDER UNDER SPACE CONDITIONS

Sunlight impinges on a fully erected cylinder from the right. It is assumed that a constant fraction, f, of the sunlight which hits any portion of the cylinder boundary for the first time is completely absorbed (the mesh fibers are assumed black here). The remaining light (1-f) goes on across the cylinder. When it traverses the cylinder boundary for the second time, a fraction f is again absorbed. The force, then, exerted by sunlight on the right-hand half of the cylinder per unit length is:

$$\frac{Sf(2r)}{c}$$

Here S is the solar constant, and c the speed of light. The force exerted by sunlight on the left-hand side of the cylinder per unit length is:

$$\frac{S(1-f)f(2r)}{c}$$

If the mass per unit length of the cylinder is m, then the acceleration of the cylinder to the left is given by:

$$\frac{Sf(2r) + S(1-f)f(2r)}{cm}$$

The force exerted on the right-hand half of the cylinder is greater than that exerted on the left-hand half. Consequently, the cylinder should flatten somewhat, the width of the figure now being smaller than its height. The cylinder flattens until stresses set up in the self-erecting material make all portions of the cylinder accelerate at the same rate.

It is arbitrarily assumed here that trouble in deployment can be expected if the radius of the fully erected cylinder, say in the absence of sunlight, is just large enough so that in the presence of sunlight the right and left extremities of the figure are regions of zero curvature. A cylinder of any larger radius would exhibit a dog-bone appearance.

Now the cylinder is accelerating to the left so one should have the x-y coordinate system also accelerating to the left at the same rate, and then perform the analysis in this accelerating system. Here we approximate this procedure by assuming that another sun produces light which shines on the cylinder from the left. The acceleration of the cylinder is now zero. Consider that "quarter" of the distorted cylinder which lies at the lower right hand, as illustrated on the following page.
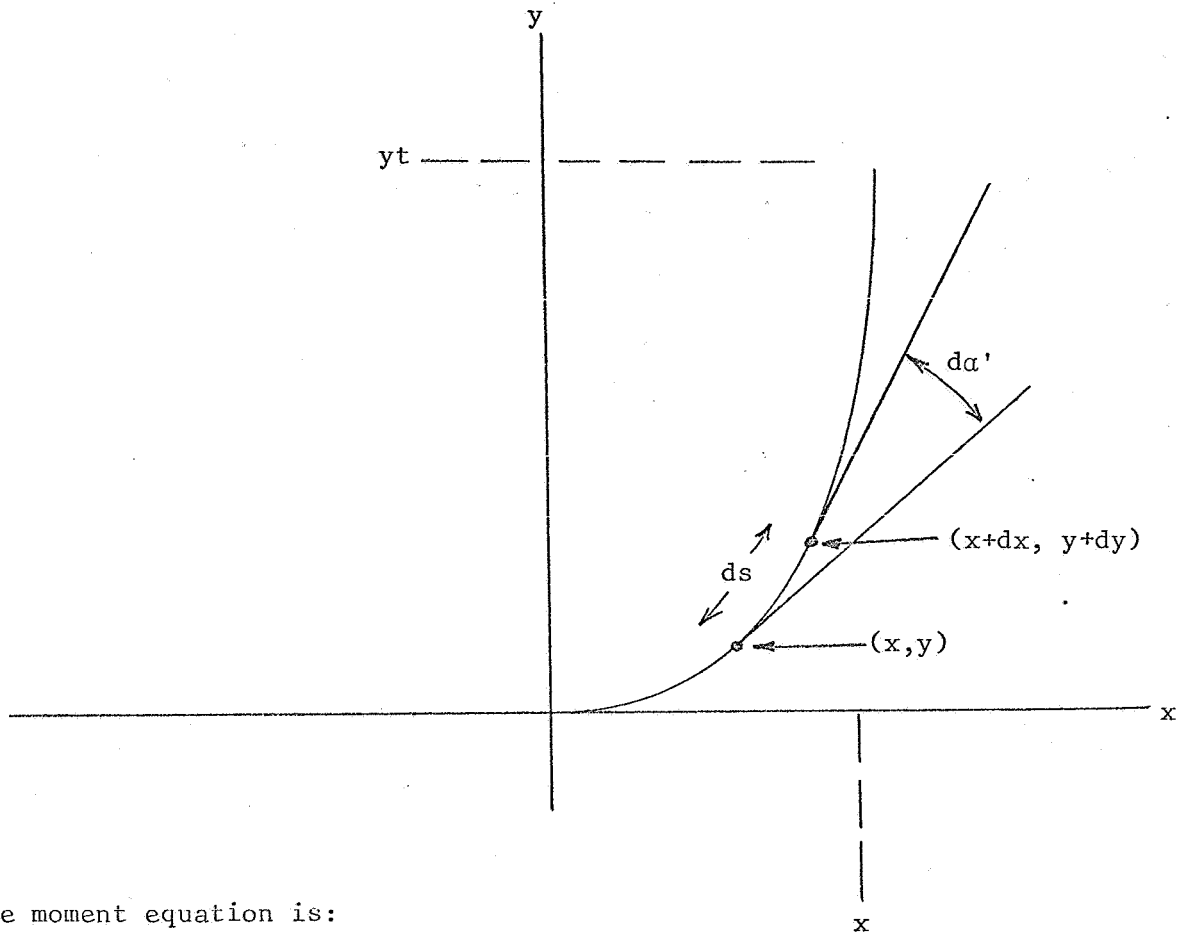
The moment equation is:

$$EI \frac{d\alpha'}{ds} = \frac{S\ f^2(yt-y)^2}{2c}$$

Here E is Young's Modulus of the material and I its moment of inertia.

Rewrite the equation as:

$$d\alpha' = ds\ \frac{S\ f^2(yt-y)^2}{2\ EIc}$$

Define a new constant C by:

$$C = \frac{S\ f^2}{2\ EIc}$$

Replace ds by S and replace $d\alpha'$ by α'_n where n=1,2,3....f-1,f. Note that the length, Z, of the illustrated band is fS and that the radius r of the undistorted cylinder which gave rise to this distorted band is given by $4Z/\alpha\pi$.

A computer program was written which gives (x,yt), Z, and r as a function of C. The basic fact which simplifies the computation is illustrated in the figure on the following page:
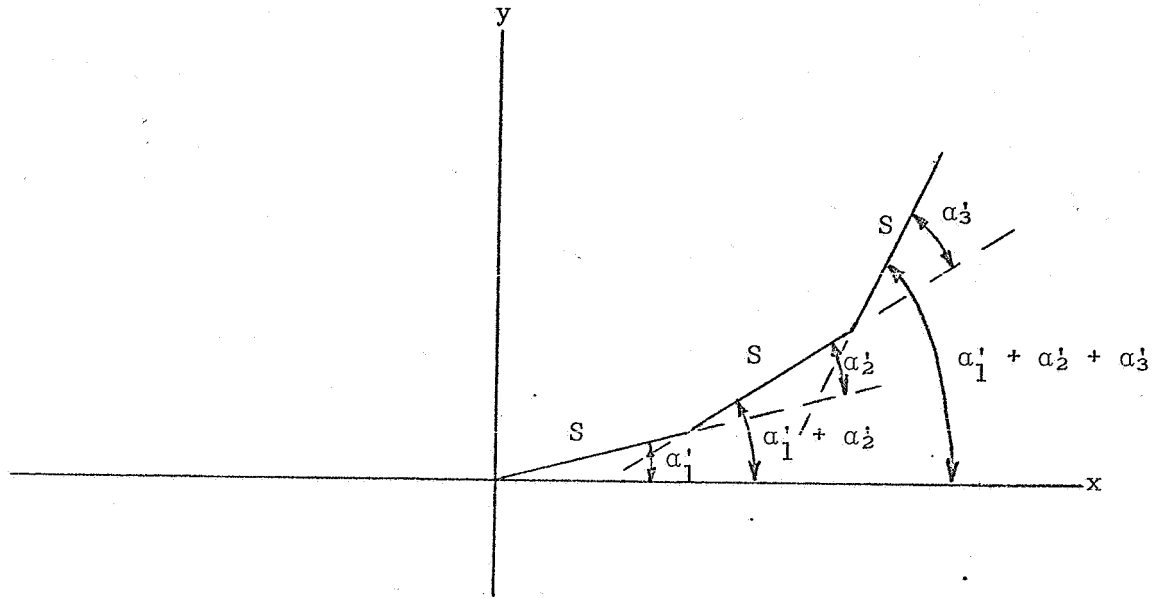
Note that:

$$y_1 = S \sin (\alpha_1' + \alpha_2')$$

$$y_2 = y_1 + S \sin (\alpha_1' + \alpha_2')$$

$$y_3 = y_2 + S \sin (\alpha_1' + \alpha_2' + \alpha_3')$$

etc.

And that

$$x_1 = S \cos \alpha_1'$$

$$x_2 = x_1 + S \cos (\alpha_1' + \alpha_2')$$

$$x_3 = x_2 + S \cos (\alpha_1' + \alpha_2' + \alpha_3')$$

etc.

The computation must stop when n becomes just large enough, say N, to make

$$\sum_{m=1}^{N} \alpha_n' = \pi/2$$

Since the expression for α_n' involves yt, and since yt can only be known after the problem is solved, the program initially requires the insertion

I-4

of a large yt as a starter which the program then adjusts as it proceeds so that it eventually converges to the correct value. The program prints out the correct value of yt and the associated x.

Now the material under study has an EI = 1000 milligram-cm = 980 dyne-cm. The speed of light is 3×10^{10} cm/sec. The solar constant,

S is $\dfrac{(2.0)(4.18) \times 10^{7}}{60} \dfrac{\text{ergs}}{\text{cm}^{2}\text{-sec}}$

Consequently C is:

$$C = 2.42 \times 10^{-6}/\text{ft}^{3}$$

With this C, an r of about 89 ft was obtained, yt being 108 ft and x about 78 ft. When the material strength EI was made ten times greater so that C was $2.42 \times 10^{-7}/\text{ft}^{3}$, the r obtained was about 190 ft, yt being about 231 ft, and x about 160 ft. Note that $10^{1/3} \approx 190/89$.

2.0 GORED SPHERE UNDER SPACE CONDITIONS

The fundamental question is, what is the maximum diameter of a self-erecting sphere which will deploy without dimples or other discontinuities, and remain stable under the action of superimposed forces after deployment.

The stability is considered first, and it is assumed tentatively that a folding technique can be devised so that a folded sphere will deploy properly. The reason for this assumption is that stability of the sphere under superimposed forces is a function of the physical properties of the material only, while deployment depends also upon the folding technique.

For the sake of analysis, the sphere is assumed to be made of gores and the effect of solar pressure is considered. In the analysis the effect of continuity between the gores has not been considered. This assumption, however, is on the conservative side and spheres of the radius so obtained should be safe under given loads with a certain factor of safety. This analysis further assumes an absorptivity equal to unity. The α of electroless-deposited copper on GT-301 is 0.35. This introduces a safety factor of 2.5 to 3.0. Figure 40, flexural rigidity vs radius, shows that a rigidity of 14,000 mg-cm would be required for a 425-ft diameter sphere.

2.1 ANALYSIS:

Assume the sunlight impinging on a fully erected sphere from the right –
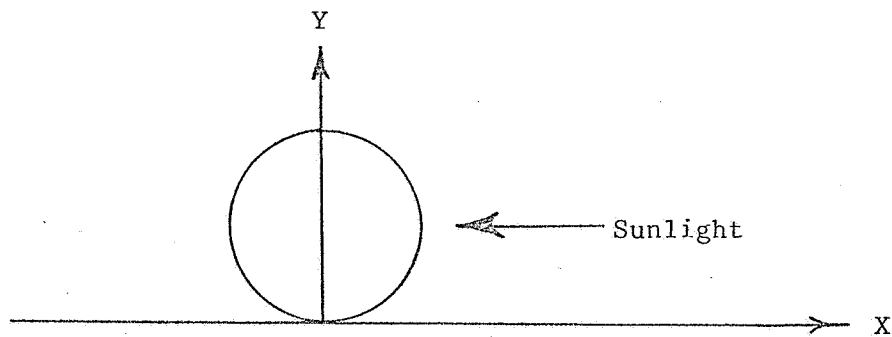
It is assumed that a constant fraction f of the sunlight which hits any portion of the sphere boundary for the first time is completely absorbed. The remaining light (1-f) goes on across the sphere. When it traverses the sphere boundary, a fraction f is again absorbed. The force then exerted by sunlight on the right hand half of the sphere is:

$$f_1 = \frac{(S)(f)(2\pi r^2)}{C}$$

where
S is the solar constant
C is the speed of light
r is the radius of sphere
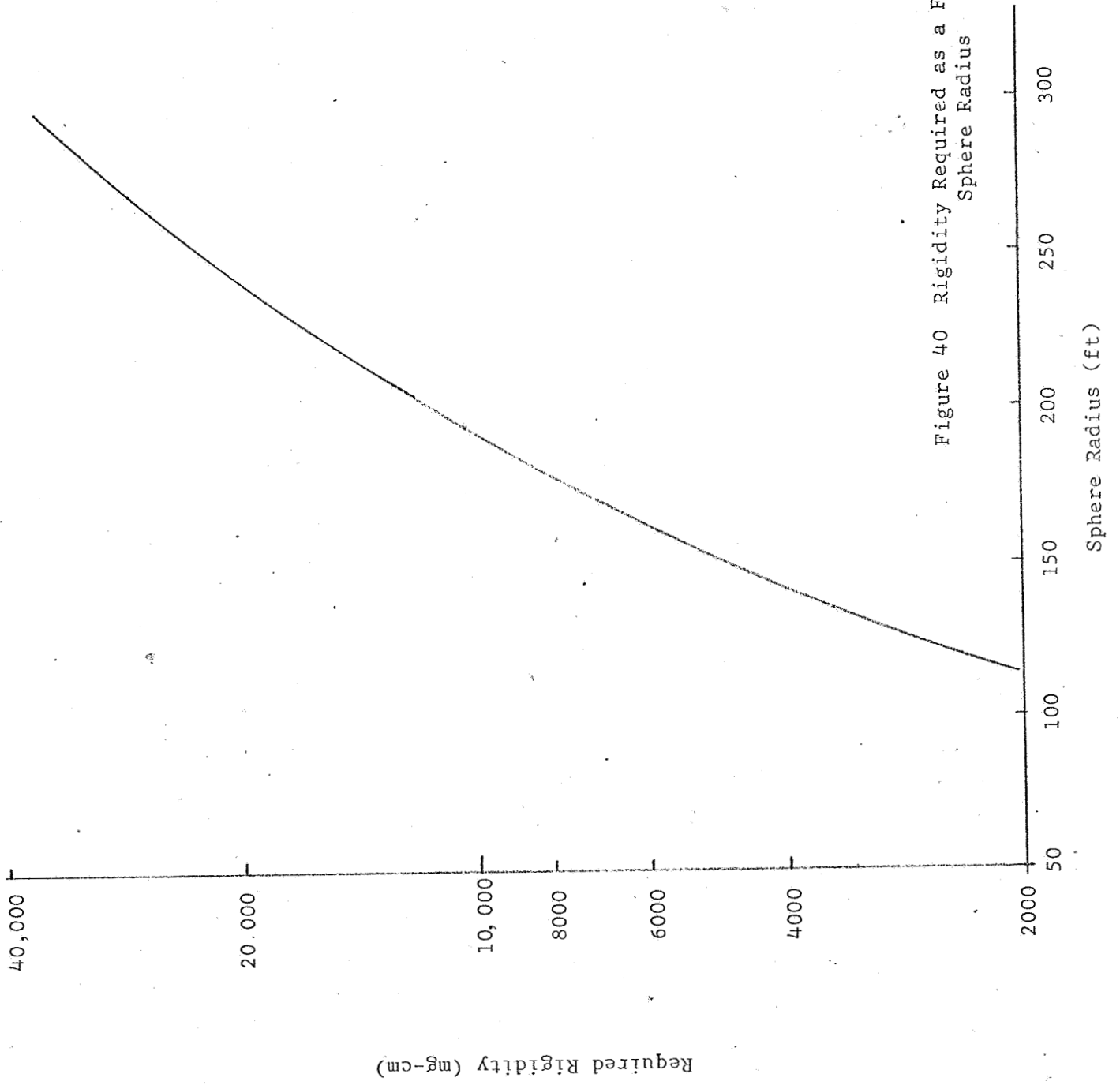
Figure 40 Rigidity Required as a Function of Sphere Radius

Force exerted by the sunlight on the left hand half of the sphere is:

$$f_2 = \frac{S\ (1-f)f\ (2\pi r^2)}{C}$$

If M is the total mass of the sphere, then the acceleration (a) of the sphere to the left is given by:

$$a = \frac{4S\ (f)\pi r^2 - S\ (f^2)\ 2\pi r^2}{CM}$$

Now the sphere is accelerating to the left so one should have the X-Y coordinate system also accelerating to the left at the same rate, and then conduct the analysis in this accelerating system. Here we approximate the procedure by assuming that another sun produces light which shines on the sphere from left hand side; thus, the resulting acceleration of the sphere is zero.

Solar pressure on a unit area

$$= \frac{S\ (f)}{C} - \frac{S\ (f)(1-f)}{C} = \frac{S\ (f^2)}{C}$$
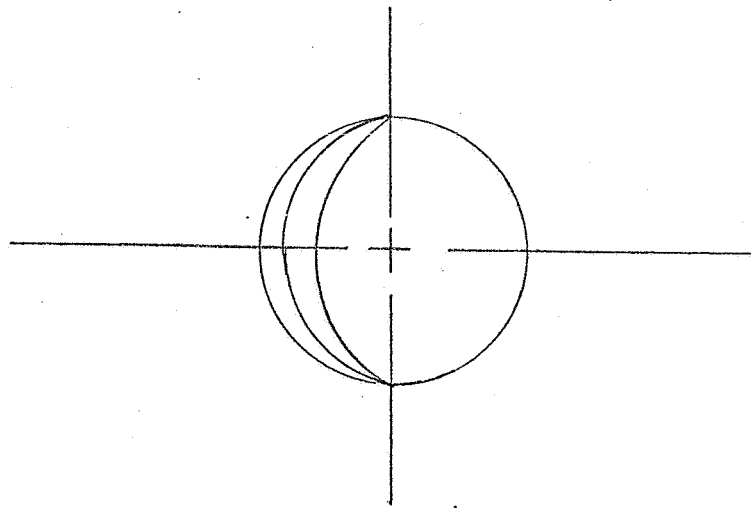
Spherical Shell
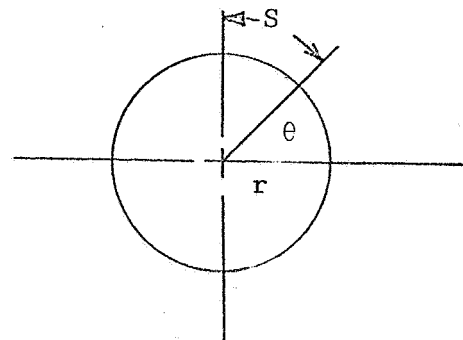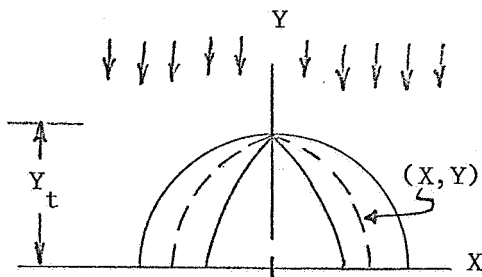
Consider one complete gore of the shell and, for the sake of analysis, consider the stability of the top half of the gore. The solar pressure is assumed acting parallel to the X-axis. The expression for the change in curvature of this gore in pure bending is given by*:

$$\frac{d\varphi}{ds} = \frac{M}{EI} \tag{1}$$

The gore width varies from apex to equator according to the following formula:

$$\text{gore width} = \frac{2\pi r \cos\left(\frac{\ell}{r}\right)}{N}$$

where r is the radius of the sphere, N is the number of gores that constitute the sphere, ℓ is the arc length from the X-axis to the point where gore width is being considered.

The moment equation (1) can now be written as:

$$\frac{d\varphi}{ds} = \int_y^{y_t} \left[\frac{S\ f^2}{C}\right]\left[\frac{2\pi r \cos\frac{\ell}{r}}{N}\right]\left[dy'\right]\left[(y' - y)\right]\left[\frac{1}{EI}\right]$$

The moment of inertia of the gore varies with the width of the gore and the above equation may be rewritten as

$$\frac{d\varphi}{ds} = \int_y^{y_t} \left[\frac{S\ f^2}{C}\right]\left[\frac{2\pi r \cos\left(\frac{\ell}{r}\right)}{N}\right]\left[dy'\right]\left[y'-y\right]\left[\frac{N}{E(2\pi r \cos \frac{\ell}{r})I}\right]$$

$$EI\ \frac{d\varphi}{ds} = \frac{S\ f^2(y_t - y)^2}{2C}$$

Some values representing the relation between the material stiffness and radius of sphere are given in the table below.

---

*Timoshenko, Strength of Materials, Part I, D. Van Nostrand Company, Inc., Third Edition, 1955

No.	EI (Milligram-in)	Radius (ft)
1	2,000	112
2	5,000	152
3	10,000	190
4	15,000	219
5	20,000	241
6	30,000	276
7	40,000	304
8	130,000	450

3.0 MEMBRANE STRESSES IN A SPHERE DUE TO SOLAR OR DYNAMIC PRESSURE

The principal external loading tending to buckle the sphere is the direct pressure of photons from the sun. The solar pressure (P) is constant in the vicinity of the earth and is 1.3×10^{-9} psi. The actual distribution over the surface of the sphere is not uniform. In terms of the angular coordinate and of any point on a meridian, as shown in figure below,
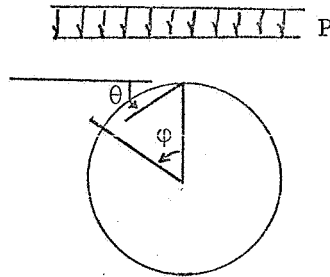
the normal pressure due to solar pressure may be given by $P \cos^2 \varphi$ over the windward half of the sphere and by zero on the leeward half. This unbalanced loading causes the sphere to accelerate through space, creating inertia forces on the skin which combine with the external pressure forces to create stresses in the skin. The total combination of forces is in equilibrium but is distributed nonuniformly over the sphere and results in nonuniform distribution of stresses in the skin. An approximation to these stresses can be given by a linear stress analysis through the use of membrane shell theory:

$$N_\varphi = \frac{-Pr}{2} + \frac{Pr}{8} \left(\frac{3 - 4 \cos \varphi}{1 - \cos \varphi} \right) \quad \frac{\pi}{2} \leq \varphi \leq \pi$$

$$N_\theta = \frac{-Pr}{2} + \frac{Pr}{8} \left(\frac{5 - 3 \cos \varphi - \cos^3 \varphi}{1 - \cos \varphi} \right)$$

where N_φ and N_θ are membrane forces per unit length of the principal normal sections of the shell, and r the radius of the sphere.

It can be seen that the maximum compressive stresses occur at the stagnation point and is given by

$$N_\varphi = N_\theta = \frac{-7}{16} Pr$$

for our present case

$$P = (1.3 \times 10^{-9}) \text{ psi}$$
$$r = (225 \times 12) \text{ in.}$$

$\therefore \quad N_\varphi = N_\theta = 1.54 \times 10^{-6} \text{ lb/in.}$

The material presently being considered is capable of much larger compressive stresses. .

A table of the normal stress for various radii follows.

Radius (feet)	Normal Stress $N_\varphi = N_\theta$ (Pounds per sq. in.)
25	0.17×10^{-6}
50	0.34×10^{-6}
100	0.68×10^{-6}
150	1.03×10^{-6}
200	1.37×10^{-6}
225	1.54×10^{-6}

This relation has been represented graphically on the following, figure 41. It can be seen that the maximum compressive stress increases less rapidly with the increase in the diameter for larger diameters of the sphere.

3.1 STRUCTURAL ANALYSIS

3.1.1 Overall Buckling:

Use the equation from p. 518, Timoshenko, Theory of Elastic Stability, 2nd Edition, 1961 –

$$P = \frac{2\ Et^2}{r^2\ \sqrt{3(1 - \mu^2}}$$

where P = solar pressure, psi
r = radius of sphere
E = modulus of elasticity of material
t = thickness of material
μ = Poisson's ratio of the material

The above equation can be rewritten as

$$P = \frac{KD}{r^2 t}$$

where D is the rigidity of the material and K is a constant and equals 13.216.

$$P = \frac{13.216}{r^2 t}$$

Since

$P = 1.3 \times 10^{-9}$

$t = 4 \text{ mils} = 4 \times 10^{-3} \text{ in}$

$r = (225 \times 12) \text{ inches}$
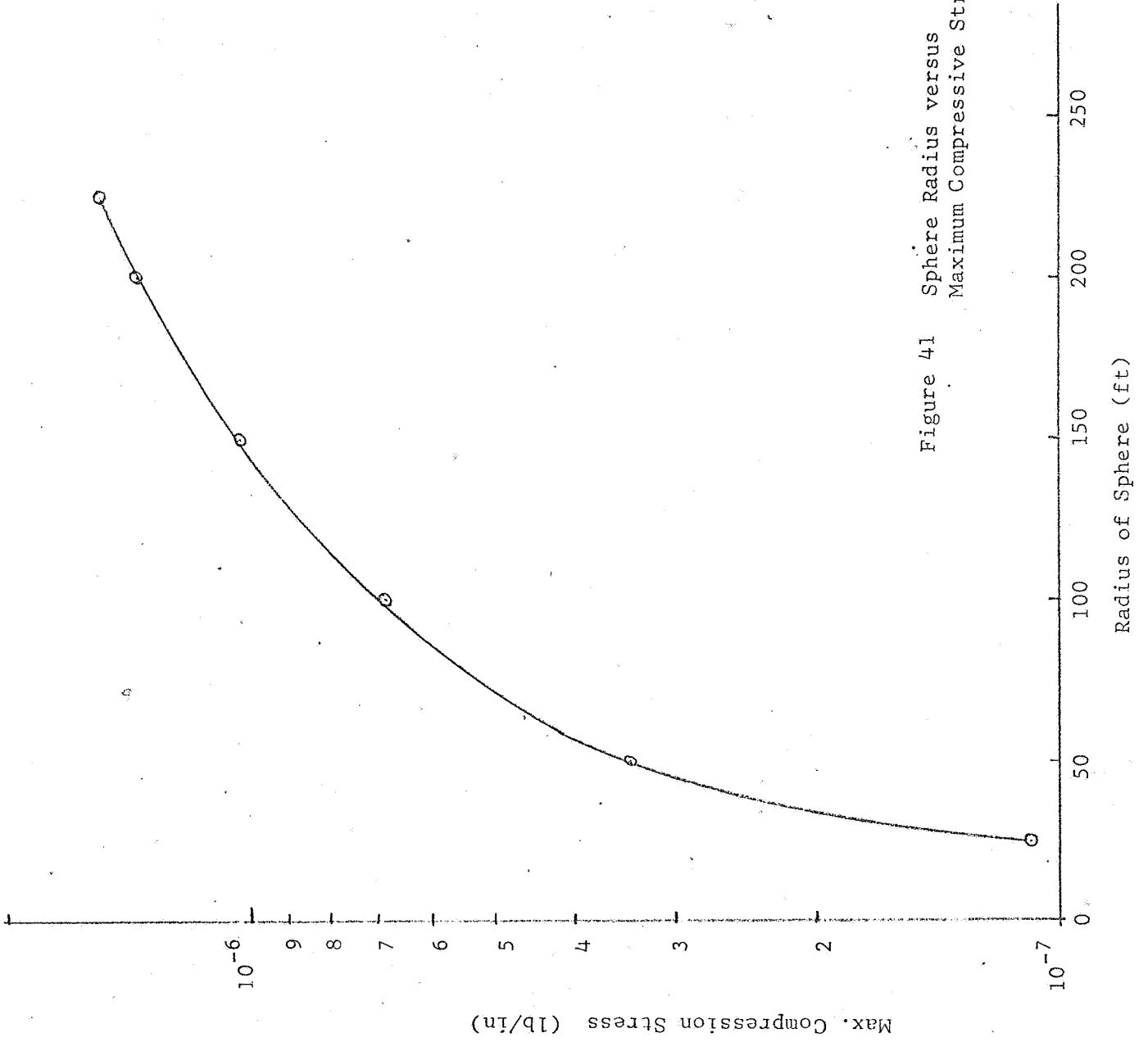
Figure 41   Sphere Radius versus
            Maximum Compressive Stress

then $\qquad$ $D = 2.87 \times 10^{-6}$ in-lb or

$\qquad\qquad\qquad$ = 3.309 mg-cm

Approximate calculations show that in the vicinity of the spherical shape of equilibrium of a compressed shell there exist forms of equilibrium slightly deviated from the spherical shape which require pressures much smaller than those given by above equations. This indicates that very small disturbance during loading or imperfection in the sphere formation may produce buckling at pressures much smaller than those given by above theory.

A table of required stiffness for various radii follows.

Radius of the Sphere (feet)	Required Stiffness (mg-cm units)
25	0.041
50	0.163
100	0.652
150	1.467
200	2.608
225	3.309

This relation has been represented graphically on the following page, figure 42. It may be concluded from this graph that the stiffness required increases less rapidly with the increase in the diameter for larger diameters of the sphere.

3.1.2 Local Buckling

Buckling of small areas of a spherical surface is a much more critical condition than general or overall buckling.

To study local buckling, reference is made to "Axially Symmetric Buckling of Shallow Spherical Shells Under External Pressure" by Reiss, Dec. 1958, Journal of Applied Mechanics.

$$Pcr = 2 \; EK^{1/2} \; p \left(\frac{h^2}{r^2} \right)$$

where
$\qquad$ Pcr = critical buckling load
$\qquad$ E = modulus of elasticity
$\qquad$ h = one half the material thickness = t/2
$\qquad$ r = radius of the sphere
$\qquad$ p = loading parameter = ω^2/ρ
$\qquad$ ω = a constant
$\qquad$ $\rho = (K)^{-1/2} \; A^3 \left(\frac{r}{h} \right)$
$\qquad$ A = semiangle of shell opening
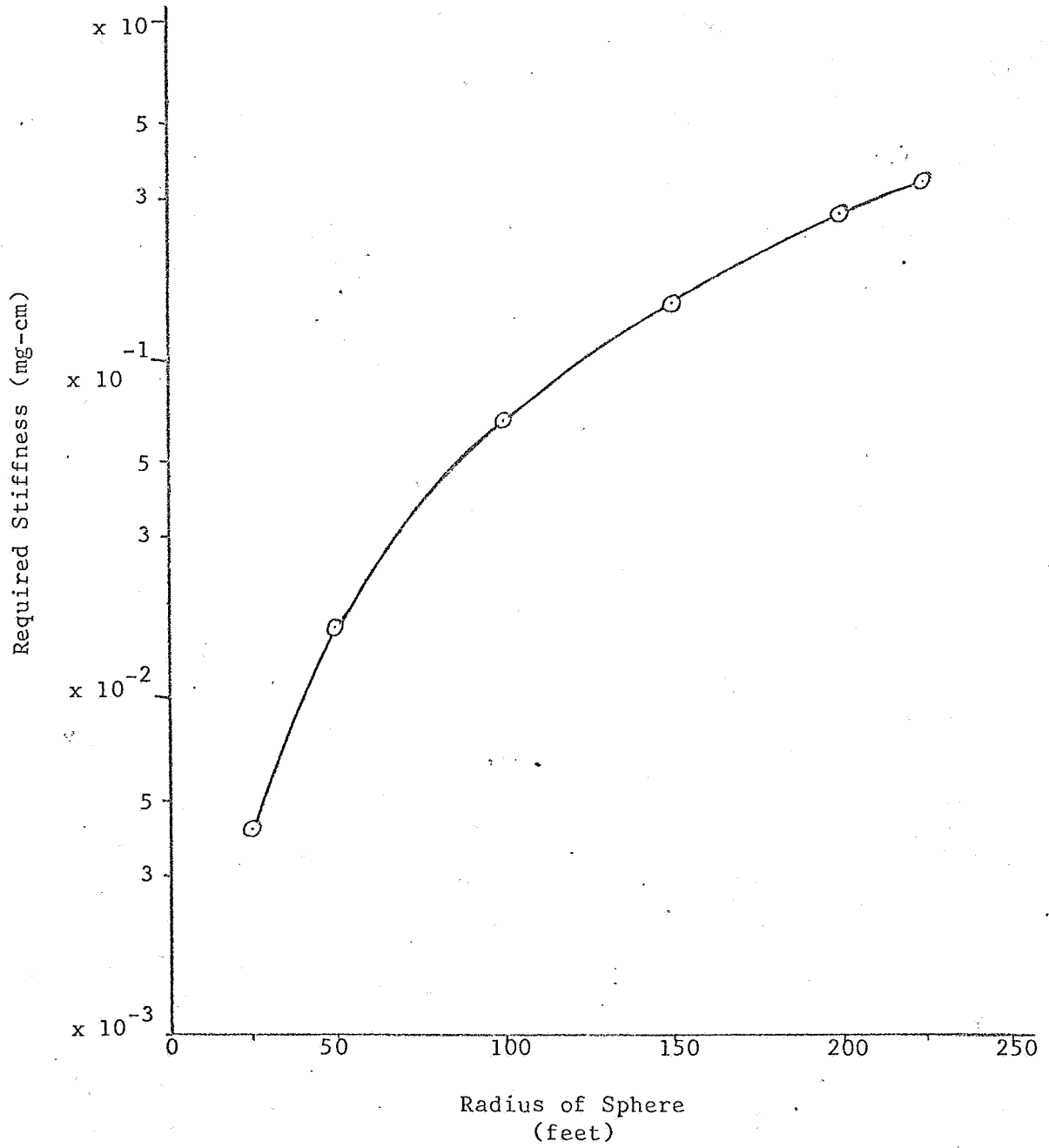
Figure 42   Radius of Spheres versus Stiffness D
(Based on Overall Buckling Criteria)

$$K^{1/2} = \frac{2}{3(1 - \mu^2)^{1/2}}$$

Since

$$\mu = 0.3$$
$$K = 0.736$$
$$K^{1/2} = 0.855$$
$$\omega = 3.83$$
$$\rho = 25.8$$
$$p = 0.57$$
$$pcr = 1.3 \times 10^{-9} \text{ psi}$$
$$E = 10^7 \text{ psi}$$

A form factor of 1/30 based on comparative stiffnesses is suggested.

$$\therefore \qquad Pcr = \frac{1}{30} \left[2 \ EK^{1/2} \ p \ \left(\frac{h^2}{r^2} \right) \right]$$

and

$$h^2 = \frac{30 \ Pcr \ r^2}{2 \ E \ K^{1/2} \ p}$$

$$\therefore \qquad h^2 = (4.0 \times 10^{-15}) \ r^2$$

The following table gives the thickness required for various radii.

Radius of Sphere (feet)	Total thickness of material (inches)
25	3.8×10^{-5}
50	7.6×10^{-5}
100	1.52×10^{-4}
200	3.04×10^{-4}
225	3.42×10^{-4}

This relation has been represented graphically on the following page, figure 43. It may again be concluded that the material thickness required increases less rapidly with the increase in the diameter for larger diameters of the sphere.
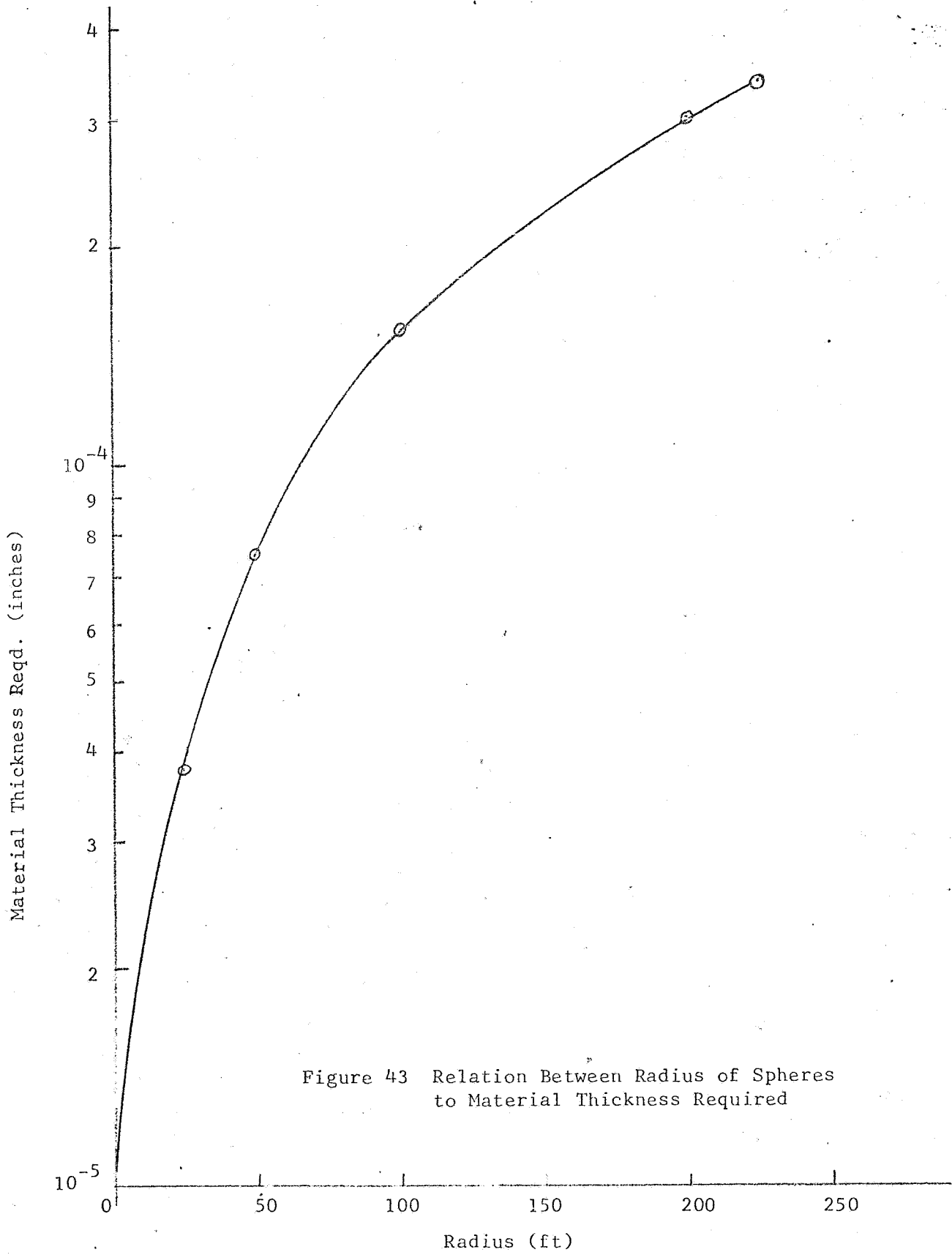
Figure 43 Relation Between Radius of Spheres
to Material Thickness Required

4.0 METHODS OF STRUCTURAL ANALYSIS

The numerical methods of structural analysis for determining stresses and displacements under prescribed applied loading can be separated into two basic types:

(1) Numerical solution of differential equations for the displacements and stresses

(2) Matrix methods based on discrete element idealization

In the first type, the differential equations of elasticity are solved for a particular structural configuration either by direct numerical integration or by finite difference techniques. In the second type, the structure is first idealized into an assembly of discrete structural elements, each having an assumed form of displacement or stress distribution, and the complete solution is then obtained by combining these individual approximate displacements or stress distributions in a manner which satisfies the force equilibrium and displacement compatibility at the junctions of these elements. Thus in general, equilibrium and compatibility are satisfied at only a finite number of points, but this does not necessarily mean that there may be an appreciable loss of accuracy and the matrix method will give good approximation to the exact solution.

Two matrix methods of analysis of a structural problem are possible:

(a) Displacement method or stiffness method

(b) Force method or flexibility method

Both methods can be successfully employed for the analysis of complex structures. In this report, displacement method has been selected.

4.1 MATRIX METHOD OF ANALYSIS

Basic Assumptions:

(1) The structure is idealized into a set of discrete elements connected together by point attachments on their boundary. These point attachments are referred to as the nodal points.

(2) The displacements within the elements may be defined by continuous functions from which the resulting strain distribution can be obtained in terms of a finite number of displacements at the nodal points of the element. These displacements are defined as element displacements.

(3) The stresses within the elements, obtained from the assumed strain distribution are balanced by equivalent boundary forces corresponding with the element displacement. These forces are referred to as element forces.

Structural Idealizations:

The first problem of idealization of the actual structure into discrete elements is the choice of structural grid. Ideally, the grid lines should be chosen as nearly as possible to correspond with the actual structure. In this particular case, the grid size for analysis is defined by the grid size of the fiber mesh.

If the structural elements of the actual structure are connected together by discrete joints, then the necessary interaction between individual elements may be introduced as joint forces, or displacements, which would ensure equilibrium and compatibility for a specified loading condition on the assembled structure. Here the transition from the differential equations of continuum mechanics into a set of algebraic equations can be easily seen. The differential equations for each element can be solved initially in terms of the boundary conditions resulting in force-displacement relationship. The satisfaction of boundary conditions leads to a set of algebraic equations which are used to determine the unknown boundary values. All these equations can be expressed in a matrix form. Thus a structure made up of elements and connected with discrete attachments lends itself ideally to a matrix method of structural analysis.

Summary of Matrix Method of Analysis:

Stiffness matrices will be formulated based on the original geometry of the structure assuming articulate joints and also assuming continuity along the main line of threads. The articulate structure is a statically determinate structure while one with continuous members is statically indeterminate. The stiffness matrices are solved yielding deflections and rotations, then in conjunction with stress matrices, the forces in all members may be obtained. This matrix formulation is limited to small deflections.

This method of direct formulation of stiffness matrix is then extended to include the effects of large deflections. The method suggested in this report is based on the notion of superposing corrections upon the general solution given by the above linear matrix method. The following two effects, ignored in the linear theory, have been accounted for in large deflection effects.

(1) Linear theory is developed on the geometry of undeformed structure while large deflection theory does account for changed geometry.

(2) The equations for strain displacement in large deflection theory are nonlinear as against linear equations in the other theory.

4.2 STIFFNESS MATRIX ASSUMING SMALL DEFLECTION THEORY

4.2.1 Articulate Structure

Coordinate System:

Radial, tangential and vertical axes form a right orthogonal triad.

Coordinate System
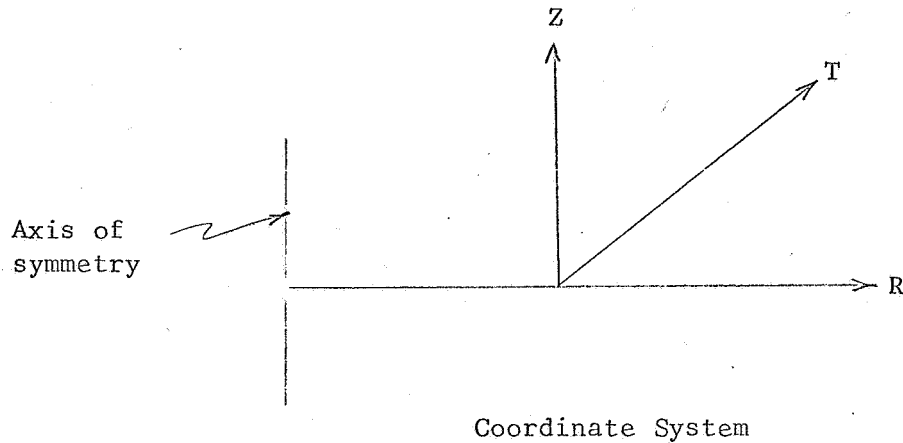
        As pointed out earlier, stiffness matrix is used as a general
solution to the problem of determining the displacements and force distri-
bution in the structure. As an introduction to stiffness matrix, we will
deal with forces produced in simple structures due to various displacements
of the ends of the members.

(1) Consider the forces in a member with pinned ends shown in figure 44a
and having length L, cross-sectional area A, and modulus of elasticity E.
The member is in the RZ plane and LR and LZ are the radial and vertical
component of the ends of the member. We will define the radial displacement
of joint 1 as U_1 and vertical displacement by W_1. Similarly radial and
vertical displacements of joint 2 will be U_2 and W_2.

        Now assume that ends (1) and (2) have been subjected to dis-
placements U_1, W_1, and U_2, W_2 respectively. To get these replacements,
certain radial and vertical forces are required at the ends (1) and (2).
Due to these displacements, LR changes by U_2-U_1, and LZ changes by W_1-W_2
(see figure 44b). The change in length is given by

$$DL = (LR/L) (U_2-U_1) + (LZ/L) (W_1-W_2)$$

Force F is the member, assuming tension to be positive is given by:

$$F = \frac{DL \cdot A \cdot E}{L}$$

        The only force transmitted by the articulate member is the force
in the direction of the principal axis of the member. Note that the lateral
displacement may be due to rigid body motion of the member. The R and Z
component of this force are

$$FR1 = F (LR/L) \text{ and } FZ1 = -F (LZ/L)$$

L

LZ

LR

(a)   SCHEMATIC VIEW

DL

L

$W_1 - W_2$

1

$U_1 - U_2$

2
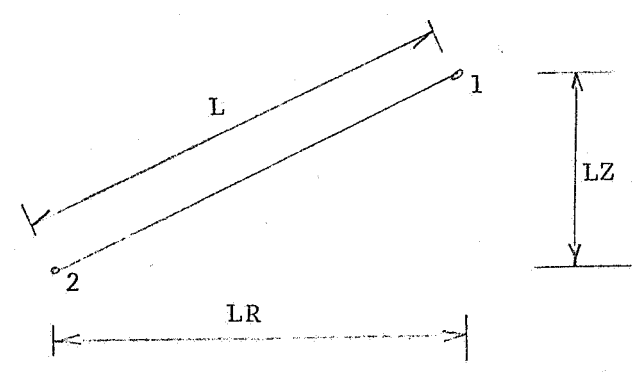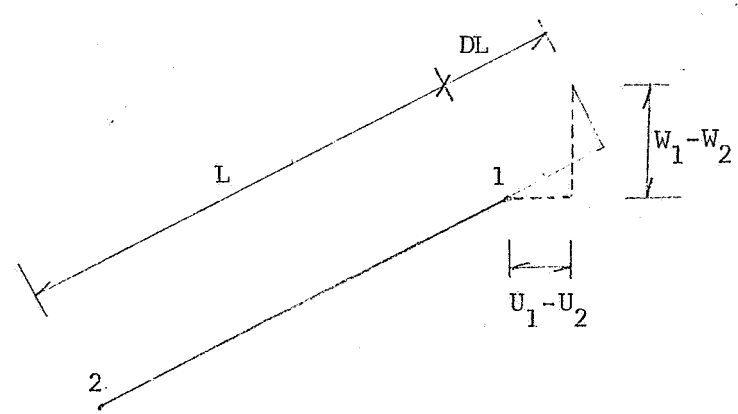
(b) Joint Translation

2

1   5

3

4
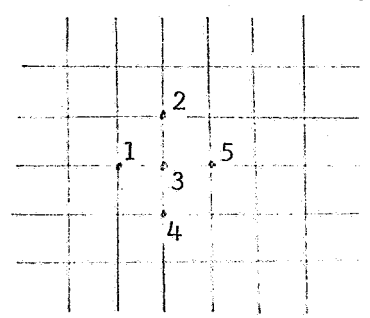
Member Designation

Figure 44   Force Diagram

A member in three dimensional space may have a tangential component of length LT and a force component in the T direction at each end. Let V_1 and V_2 be the tangential displacements at joints 1 and 2. Assume joint 2 to be in the positive T direction from joint 1. The change in length of the member is

$$DL = (LR/L) (U_2 - U_1) + (LT/L) (V_2 - V_1) + (LZ/L) (W_1 - W_2)$$

Force F in the member is

$$F = \frac{DL \cdot A \cdot E}{L}$$

The R, T, and Z components of this force on joint 1 are

$$FR1 = F(LR/L), \quad FT1 = F(LT/L), \quad \text{and} \quad FZ1 = -F(LZ/L)$$

while the components of joint 2 are

$$FR2 = -F(LR/L), \quad FT2 = -F (LT/L); \quad FZ2 = F(LZ/L) \ .$$

Using $r = LR/L$
$t = LT/L$
$Z = LZ/L$

We can transform the above equations in a matrix form.

$$
\begin{vmatrix} FR1 \\ FT1 \\ FZ1 \\ FR2 \\ FT2 \\ FZ2 \end{vmatrix}
= \frac{AE}{L}
\begin{vmatrix}
-r^2 & -rt & rZ & r^2 & rt & rZ \\
-tr & -t^2 & tZ & tr & t^2 & -tZ \\
Zr & Zt & -Z^2 & -Zr & -Zt & Z^2 \\
r^2 & rt & -yZ & -r^2 & -rt & rZ \\
tr & t^2 & -tZ & -tr & -t^2 & tZ \\
-Zr & -Zt & Z^2 & Zr & Zt & -Z^2
\end{vmatrix}
\times
\begin{vmatrix} U_1 \\ V_1 \\ W_1 \\ U_2 \\ V_2 \\ W_2 \end{vmatrix}
$$

This gives force components along the principal axes of a single articulate member due to joint displacements.

If a number of members were framing at a joint, similar force components could be outlined for every member. To obtain equilibrium, the sum of these internal forces and the externally applied forces, along all

principal axes at all joints must equal zero. We have one equation for
each principal direction of motion at each joint. The articulate sphere
has three principal directions of motion at each joint. If there are n
joints, we shall have 3n unknowns and 3n equations. The coefficients of
these equations are the elements of a 3n by 3n stiffness matrix.

Consider 3 as a typical joint and we shall write the equations
of equilibrium for this joint in the articulate sphere. The internal forces
are introduced through the forces in members 1-3, 2-3, 4-3, and 5-3, as
seen in figure 44.

We shall use the following notation for the equations of equi-
librium:

Ui	radial displacement of joint i
Vi	tangential displacement of joint i
Wi	vertical displacement of joint i

FBRi	radial component of force in the rib member below joint i
FBTi	tangential component of force in the upper rib member at joint i
FBZi	vertical component of force in the upper rib member at joint i
FRRi	radial component of force in the band member to the right of joint i
FRTi	tangential component of force in the band member to the right of joint i
FRZi	vertical component of force in the band member to the right of joint i
FLRi	radial component of force in the band member to the left of joint i with respect to the coordinates at joint i
FLTi	tangential component of force in the band member to the left of joint i with respect to the coordinates at joint i
FLZi	vertical component of force in the band member to the left of joint i with respect to the coordinates at joint i
LRi	length of rib below joint i
LBi	length of band to the left of joint i
AR	area of rib members
AB	area of band members
E	modulus of elasticity of the material

All original components of all members will be considered positive.
The tangential components of the rib i will be considered positive if joint
i + 1 is in the positive T direction from joint i.

Radial equilibrium requires that the sum of internal and external
forces in radial direction be zero.

$$-FBRZ \cdot \frac{AR\ E}{(LR2)^3} \left[FBR2\ (U3-U2) + FBT2\ (V3-V2) + FBZ2\ (W2-W3) \right]$$

$$-FRR3 \cdot \frac{AB \cdot E}{(LB3)^3} \left[FLR5 + U5 + FRR3 \cdot U3 + FLR5 \cdot V5 - FRT3 \cdot V3 \right.$$
$$\left. + FRZ3\ (W3-W5) \right]$$

$$+ \text{FBR3} \cdot \frac{\text{AR} \cdot \text{E}}{(\text{LR3})^3} \left[\text{FBR3} \ (\text{U4}-\text{U3}) \ + \ \text{FBT3} \ (\text{V4}-\text{V3}) \ + \ \text{FBZ3} \ (\text{W3}-\text{W4}) \right]$$

$$- \text{FLR3} \cdot \frac{\text{AB} \cdot \text{E}}{(\text{LB3})^3} \left[\text{FLR3} \cdot \text{U3} \ + \ \text{FLT3} \cdot \text{V3} \ - \ \text{FLZ3} \ (3) \right]$$

+ external force in the radial direction = 0.

Equations for tangential and vertical equilibrium can be written in a similar manner. The coefficients of these equations are the elements of the stiffness matrix for an articulate structure. The solution of stiffness matrix gives deflections of the joints and finally the member forces can be computed.

4.2.2 Continuous Structure

We shall now consider the forces produced when ends of a beam with bending resistance are subjected to various displacements and rotations.

Forces considered to be distributed by the member are the forces in the direction of the principal axis of the member and forces normal to it. As the force transmitted in the direction of the principal axis of the member is the same as that for an articulate member, we shall consider only the forces transmitted normal to the principal axis of member. These forces and the forces transmitted by an articulate member can then be superposed.

Consider a member as shown in figure with length L, cross-sectional area A, moment of inertia I and modulus of elasticity E. This member is oriented in RZ plane such that LR, the radial component of the length of the member previous to rotation and displacements of the ends of the member is equal to L and LZ, the vertical component is zero.

We shall define the Z component of deflections at points 1 and 2 as W1 and W2 respectively. The clockwise rotations will be designated $\theta 1$ and $\theta 2$ respectively. Let FZ1 and FZ2 be the Z component of the force at joints 1 and 2 respectively and let M_1 and M_2 be the clockwise moments at these node points. Using these notations, we find

$$\text{FZ1} = \frac{\text{EI}}{\text{L}^3} \left[12(\text{W2}-\text{W1}) \ - \ 6\text{L}(\theta 1 \ + \ \theta 2) \right]$$

$$\text{FZ2} = \frac{\text{EI}}{\text{L}^3} \left[12(\text{W2}-\text{W1}) \ + \ 6\text{L}(\theta 1 \ + \ \theta 2) \right]$$

$$\text{M1} = \frac{\text{EI}}{\text{L}^2} \left[6(\text{W2}-\text{W1}) \ - \ 2\text{L}(\theta 2 \ + \ 2\theta 1) \right]$$

$$\text{M2} = \frac{\text{EI}}{\text{L}^2} \left[6(\text{W2}-\text{W1}) \ - \ 2\text{L} \ (\theta 1 \ + \ 2\theta 2) \right]$$
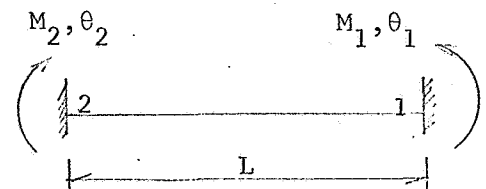
Continuous Member

Using the following notation

θ1X   rotation in RZ plane of the end 1 of the member

θ2X   "   " "   "   "   "   " 2 " "   "

θ1Y   rotation normal to the plane RZ of end 1 of member

θ2Y   "   "   "   "   "   " "   " 2 "   "

M1X   bending moment on the member in RZ plane, at end 1

M2X   "   "   " "   "   "   "   "   ". 2

M1Y   "   "   " "   "   , normal to RZ plane, at end 1

M2Y   "   "   " "   ".   "   " "   "   . " " 2

IX   moment of inertia, in RZ plane, of the rib member

IY   "   "   "   , normal to RZ plane, of the rib member

 x EIX/L^3

 y EIY/L^3

 K . AE/L

 r LR/L

 t LT/L

 z LZ/L

    In matrix form, forces 4 moments on joints 1 and 2 of a continuous
member are

$$\{F\} = [K]\,\{d\}$$

$$
\begin{Bmatrix} FR1 \\ FT1 \\ FZ1 \\ M1X \\ M1Y \\ FR2 \\ FT2 \\ FZ2 \\ M2X \\ M2Y \end{Bmatrix}
= [K] \times
\begin{Bmatrix} U1 \\ V1 \\ W1 \\ \theta 1X \\ \theta 1Y \\ U2 \\ V2 \\ W2 \\ \theta 2X \\ \theta 2Y \end{Bmatrix}
$$

	$U1$	$V1$	$W1$	$\theta 1X$	$\theta 1Y$	$U2$	$V2$	$W2$	$\theta 2X$	$\theta 2Y$
$FR1$	0	$-6Ly$	0	0	$-2L^2y$	0	$6Ly$	0	0	$-4L^2y$
$FT1$	$-6Lxz$	0	$-6Lxr$	$-2L^2x$	0	$6Lxz$	0	$6Lxr$	$-4L^2x$	0
$FZ1$	$-rZK+12xrZ$	$-tZK$	$Z^2K+12xr^2$	$6Lxr$	0	$rZK-12xrZ$	tZK	$-Z^2K-12xr^2$	$6Lxr$	0
$M1X$	rtK	t^2K+12y	$-tZK$	0	$6Ly$	$-rtK$	$-t^2K-12y$	tZK	0	$6Ly$
$M1Y$	$r^2K+12xZ^2$	rtK	$-rZK+12xrZ$	$6LxZ$	0	$-r^2K-12xZ^2$	$-rtK$	$rZK-12xrZ$	$6LxZ$	0
$FR2$	0	$-6Ly$	0	0	$-4L^2y$	0	$6Ly$	0	0	$-2L^2y$
$FT2$	$6Lxz$	0	$6Lxr$	$-4L^2x$	0	$-6Lxz$	0	$-6Lxr$	$-2L^2x$	0
$FZ2$	$rZK-12xrZ$	tZK	$-Z^2K-12xr^2$	$6Lxr$	0	$-rZK+12xrZ$	$-tZK$	$Z^2K+12xr^2$	$-6Lxr$	0
$M2X$	$-rtK$	$-t^2K-12y$	tZK	0	$6Ly$	rtK	t^2K+12y	$-tZK$	0	$-6Ly$
$M2Y$	$-r^2K-12xZ^2$	$-rtK$	$rZK-12xrZ$	$6LxZ$	0	$r^2K+12xZ^2$	rtK	$-rZK+12xrZ$	$-6LxZ$	0

We have thus found the moments and force components along the principal axes of a single continuous member due to joint rotations and displacements. If a number of members were framing together at a joint, similar force components could be obtained for each member. To satisfy equilibrium, the sum of internal and external forces, as well as moments, must equal zero. We thus have one equilibrium equation for each direction of translation and rotation at a continuous joint. The coefficients of these equations are the elements of the stiffness matrix. The solution of the stiffness matrix yields displacements and rotations of the ends of all members in the structure. The forces and moments to which these members are subjected then be calculated.

4.3 EFFECT OF LARGE DEFLECTIONS

The approach to large deflection problem is to superimpose corrective terms into small deflection equations to eliminate the errors resulting from the small deflection assumptions. The corrective terms include effects of deformed geometry of the structure and nonlinear load deformation relationship.

Let us again consider the case of a member with articulate joints, shown in figure 45 below.

Forces on a Member with Articulate Joints
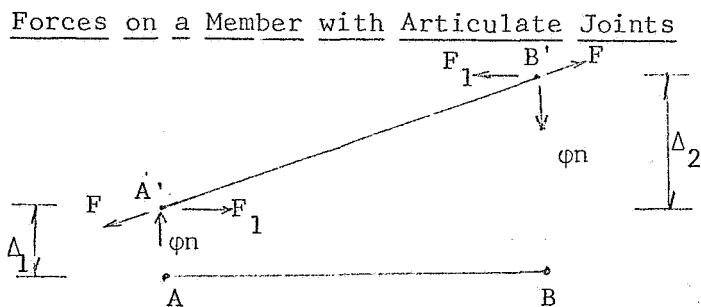
Figure 45

Let AB and A'B' represent the positions of the member before and after deformation. The member is in the state of equilibrium under the action of:

(1) member force F

(2) linear force F_1

(3) corrective force φn

If the deformation of member was neglected, the linear force F_1 would have been the member force. Thus the force φn may be thought of as the correction to the linear force F_1, correction being considered for the effect of deflection. This force may be expressed as:

$$\varphi n = (F/L)\ (\Delta 2 - \Delta 1)$$

Thus the corrective force φn is a linear in F and may be expressed as

$$\varphi n = BF$$

where φn is a matrix of corrective forces, B is a linear transform and F is a matrix of member forces.

The equation for member deformation must also be revised to account for large deflections.

Original and Deformed
Position of Member

Figure 46

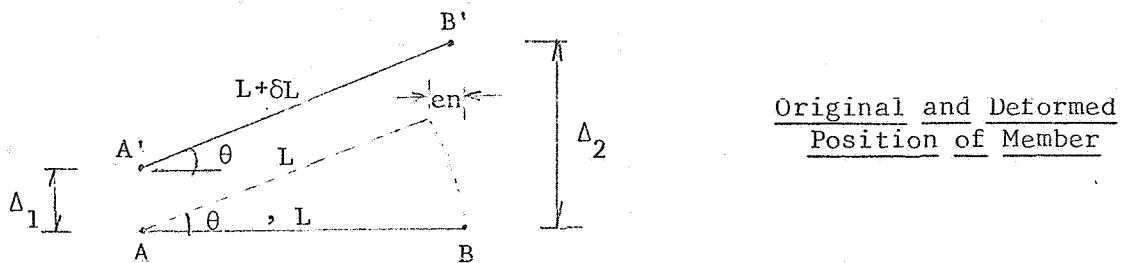Figure 46 shows the original position AB and deformed position B'B' of the articulate member. The previous theory was developed in terms of the deformation of the bar δL and the original geometry of the structure. In this case, the change in length may be given by

$$(L + \delta L) \cos \theta - L \simeq \delta L - \frac{L}{2} \theta^2$$

Thus the effect of rotation of a bar can be approximately described by adding the corrective deformation

$$en = \frac{L}{2} \theta^2$$

to the linear equations of member deformation derived previously.

For a linear structure, the internal forces and deflections due to applied loading can be described in terms of influence coefficients by the matrix equations

$$FL = F\varphi \cdot \varphi + Fe \cdot e$$

$$\Delta L = \Delta\varphi \cdot \varphi + \Delta e \cdot e$$

FL = matrix of linear internal forces due to applied loading

ΔL = matrix of deflections due to applied loading

Fφ = influence matrix of element forces resulting from unit values of external load

Fe = influence matrix of element forces resulting from unit values of element deformations

Δφ = influence matrix of deflections resulting from unit values of applied loads

Δe = influence matrix of deflections resulting from unit values of element deformations

I-28

φ = matrix of est. loads

e = matrix of element deformations

Influence matrices Fφ, Fe, $\Delta\varphi$, Δe can be computed by linear displacement methods and φ and e are known matrices.

Now the corrective forces are of the same physical form as φ and the corrective member deformations are of the same physical form as e. Since φn and en are corrections to the linear solutions for large deflections, the forces and deflections for geometrically nonlinear structures are:*

$$F = F\varphi\ (\varphi + \varphi n) + Fe(e + en) \tag{1}$$

$$\Delta = \Delta\varphi\ (\varphi + \varphi n) + \Delta e(e + en) \tag{2}$$

where φn = matrix of corrective external loads

en = matrix of corrective element deformations

φn   and en are functions of deflections

F = matrix of element forces ⎫
                            ⎬ accounting for large deflection
Δ = matrix of deflections   ⎭

Because of the dependence of φn and en on Δ, the equations (1) and (2) are nonlinear and must be solved by repetitive means. To reduce the computational work, the following simplification may be used:

The corrective loads are linear functions of the element forces, therefore

$$\varphi n = BF \tag{3}$$

where B is a matrix of corrective loads resulting from unit values of element forces, and from deflections. Eliminate φn and F from equations (1) and (2)

$$F = \left[I - F_\varphi \cdot B\right]^{-1} \left[F\varphi \cdot \varphi + Fe(e + en)\right] \tag{4}$$

therefore from equation (3)

$$\varphi n = B\left[1 - F\varphi \cdot B\right]^{-1} \left[F\varphi \cdot \varphi + Fe(e + en)\right] \tag{5}$$

Eliminate φn from (2) and (5)

$$\Delta = \Delta\varphi \cdot \varphi + \Delta\varphi \cdot B\left[I - F\varphi \cdot B\right]^{-1}\left[F\varphi \cdot \varphi + Fe(e + en)\right] + \Delta e(e + en) \tag{6}$$

*Matrix Methods of Structural Analysis, edited by F. de Veubeke, The Macmillan Company, New York, 1964.

Expand the matric $(I - F\varphi \cdot B)^{-1}$

$$\Delta = \Delta\varphi \cdot \varphi + \Delta\varphi \cdot B \left[I + F\varphi \cdot B + (F\varphi \cdot B)^2 + --- \right] * \left[F\varphi \cdot \varphi + Fe(e+en) \right]$$

$$+ \Delta e(e + en) \qquad\qquad (7)$$

Rearranging the terms in (7) and substituting $\varphi n\varphi = BF\varphi$ and $\varphi ne = B \cdot Fe$

$$\Delta = \Delta\varphi(I + \varphi n\varphi + \varphi^2 n\varphi + ---)\varphi + \left[\Delta e + \Delta\varphi(I + \varphi n\varphi + \varphi^2 n\varphi + ---)\varphi ne \right] \left[(e+en) \right]$$

where $\varphi n\varphi$ is a matrix of corrective loads resulting from the linear element forces resulting from unit external loads and φne is a matrix of fictitious loads resulting from the linear element forces resulting from unit element deformations. As an approximation, neglect all powers of $\varphi n\varphi$ higher than the first and all terms involving products of the form $\varphi n\varphi \cdot \varphi ne$.

$$\Delta = \Delta\varphi(I + \varphi n\varphi)\varphi + (\Delta e + \Delta\varphi \cdot \varphi ne)(e + en) \qquad (8)$$

The matrices $\varphi n\varphi \cdot \varphi$ and $\varphi ne \cdot e$ involve the deflections Δ. As an approximation, assume that $\varphi n\varphi \cdot \varphi$ and $\varphi ne \cdot e$ are linear functions of Δ, such that

$$\varphi n\varphi \cdot \varphi = \varphi n\varphi\Delta \cdot \Delta$$

$$\varphi ne \cdot e = \varphi ne\Delta \cdot \Delta$$

substituting these in (8) and rearranging

$$\left[I - \Delta\varphi(\varphi n\varphi\Delta + \varphi ne\Delta) \right] \Delta = (\Delta\varphi\varphi + \Delta ee) + (\Delta e + \Delta\varphi\varphi ne)en \qquad (9)$$

where $\varphi n\varphi\Delta$ and $\varphi ne\Delta$ are matrices of influence coefficients for the corrective forces due to the combined effect of the unit deflections and the linear internal forces due to applied load and member deformation (may be due to temperature, etc.). The homogeneous form of the equation

$$I - \left[\Delta\varphi(\varphi n\varphi\Delta + \varphi ne\Delta) \right] \Delta = 0$$

is the linearized stability criteria for buckling due to mechanical loading.

APPENDIX II

Deployment Machine

Figure 47 shows the deployment machine and canister assembly used
for the tests at Goddard. The machine was designed as simply as possible
to assure reliability. Velocity was imparted by springs spaced around
the plunger. The plunger was cocked and tied with 1000-lb test nylon line.
This line had a squib-fired line cutter triggered by a 2 to 6 volt charge.
This means of triggering was felt to be as foolproof as possible. The
spring rate for each spring was 30 lbs/ft. Knowing the initial velocity
required to send the sphere 30 to 35 feet high, the total spring rate
needed could be determined. Since the initial velocity required was
51 ft/sec, 12 springs were required.

The canister assembly was a split cylinder with a loose bottom.
The three components of this canister were attached to the catapult
plunger so that the bottom was pulled out first allowing the canister
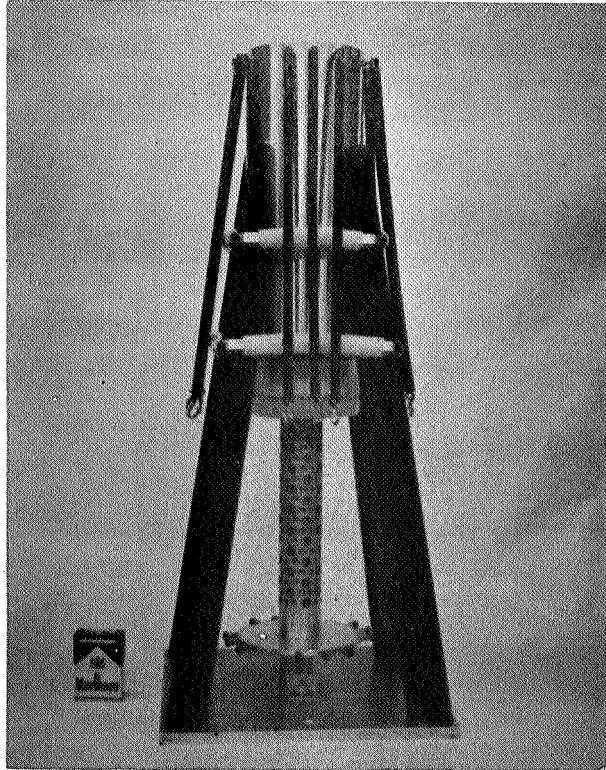halves to be pushed open by the self-erecting material.

Figure 47   Development Machine and Canister Assembly

APPENDIX III

Items Shipped

The following list contains the shipping date, description of items, quantity and/or unit identification numbers of deliverable items made under the contract. Figures 48 and 49 show the configurations of spherical segments and panels. All panels were 4 by 6 feet.

SHIPPING DATE	DESCRIPTIONS OF ITEMS	QUANTITY AND/OR UNIT IDENTIFICATION NUMBER
8/16/65	7-1/2 in by 12 in cylinder	1 unit
	Polyethylene bladder	1 unit
	Panel - with seals	1 unit
	Panel - without seals	1 unit
12/10/65	Made from 129 material	105-76-1 and 105-76-2
1/25/66	30-inch sphere (18 gores) made from 129 material	105-84-1
2/18/66	Spherical segment made from 130 material. Type A seal.	105-85-1
	Spherical segment made from 130 material. Type A seal.	105-85-2
6/1/66	Type A panel made from 131 material.	105-118-1
	Type B panel made from 131 material.	105-118-2
6/30/66	Type A panel made from I-8601 scrim having been sized with a 10 per cent solution of polyvinyl alcohol. The material was also coated with 25 microinches of vacuum deposited aluminum.	105-123-11
	Type A panel made from I-8601 scrim having been sized with a 6 per cent solution of polyvinyl alcohol. The material was also coated with 25 microinches of vacuum deposited aluminum.	105-123-12

SHIPPING DATE	DESCRIPTION OF ITEMS	QUANTITY AND/OR UNIT IDENTIFICATION NUMBER
9/29/66	Type A panel made from 133 material. Resistance side 1 - 7.2 $\Omega/\square$ Resistance side 2 - 4.4 $\Omega/\square$ Resistance across seal - 4.9 Ω	105-135-1
	Type A panel made from 132 material. Resistance side 1 - 7.0 $\Omega/\square$ Resistance side 2 - 2.9 $\Omega/\square$ Resistance across seal - 31.3 Ω	105-135-2
12/27/66	One 30-inch diameter sphere made from 136 material. The sphere was sealed as shown, figure 36. It was used for deployment tests at Goddard Space Flight Center.	1 unit
	One 30-inch diameter sphere made from 137 material. The sphere was sealed as shown, figure 36. It was used for deployment tests at Goddard Space Flight Center.	1 unit
1/23/67	One spherical segment made from 139 material. The segment was fabricated as shown in figure 48. Type B seals were used. Average gore resistance - 8.4 $\Omega/\square$ Resistance across seals - 2000 Ω	341-6-1
	One spherical segment made from 139, 141, and 143 material. Type A seals. Average gore resistance - 2.0 $\Omega/\square$ Resistance across seals - 500-1000Ω	341-6-2
	One spherical segment made from 140 material. Type A seals.	341-6-3
	Type A panel made from 137 material with overlapping joint	341-7-1
	Type A panel made from 134 material with butt joint.	341-7-2
	Type B panel made from 139 material with overlapping joints.	341-7-3

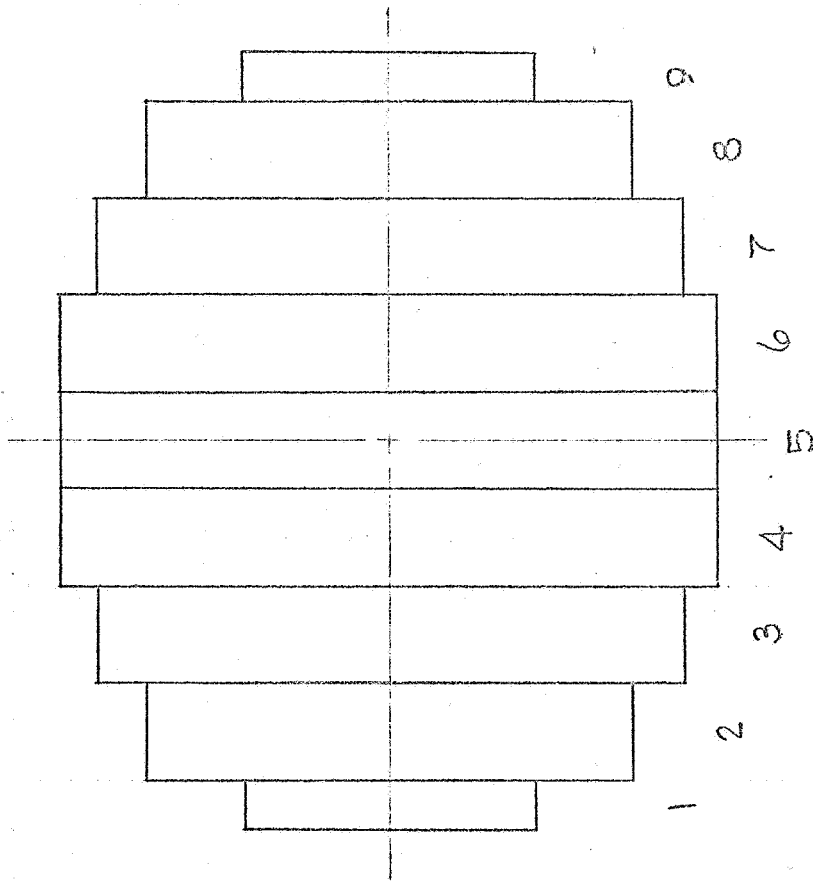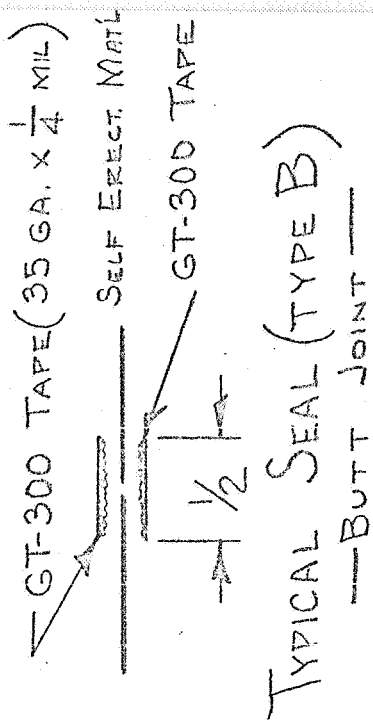| SHIPPING DATE	DESCRIPTION OF ITEMS	QUANTITY AND/OR UNIT IDENTIFICATION NUMBER
1/24/67	Panel made from 140 material. This panel had four sections with overlapping joints and bi-tape seals.	341-7-4
	Type A panel made from 142 material with butt joint.	341-7-5
	Type A panel made from 142 material with overlapping joints.	341-7-6
	Type B panel made from 142 material with butt joints.	341-7-7
	Type B panel made from 142 material had overlapping joints.	341-7-8
	Type A panel made from 144 material with butt joint.	341-7-9

GORE	LENGTH FEET	WIDTH INCHES
1	12	21
2	20	41
3	24	41
4	27	41
5	27	41
6	27	41
7	24	41
8	20	41
9	12	21

GORE SEALING CONFIGURATION

GT-300 TAPE (35 GA. × $\frac{1}{4}$ MIL)

SELF ERECT. MAT'L.

GT-300 TAPE

$\frac{1}{2}$

TYPICAL SEAL (TYPE B)
— BUTT JOINT —

GT-300 TAPE (35 GA. × $\frac{1}{4}$ MIL)

SELF-ERECT. MAT'L.

GT-300 TAPE
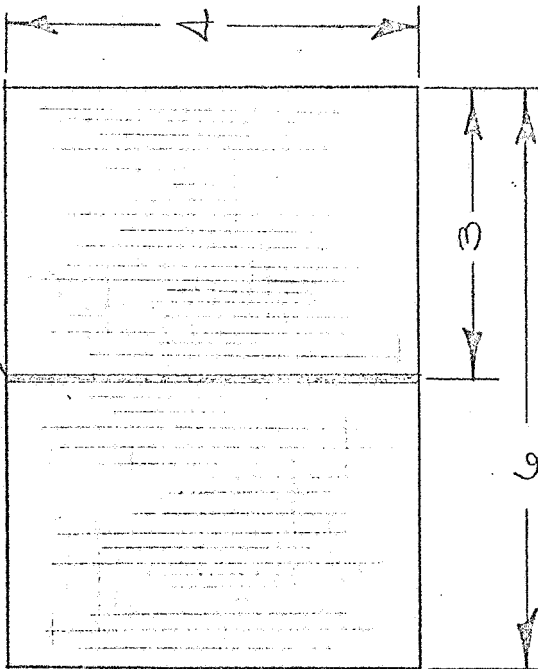
SELF-ERECT. MAT'L.

$\frac{1}{2}$
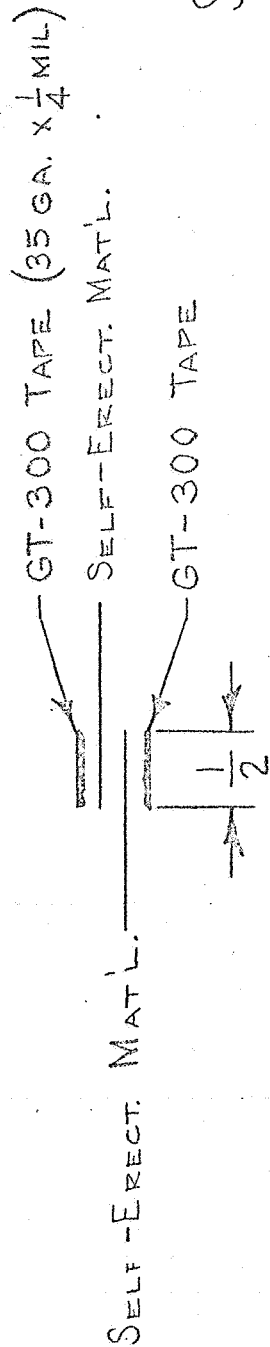
TYPICAL SEAL (TYPE A)
— OVERLAPPING JOINT —

Figure 48

SPHERICAL SEGMENT AND
TYPICAL GORE SEAL

MARCH 24, 1966

GT 300 Bi-Tape Seal

Note: Type A
Used on 105-118-1

4

3

6

MD

GT 300 Bi-Tape Seals
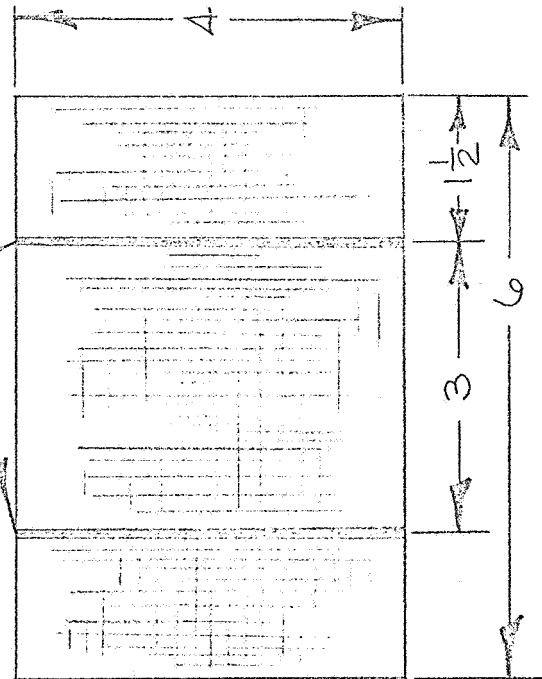
Note: Type B
Used on 105-118-2

4

$\frac{1}{2}$

6

3

MD

4 FT. X 6 FT. PANELS
24456-17 6-25-66

Figure 49

APPENDIX IV

Specifications

SPECIFICATION

CLASSIFICATION

Page _____ 1 _____ of _____

Specification NO. _____

Date Issued _____

Revision _____

PROCESSING SELF-ERECTING MATERIAL

	REV.	E C O	CHANGED

Prepared By: _T. F. Origen_

Approved By: _William Jacobi_

Approved By:

Released By:

1.0 SCOPE

This specification is applicable to the pretreatment, binding, and/or electroless copper plating of self-erecting material made to deploy without an inflatant or additional hardware.

2.0 PURPOSE

The purpose of this specification is to describe the equipment and procedures for pretreatment, binding, and/or electroless copper plating self-erecting material.

3.0 MATERIALS

3.1 Paint rollers (54 inch)

3.2 GT-201 adhesive (12% solids)

3.3 duPont red dye (C003500)

3.4 Deionized water

3.5 Enplate Cu-400-A (Enthone)

3.6 Enplate Cu-400-B (Enthone)

3.7 Enplate sensitizer #432 (Enthone)

3.8 Enplate activator #440 (Enthone)

Schjeldahl Company
G.T. SCHJELDAHL COMPANY ∘ NORTHFIELD, MINNESOTA 55057

	REV.	E C O	CHANGED

4.0 EQUIPMENT

    4.1 Continuous copper plating machine having
        tanks and rollers as shown on attached
        diagram.

    4.2 pH meter

5.0 PRETREATMENT AND/OR BINDING

    5.1 Section B of the plating machine will be used
        (ref. attached diagram).*

    5.2 Web the machine as shown using the second
        unwind. Install new coating rolls (3.1) to
        run in tank 10. Check to be sure that the nap
        of the paint roller covers will lay down as it
        comes into contact with the web. Having
        the rolls in the wrong way will result in the
        web shifting to one side and not going through
        the machine straight.

    5.3 Move coating tank (10) into position and fill
        with the material to be applied. The level in
        the tank will be maintained by periodic
        additions.

    5.4 Turn on exhaust fan and start machine. The
        machine may be operated at 6 in/min, 1 ft/min,
        1.3 ft/min, or 6 ft/min as desired.

    5.5 Turn on the 2 banks of heat lamps.

*Figure 10 in text.

Schjeldahl Company

G.T. SCHJELDAHL COMPANY • NORTHFIELD, MINNESOTA 55057

SPECIFICATION

CLASSIFICATION

Page __3__ of _____

Specification NO. _____

Date Issued _____

Revision _____

	REV.	E C O	CHANGED

5.6 After processing the desired amount of material stop the machine after the end of the web has come through the coating rolls. Allow the web to dry for 5 minutes in drying tower number 2 before rewinding. Cover the coating rolls with polyethylene so that the material will not fall on them.

5.7 Turn the heat lamps off and complete the rewinding of the material. When coating GT-201 (3.2), polyethylene must be wound into the roll to prevent blocking. The roll should be wound as loose as possible to facilitate the curing of the GT-201 coating.

5.8 Upon completion of the run, remove the coating roll covers and clean tank 10.

5.9 For material coated with GT-201: Place roll in cure room for 96 hours.

6.0 ELECTROLESS COPPER PLATING

6.1 Section A of the plating machine will be used (ref. attached diagram).

6.2 General operating conditions are as follows:

6.2.1 Web speed: 1 ft/min (6 in/min optional)

6.2.2 Air agitation: 14 psi gauge

6.2.3 Residence times:

Sensitizer solution   1.7 min

Activator solution   1.7 min

Plating solution   10 min

Drying tower   10 min

6.2.4 Process control temperatures:

SPECIFICATION

CLASSIFICATION

Page ___4___ of _____

Specification NO. _____

Date Issued _____

Revision _____

	REV.	E C O	CHANGED

Sensitizer and activator   18 to 22 C

Plating   20 to 22 C

Rinse tanks   40 to 50 C

Drying tower   18 to 22 C

6.3   Normal web speed is 1 ft/min. The optional speed (6 in/min) may be used. When operating at the slower speed use 1/2 the normal amount of sensitizer, activator, and plating solution.

6.4   Web the machine as shown on the attached diagram. Run the web from drying tower 1 directly to the rewind station.

6.5   Fill the tanks as follows:

1 - Sensitizer (3.7) - 8 in deionized water

6 qt sensitizer (3.7)

2 - Rinse - deionized water

3 - Activator (3.8) - 8 in deionized water

6 qt activator (3.8)

4 & 5 - Rinse - deionized water

6 & 7 - Plating - 15 3/4 in deionized water

3 1/2 in Cu-400-A (3.5)

8 3/4 in Cu-400-B (3.6)

8 - Rinse - deionized water

SPECIFICATION

CLASSIFICATION

Page ___5___ of _____

Specification NO. _____

Date Issued _____

Revision_____

	REV.	E C O	CHANGED

The sensitizer and activator are mixed with
1 part sensitizer or activator per 15 parts
deionized water. The plating solution is
mixed with 2 parts Cu-400-A and 5 parts
Cu-400-B per 9 parts deionized water.

6.6   Start the machine and process the desired
amount of material. Check and record the
pH (4.2) and the temperature of the plating
tank or tanks every hour during the run.
All in-process information will be recorded
on the attached data sheet.

6.7   If it is necessary to splice the web use
a bi-tape splice of D000800 tape. Reinforce
the splice with staples.

6.8   Upon completion of the run, remove the
completed material from the rewind and seal
in a Scotchpak (M001200) bag with a desicant.

Metal Deposition

Date _____   Amount Processed _____ ft

ype   _____   Electroless Plating (Use "Plating Log" Below)

    _____   Vapor Deposition (Use "Remarks")

    _____   Other   (Use "Remarks")

emarks -

           Type of Metal _____

           Thickness _____ Angstroms

           No. of Shots _____

Plating Log: Machine Speed _____ fpm

Feet	Time	Plating Tank pH #1	Plating Tank pH #2	Temperature	Resistivity	Remarks

Chemical Consumption: (Record Time & Amt.)	Sensitizer	Activator	Cu400A	Cu400B	NaOH	
	Deionized Water Tanks Start _____ End _____					

SPECIFICATION

Page 1 of 7

Specification NO. Q-132

Date Issued 6-28-66

Revision _____

TESTING OF SELF-ERECTING MATERIAL

	REV	ECO	CHANGED

Prepared By: _____

Approved By: _____

Approved By: _____

Released By: _____

1.0 SCOPE

This specification is applicable to the testing and evaluation of self-erecting material made to deploy without an inflatant or additional hardware.

2.0 PURPOSE

The purpose of this specification is to describe the apparatus and procedures for performing the following tests:

1. Resistivity measurement
2. Ultimate tensile (MD, TD, 45°)
3. Bend radius tensile
4. Rigidity
5. Folded rigidity

3.0 MATERIALS

The sample shall be properly identified with the roll number and an arrow indicating machine direction.

4.0 APPARATUS

4.1 Ohm meter

4.2 Test jig for resistivity measurement (ST-21-1)

4.3 Instron tester with CT load cell and chart recorder

4.4 Five (5) pound weight accurate within 2.0 grams

4.5 Rigidity test fixture per ASTM-D-1388

4.6 Bend radius test fixture

G. T. SCHJELDAHL COMPANY
NORTHFIELD, MINNESOTA

SPECIFICATION

CLASSIFICATION

Page __2__ of __7__

Specification NO. __Q-132__

Date Issued __6-28-66__

Revision _____

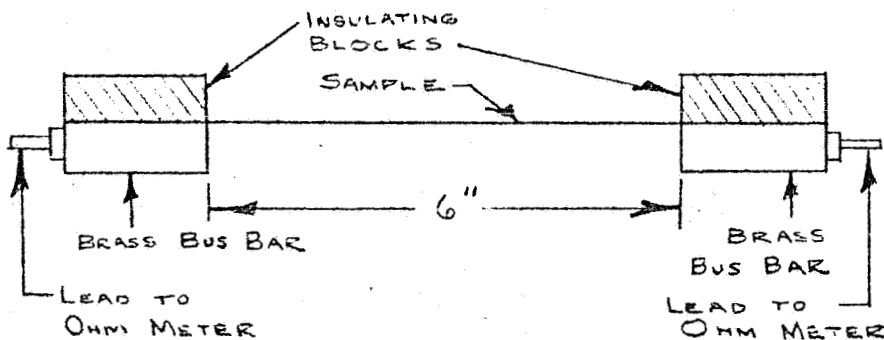|	REV	E C O	CHANGED

4.7 Mettler gram-atic balance

5.0 RESISTIVITY MEASUREMENT

The resistivity measurement shall be made on a 1" x 8" sample with brass bus bars contacting one square inch of area on each end of the sample. This leaves a 1" x 6" test area.

5.1 Connect the ohm meter to the resistivity jig (ST-21-1) and zero ohm meter.

5.2 Cut sample of material (1" x 8") and place in resistivity jig (jig has spring loaded clamps which exert constant pressure on the specimen) as shown in sketch above.

5.3 Take reading on ohm meter and record on data sheet. Remove specimen from resistivity jig.

5.4 Calculate ohms per square as follows and record on data sheet. Ohms per square is calculated from the resistance in ohms divided by 6.

6.0 ULTIMATE TENSILE

One inch wide samples shall be tested having the threads running in either the machine direction, transverse direction, or at a 45° angle.

SPECIFICATION

	REV	ECO	CHANGED

6.1 Cut the required number of one inch samples (note the direction which the threads run in the sample). The threads in the samples shall be straight and continuous from one end to the other.

6.2 The Instron shall be operated in accordance with Q-101.

6.3 Balance, zero, and calibrate the load weighing and recording system using the five pound calibrated weight.

6.4 Set crosshead speed at two (2) inches per minute, chart speed at two (2) inches per minute, and jaw separation at two (2) inches.

6.5 Set the "Full Scale Load" at a setting which will put the breaking point between the lower one quarter (1/4) and upper one quarter (1/4) portion of the graph.

6.6 Mount the specimen in the Instron jaws in such a manner that the length of the specimen is parallel to the lines of force exerted on it.

6.7 Run test, record elongation and ultimate tensile on chart.

6.8 Record elongation and ultimate tensile on data sheet.

7.0 BEND RADIUS TENSILE

One inch wide samples shall be tested having the threads running in either the machine direction, transverse direction, or at a 45° angle.

G. T. SCHJELDAHL COMPANY
NORTHFIELD, MINNESOTA
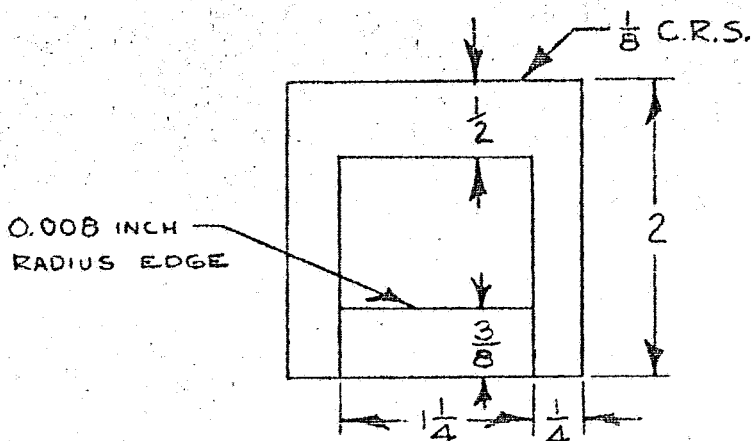
SPECIFICATION

CLASSIFICATION

Page __4__ of __7__

Specification NO. __Q-132__

Date Issued __6-28-66__

Revision _____

	REV	ECO	CHANGED

7.1 Clamp the bend radius fixture (see sketch below) in the upper jaw of the Instron.

7.2 Repeat steps 6.1 through 6.5.

7.3 Mount the specimen in the Instron so that the material makes a 180° bend over the bend radius fixture (.008 inch radius edge) and clamp both ends in the lower jaw. The specimen should be mounted in such a manner that the length of the specimen is parallel to the lines of force exerted on it.

7.4 Run test, record elongation and ultimate tensile on chart.

7.5 Record elongation and ultimate bend radius tensile on data sheet.

8.0 RIGIDITY TEST

One inch wide samples shall be tested having the threads running in either the machine direction, transverse direction or at a 45° angle.

8.1 The test shall be performed according to the procedures outlined in ASTM-D-1388. Measurements will be made at 10°, 20°, and 41.5°.

G. T. SCHJELDAHL COMPANY
NORTHFIELD, MINNESOTA

SPECIFICATION

CLASSIFICATION

Page __5__ of __7__

Specification NO. __Q-132__

Date Issued __6-28-66__

Revision _____

	REV	ECO	CHANGED

8.2 Cut the necessary samples (1" x 8"). The threads should be straight and continuous from one end to the other. Also cut a sample 6" x 6", this will be weighed later.

8.3 Place one specimen (1" x 8") on the smooth surface of the test fixture. The end of the sample should be even with the edge of the test fixture. Place the top weight, with the rubber pad against the sample, on the test fixture.

8.4 Slide the sample over the edge until the overhanging edge of the sample meets the desired angle 10°, 20°, or 41.5°. Note the length of overhang (in centimeters) and record this value on the data sheet.

8.5 This should be repeated for the top and bottom and each end of the sample (four measurements will be taken).

8.6 Average the readings obtained in 8.4 and 8.5 for each angle. This value will be used to calculate the flexural rigidity.

8.7 Weigh the 6" x 6" sample cut in 8.2 on the Mettler gram-atic balance.

$$\frac{\text{Weight of 6" x 6" sample}}{232} = \text{weight of sample in grams/cm}^2$$

Record the weight of the sample and the weight in grams/cm^2 on the data sheet.

-8.8 The formula for calculating flexural rigidity, G, is as follows:

$$G = W\, C^3$$

where W is the weight of the material expressed in mg/cm^2 and C is the bending length in cm. The bending length is determined as follows:

G. T. SCHJELDAHL COMPANY
NORTHFIELD, MINNESOTA

SPECIFICATION

CLASSIFICATION

Page __6__ of __7__

Specification NO __Q-132__

Date Issued __6-28-66__

Revision _____

	REV	ECO	CHANGED

10° - multiply the length of overhang (length to meet 10° angle) (value from 8.6) by 0.890

20° - multiply the length of overhang by 0.695

41.5° - multiply the length of overhang by 0.500

Record the flexural rigidity on the data sheet.

9.0 FOLDED RIGIDITY TESTS

The folded rigidity test is similar to the standard rigidity test (ref. 8.0) only the sample will be folded and creased prior to testing.

9.1 Cut the samples per 8.2.

9.2 Fold the sample to be tested in the center (approx. at the 4 inch mark) 180° and press under a seven pound weight for the desired amount of time (to be indicated on the test data sheet).

9.3 After folding, place the sample on the test fixture so that the fold is even with the edge. Place the top weight, with the rubber pad against the sample, on the test fixture to hold the specimen in place.

9.4 Starting with the 41.5° angle, cut off the sample (the overhanging end) until it meets 41.5°. Measure the remaining length of material overhanging (measured in centimeters).

9.5 Repeat step 9.4 for 20° and 10°. The same end of the sample may be used for the three measurements. Record the remaining overhang on the data sheet each time.

9.6 Steps 9.3 through 9.5 should be repeated for the other end of the sample.

G. T. SCHJELDAHL COMPANY
NORTHFIELD, MINNESOTA

SPECIFICATION

CLASSIFICATION

Page __7__ of __7__

Specification NO. __Q-132__

Date Issued __6-28-66__

Revision _____

	REV	ECO	CHANGED

9.7 Average the readings obtained in 9.4, 9.5 and 9.6 for each angle. This value will be used to calculate the flexural rigidity.

9.8 Weigh the 6" x 6" sample cut in 9.1 and calculate the weight (in grams/cm^2) of the material (ref 8.7). Record the weight of the sample and the weight in grams/cm^2 on the data sheet.

9.9 Calculate the flexural rigidity as in 8.8. Record the flexural rigidity (after folding) on the data sheet.